SEMMELWEIS EGYETEM
DOKTORI ISKOLA

Ph.D. értekezések

3038.

GANTSETSEG GARMAA

Transzlációs vesekutatások és szervtranszplantáció
című program

Programvezető: Dr. Zsembery Ákos, egyetemi docens

Témavezető: Dr. Gábor Kökény, egyetemi docens

UNRAVELING CHRONIC KIDNEY DISEASE: EVIDENCE FROM TGF-β-INDUCED IN VITRO AND IN VIVO FIBROSIS MODELS AND META-ANALYSES

PhD thesis

Gantsetseg Garmaa

Theoretical and Translational Medicine Division
Semmelweis University

Supervisor: Gábor Kökény, MD, PhD, Associate Professor

Official reviewers: András Balla, MD, PhD, Associate Professor

Péter Légrády, MD, PhD, Associate Professor

Head of the Complex Examination Committee:

Péter Reismann, MD, PhD, Associate Professor

Members of the Complex Examination Committee:

Tamás Kaucsár, MD, PhD

Balázs Sági, MD, PhD, Assistant Professor

Budapest
2024

TABLE OF CONTENTS

Abbreviations

ACTA2	Actin Alpha 2, Smooth Muscle
AGEs	Advanced glycation end products
AGO1-4	Four Argonaute proteins
Ang II	Angiotensin II
AKI	Acute Kidney Injury
AUC	Area under the curve
BMP-7	Bone morphogenetic protein 7
Ccl2	C-C Motif Chemokine Ligand 2
C3	Complement C3
CoR	Corepressor
Col1a1	Collagen Type I Alpha 1 Chain
COL4A1	Collagen Type IV Alpha 1 Chain
Clu	Clusterin
CKD	Chronic kidney disease
CPT-1	Carnitine palmitoyltransferase 1α
CTGF	Connective Tissue Growth Factor
CTL	Control
DAPI	4',6-diamidino-2-phenylindole
D-control	Diseased control
DMEM 2%	DMEM with 2% FBS-supplemented medium
DMEM 5%	DMEM with 5% FBS-supplemented medium
DMEM 10%	DMEM with 10% FBS-supplemented medium
DMEM/F12 10%	DMEM F12 with 10% FBS-supplemented medium
DKD	Diabetic kidney disease
DNA	Deoxyribonucleic acid
DN	Diabetic nephropathy
DM	Diabetes mellitus
DGCR	DiGeorge syndrome critical region 8
ECM	Extracellular matrix
E-cadherin	Epithelial cadherin
EnMT	Endothelial-to-mesenchymal transition
EMT	Epithelial-to-mesenchymal transition

EGR2	Early Growth Response-2
EGR1	Early Growth Response-1
FAO	Fatty acid oxidation
FN	Fibronectin
Fog2	Friend Of GATA 2
GAPDH	Glyceraldehyde-3-phosphate dehydrogenase
G2/M	Gap2 phase and Mitosis
H-control	Healthy control
HDAC	Histone deacetylase
IFN-γ	Interferon-gamma
IRI	Ischemia-reperfusion injury
IL-6	Interleukin-6
JAK1	Janus kinase
KFSM	Keratinocyte Serum-Free Growth Medium
Lgals3	Galectin-3
LAP	Latency-associated peptide
LBD	Ligand-binding domain
Lc3	Microtubule-associated proteins 1A/1B light chain 3
lncRNA	Long noncoding RNA
LN	Lupus nephritis
LRRC32	Glycoprotein-A repetitions predominant
LTBP	Latent TGF-β binding protein
miRNA	Microribonucleic acid
miRISC	miRNA-induced silencing complex
mRNA	Messenger RNA
MMP	Matrix metalloproteinase
MMT	Macrophage to myofibroblast transition
NF-κB	nuclear factor κB
Nox4	NADPH Oxidase 4
pAUC	Pooled Area under the curve
PAK1	P21 Activated Kinase 1
PI3K/AKT	Phosphoinositide 3-kinase / protein kinase B
PKC	protein kinase C

p53	Tumor protein 53
PTECs	Proximal tubular epithelial cells
PTEN	Phosphatase And Tensin Homolog
PGC-1α	Peroxisome proliferator-activated receptor gamma coactivator
PPARα	Peroxisome proliferator receptor-alpha
PPARγ	Peroxisome proliferator receptor-gamma
PPAR	Peroxisome proliferator-activated receptor
PPARGC1B	PPARG Coactivator 1 Beta
pre-miRNAs	Precursor miRNAs
PTEC medium	Hormonally defined medium
RAS	Renin-angiotensin system
Ran-GTP	RAS-related nuclear protein guanosine-5′-triphosphatase
Rho kinase	Rho-associated protein kinase
RI-III	Serine/threonine kinase receptor I-III
RISC	RNA-induced silencing complex
RNA pol II	RNA polymerase II
ROC	Receiver operating characteristic
ROS	Reactive oxygen species
RXR	Retinoid X receptors
rRNA	Ribosomal RNA
RRA	Robust Rank Aggregation
RUNX1	RUNX Family Transcription Factor 1
SD	Standard deviation
SEN	Sensitivity
Shh	Sonic Hedgehog signaling ligands
SLE	Systemic lupus erythematosus
Smad	Sma- and Mad- related protein
Snail	Snail family zinc finger
SPE	Specificity
α-SMA	Smooth muscle alpha-actin
STAT	Signal transducer and activator of transcription
Spry-1	Sprouty homolog 1
SQSTM1	Sequestosome 1

SOD1/2	Superoxide Dismutase 1/2
TECs	Tubular epithelial cells
T2DM	Type 2 diabetes mellitus
3′ UTR	3′ untranslated region
TIF	Tubulointerstitial fibrosis
TIMP	Tissue inhibitors of metalloproteinases
TNF-α	Tumor necrosis factor
TGF-β	Transforming growth factor-beta
TGFb	Transforming growth factor-beta 1 treated group
TGFBR1	TGF- β receptor type - 1
TRBP	Transactivation – responsive RNA – binding protein
UCP2	Uncoupling Protein 2
UPR	Unfolded protein response
UUO	Unilateral ureteral obstruction
Wnts	Wnt/β-catenin signaling ligands
Ybx1	Y-Boksz Binding Protein 1
VEGF-A	Vascular Endothelial Growth Factor A
VIM	Vimentin
Zeb 1/2	Zinc Finger E-Box Binding Homeobox

1. INTRODUCTION

1.1. Fibrosis in Chronic Kidney Disease

Chronic kidney disease (CKD) is a condition that results in structural (usually detected as urinary albumin excretion of ≥30 mg/day or equivalent) or functional abnormalities (defined as estimated glomerular filtration rate (eGFR) <60 mL/min/1.73 m^2) in the kidneys lasting for at least three months (1, 2). It affects 13.4% of the adult population worldwide (3) and significantly contributes to mortality rates (4, 5). The most common causes of CKD are diabetes mellitus, hypertension, glomerulonephritis, and others. Acute kidney injury (AKI) may cause CKD. The kidney repair itself after AKI is considered an adaptive process, but it can be maladaptive, especially when the acute injury is superimposed on CKD. CKD is classified based on its cause, GFR category (G1-G5), and albuminuria (A1-A3) (6). Unfortunately, CKD patients are often asymptomatic in the early stages of the disease, making early detection and therapeutic intervention challenging (7, 8). Patients with CKD are typically initially identified due to a gradual, asymptomatic rise in serum creatinine. However, at advanced stages of the disease, patients may present symptoms such as fluid overload (peripheral edema) and/or uremia (e.g., fatigue, pruritis).

Renal fibrosis is a pathological feature of CKD, identified by the presence of tubulointerstitial inflammation, fibrogenesis, glomerulosclerosis, tubular atrophy, irreversible depletion of parenchymal cells, and vascular rarefaction, leading to irreversible structural and functional loss in the kidneys. The stages involved in the development of renal fibrosis include the activation of an inflammatory response, fibroblast accumulation, excessive extracellular matrix accumulation, overexpression of pro-fibrotic factors, irreversible loss of parenchymal cells, phenotypic change and reduction in renal microvasculature. Therefore, comprehending the molecular mechanisms that play a key role in developing renal fibrosis is of utmost importance.

1.1.1. Overview of TGF-β signaling and renal fibrosis

Transforming growth factor beta (TGF-β) is a fibrogenic cytokine known to cause kidney fibrosis by activating both non-canonical (non-Smad-based) and canonical (Smad-based) signaling pathways (9). TGF-β belongs to the transforming growth factor superfamily and has three isoforms: TGF-β1, TGF-β2, and TGF-β3. These isoforms bind to the TGF-β type 2 receptor as homodimers, activating the type 1 receptor to initiate receptor signaling (9). TGF-β is initially synthesized in a precursor form, where the latency-associated peptide (LAP) is

cleaved near the N-terminus. Then, to promote attachment with latent TGF-β binding protein (LTBP), LAP binds to mature TGF-β homodimers (9). The latent TGF-β complex, consisting of LAP and LTBP, keeps TGF-β inactive. However, proteases, such as matrix metalloproteinases (MMPs), MMP2, MMP9, and plasmin, can cleave this complex, releasing active TGF-β. The LAP/TGF-β complex can also bind to glycoprotein-A repetitions predominant (known as LRRC32), a receptor expressed in regulatory T cells, regulating their functions and phenotypes (9). This binding may explain why overexpressing latent TGF-β1 can stop both fibrosis and inflammation in kidney disease models (10).

It has been hard to directly target TGF-β due to its involvement in other biological processes, such as immune activity (9). All three isoforms of TGF-β have been identified in mammals, sharing 70–82% amino acid homology (11), which made it possible to understand molecular mechanisms in animal models. Overexpression of active TGF-β1 in the liver of transgenic mice is sufficient to induce fibrotic disease in multiple organs, including the kidneys (12).

TGF-β facilitates renal fibrosis through various potential mechanisms (10) (**Fig. 1**): **1)** TGF-β1 plays a crucial role in the transdifferentiation of several cell types, such as epithelial cells, endothelial cells, pericytes, and bone marrow-derived macrophages, towards myofibroblasts. This process is known as epithelial-to-mesenchymal transition (EMT), endothelial-to-mesenchymal transition (EnMT), and macrophage-to-myofibroblast transition (MMT); **2)** TGF-β1 inhibits MMPs and promotes natural inhibitors of MMPs, such as tissue inhibitors of metalloproteinases (TIMPs) to suppress the degradation of extracellular matrix (ECM); **3)** TGF-β1 induces the synthesis of ECM by directly affecting Smad3-dependent or Smad3-independent pathways; **4)** TGF-β1 acts directly on various renal resident cells, which may result in the proliferation of mesangial cells and the elimination of tubular epithelial cells (TECs), podocytes, and endothelial cells, leading to severe renal damage and fibrosis (13, 14).

In addition, the pro-fibrotic effect of TGF-β is mediated by epigenetic mechanisms, such as non-coding RNAs (15). Targeting TGF-β is not the most effective approach as it plays various roles in other biological processes, such as immune regulation. Identifying the mechanisms behind TGF-β regulation in fibrotic diseases will advance the discovery of potential targets. These targets can serve as therapeutic solutions to either delay or prevent fibrosis progression in kidney diseases.

1.1.1. The pathogenesis of kidney tubular injury and chronic fibrosis

The functional unit of the kidney is the nephron, which filters blood in the glomerulus. The resulting ultrafiltrate passes through specialized epithelia-lined tubules that reabsorb water, electrolytes, and organic solutes such as glucose, amino acids, and vitamins. When matrix proteins accumulate in the glomerulus, it is called glomerulosclerosis. In contrast, when matrix proteins replace the tubules and/or surrounding interstitium, it is referred to as tubulointerstitial fibrosis (TIF).

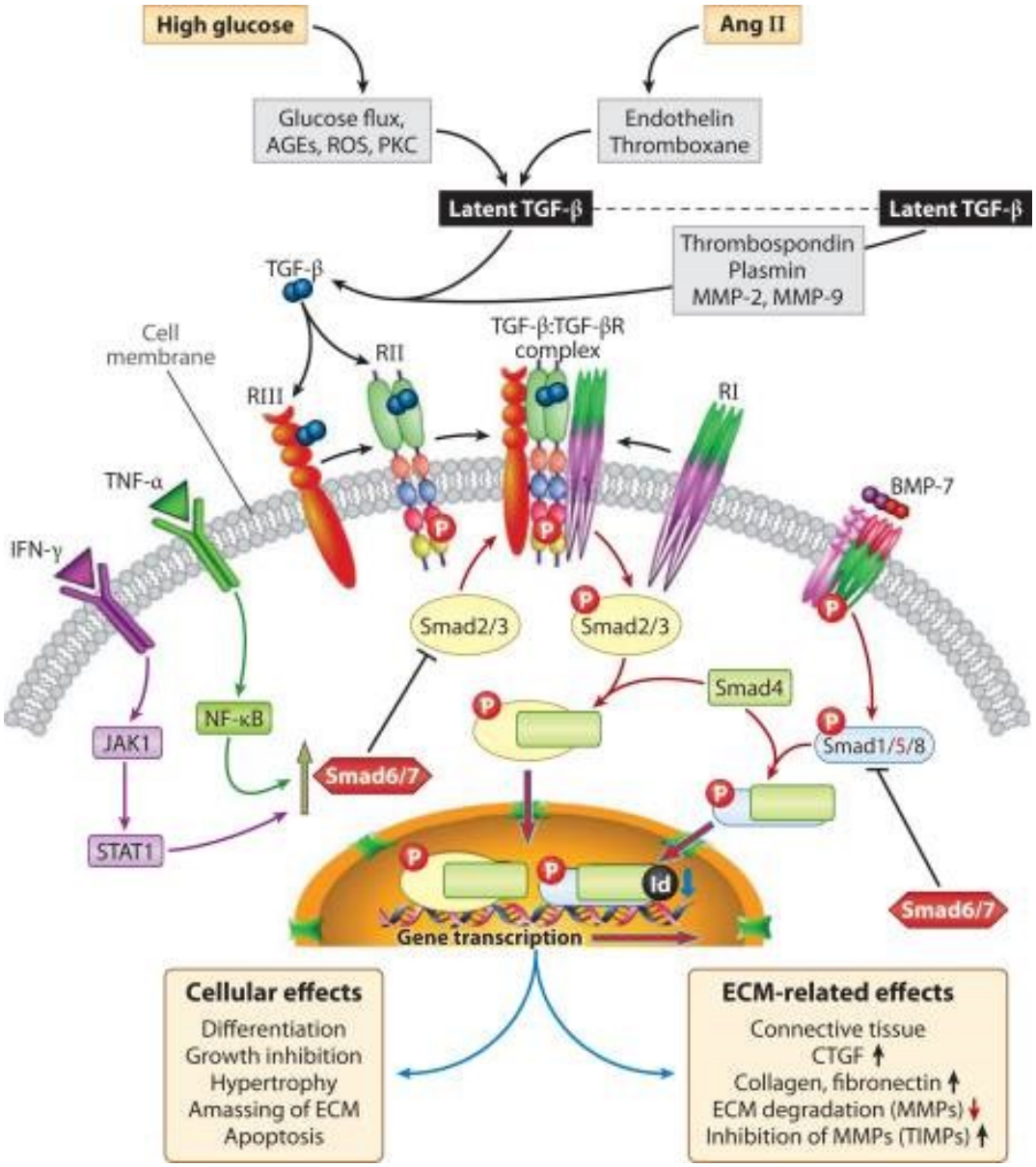

Figure 1. The overall scheme of the TGF-β signaling pathway and related molecules. *Image adapted from Y. S. Kanwar and colleagues (16).* ***Abbreviations:*** *AGEs - Advanced glycation end products; Ang II - Angiotensin II; BMP-7 - Bone morphogenetic protein 7; CTGF - Connective tissue growth factor; ECM - Extracellular matrix; IFN-γ - Interferon-gamma; JAK1 - Janus kinase; MMP - Matrix metalloproteinase; NF-κB - Nuclear factor κB; PKC - Protein*

kinase C; RI-III, Serine/threonine kinase receptor I-III; ROS - Reactive oxygen species; Smad - Sma- and Mad- related protein; STAT1 - Signal transducer and activator of transcription 1; TGF-β - Transforming growth factor β; TNF-α - Tumor necrosis factor α.

Recent research points to proximal tubule response as a key player in TIF progression. The primary site of damage during AKI is the proximal tubule, which is highly responsive to alterations in oxygen delivery. Proximal tubule cells reabsorb over 60% of filtered electrolytes and water because the rich mitochondria support a high metabolic rate and brush border, increasing the surface area for reabsorption (17).

Chronic injuries of various causes result in proximal tubular responses that can be adaptive or maladaptive, depending on the severity and chronicity of the injury. These injuries may be caused by several factors, such as high levels of glucose, free fatty acids, advanced glycation end products, TGF-β, physical stretch, detachment, and a reduction in nutrient availability caused by capillary loss (18). In general, initially, adaptive responses of the proximal tubule, including de-differentiation, cell cycle changes, autophagy, and metabolic changes, can eventually become maladaptive and promote TIF through autocrine and paracrine effects (**Fig. 2**). The proximal tubule cells that are injured tend to lose their brush border and undergo de-differentiation. This can be observed by decreased **epithelial cadherin** (E-cadherin) expression, increased **vimentin** (VIM) expression**,** and cytoskeletal changes (17). While de-differentiation can lower oxygen consumption and promote survival, it can also increase the production of pro-fibrotic factors like TGF-β that act on neighboring myofibroblasts and lead to TIF (17).

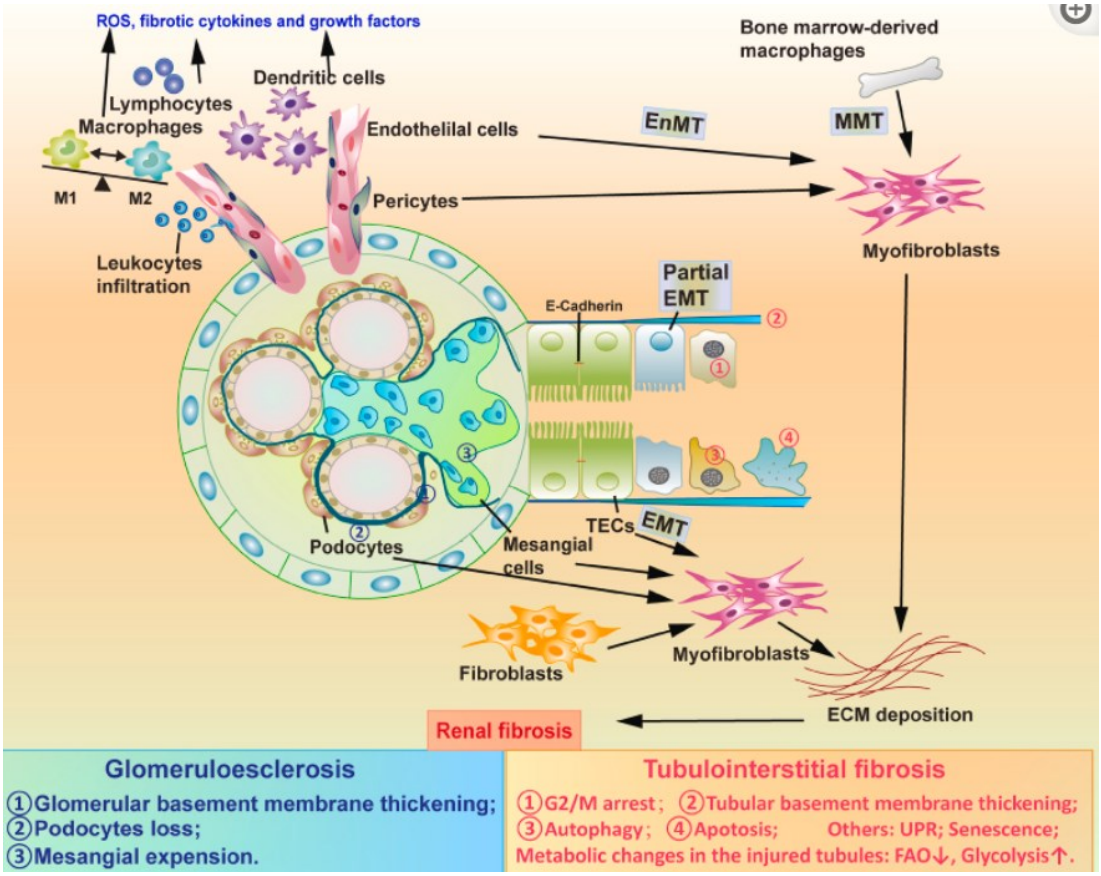

Figure 2. Major events in renal fibrosis. *Kidney injury causes inflammation. T-lymphocytes, macrophages, and dendritic cells penetrate the peritubular area and produce ROS, which damages tissue and triggers fibrotic cytokines and growth factors. The inflammatory milieu following renal injury stimulates fibroblasts, TECs, endothelial cells, podocytes, pericytes, mesangial cells, and macrophages to create a matrix similar to myofibroblasts.* ***Abbreviations:*** *ECM - Extracellular matrix; EMT - Epithelial to mesenchymal transition; EnMT - Endothelial to mesenchymal transition; FAO - Fatty acid oxidation; G2/M arrest - Gap2 phase and Mitosis arrest; MMT - Macrophage to myofibroblast transition; ROS - Reactive oxygen species; TECs - Tubular epithelial cells; UPR - Unfolded protein response. Image adapted from Z. Peng and colleagues (19).*

The kidney has a relatively low glycolytic capacity, so it relies on beta-oxidation of **free fatty acids** for energy in mitochondria, particularly in proximal tubule cells. Chronic injury affects proximal tubule cell metabolism, disrupting their reliance on **fatty acid oxidation** (FAO) for energy (18). In human and animal models of CKD, the expression of FAO-related genes is decreased due to the downregulation of peroxisome proliferator-activated receptor (PPAR)-gamma coactivator (PGC-1α), a crucial regulator of the PPAR family (20). The

reduced expression of **PPARγ** and PPARα contributes to diabetic kidney disease (DKD) (20). In addition, the PPARγ agonist pioglitazone has been found to be effective in treating diabetes-induced renal fibrosis (21). Our research group also reported that pioglitazone ameliorated renal fibrosis in TGF-β transgenic mice (22); however, the role of PPARγ in the fibrotic process is not fully answered elsewhere.

Additionally, injured proximal tubule cells also undergo the unfolded protein response (UPR) and cell senescence, both of which can have adaptive or maladaptive effects, as shown (17). UPR is a protective mechanism adopted by cells in response to the endoplasmic reticulum stress, which occurs when kidney cells are stimulated by TGF-β1 or platelet-derived growth factor (23). It inhibits protein translation, refolds unfolded proteins, and removes unfolded proteins to maintain cell survival. Sustained ER stress can activate **inflammatory pathways**, leading to the occurrence of TIF (19). It has been suggested that UPR and autophagy could work together to alleviate protein misfolding in kidney disease. Senescent renal tubular cells can protect against aging, but their abnormal accumulation can lead to renal disease (24). Senescent cells contain a senescence-associated secretory phenotype that can recruit inflammatory cells and increase **inflammatory paracrine secretion**, exacerbating TIF (19).

Moreover, various transcription factors have been linked to fibrotic diseases. The signaling pathways of **signal transducers and activators of transcription** (STAT) are also significant in renal disorders (25). STAT3, for instance, can trigger cell proliferation (26, 27) and enhance fibrosis via TGF-β_1 (28-30). It can also activate **monocyte chemoattractant protein 1, CCL2** (known as MCP-1), fostering inflammation conducive to liver tumor growth, which is also crucial in renal inflammation (31). Additionally, CCL2 is essential for renal tubulointerstitial inflammation (32). **Galectin-3** (Lgals3) is another factor in the inflammatory response, with elevated levels observed in the Unilateral ureteral obstruction (UUO) mouse model of progressive renal fibrosis. Its absence protects against renal myofibroblast accumulation, activation, and fibrosis (33). **Interleukin-6** (IL-6) can further stimulate proximal tubular epithelial cells (PTECs) to produce **collagen I**, accelerating tubulointerstitial fibrosis and increasing STAT3 phosphorylation (34). **Complement component C3** can induce tubulointerstitial inflammation and fibrosis through the TGF-β1 and Connective Tissue Growth Factor (CTGF) signaling pathway (35, 36). Moreover, the upregulation of **Runt-related transcription factor 1 (Runx1**) has been shown to increase the expression of EMT marker genes in renal tubular epithelial cells (37). In contrast, the targeted deletion of Runx1 in mouse TECs reduced renal fibrosis caused by UUO and folic acid treatment (37). Nevertheless, the

impact of pioglitazone on these transcription factors and inflammatory markers during TGF-β-induced renal fibrosis remains uncertain.

1.1.2. From Epithelial to mesenchymal transition to renal fibrosis

EMT is considered one of the initiating factors in the development of renal TIF. When renal TECs go through the EMT process, they go through the following steps (38): **first**, loss of cell polarity and tight junctions between cells and cells, downregulation of **E-cadherin** and showing **mesenchymal cell markers**, **fibronectin (FN)** and **VIM**; **second**, destruction of renal tubular basement membrane, **third**, the TECs enter the interstitium through the damaged basement membrane, **fourth**, the TECs transform into myofibroblasts expressing **alpha-smooth muscle actin (α-SMA)**. Inhibiting EMT prevents tubular cell damage, restores repair and regeneration, and reduces myofibroblast accumulation.

In fact, how tubular injury activates fibroblasts and overproduces extracellular matrix is still under debate (39). A common theory is that after injury, kidney tubular cells can undergo EMT, a phenotypic transition in which the cells lose epithelial markers and gain mesenchymal features, as mentioned earlier. However, until recently, it was thought for a while that epithelial cells, through an EMT, made an immense contribution to the interstitial myofibroblast pool; some evidence has shown that myofibroblasts are derived from resident stromal cells (40), such as kidney pericytes, perivascular fibroblasts, or mesenchymal stem cell-like cells, endothelial cells, macrophages, and "fibrocytes" that come from bone marrow contribute to the myofibroblast pool in the kidney (39). Based on extensive confirmatory studies, which included genetic cell lineage tracing (41), it has been found that the phenotypic transformation of TECs into a myofibroblast phenotype is improbable, even if it happens at all (42). These studies also discovered that TECs only undergo a **partial EMT** during kidney fibrosis. These cells show signs of being both epithelial and mesenchymal cells and remain in contact with their basement membrane.

Nevertheless, even partial EMT is sufficient to cause tubular dysfunction, which in turn causes cell cycle arrest and promotes the release of fibrogenic cytokines. EMT is categorized into three types based on the biological context (43, 44). Our project investigated type 2 EMT in human immortalized proximal tubular cells, mouse primary TECs, and TGF-β transgenic mice. In type 2 EMT, fibroblasts are generated after inflammation and injury, replacing and restoring tissue integrity. This process leads to the acceleration of wound healing, tissue regeneration, and organ fibrosis (**Fig. 2**).

1.1.3. Models used in EMT and renal fibrosis

In vitro model

Several studies show that TECs undergo phenotypic conversion *in vitro* after being incubated with fibrogenic TGF-β1 (45). Most of what we know about how EMT is controlled in the kidney comes from *in vitro* studies performed in renal TECs. TGF-β1 is the main factor that induces EMT in the kidney and other body parts (9). Currently, HK-2 is the most commonly used *in vitro* cell line to study tubular cell EMT (46), despite the absence of some transporters. However, new development methods are emerging; for example, researchers created microfluidic chips that mimic the environment of PTECs. They induced EMT in HK-2 cells using different doses of TGF-β (47).

In vivo model

The animal models of renal fibrosis closely mimic the three primary causes of AKI in humans: ischemia, toxin exposure, and ureteral obstruction (48). The most often used models for acute kidney injury and chronic kidney fibrosis in murine animals include severe bilateral ischemia-reperfusion injury (IRI), unilateral IRI, aristolochic acid nephropathy for acute, and UUO, 5/6 subtotal nephrectomy, type 1 and 2 DKD models, and genetic engineering (49, 50). In this project, we used a widely recognized TGF-β transgenic mouse model (12, 51).

Genetically modified mice offer valuable opportunities to study protein effects on phenotype and therapy responsiveness (52). Sanderson and his colleagues created one of the primary **TGF-β transgenic models** (12). As a result, these mice showed elevated levels of mature TGF-β1 in their plasma and liver, causing multiple tissue lesions, hepatic fibrosis, severe glomerulonephritis, and renal failure (12). The pathological changes and progress of fibrosis in TGF-β transgenic mice kidneys were extensively studied in previous publications from our research group (51). Diabetic kidney fibrosis is a major cause of fibrotic kidney disease nowadays. Recent studies have identified a mouse model called Akita$^{+/-}$ Ren$^{+/-}$ mouse (53). This model exhibits several characteristics of human diabetic nephropathy, including hyperglycemia, hypertension, albuminuria, reduced glomerular filtration rate, glomerulosclerosis, and interstitial fibrosis (53).

1.2. Discovery of microRNAs and their biogenesis

Lee and colleagues made the initial discovery of microribonucleic acids (miRNA) in 1993 (54). Subsequently, there has been a significant surge in fascination with miRNAs, supported by mounting evidence indicating their role in controlling most transcriptional or translational pathways in all organs. Since the discovery of the first miRNA, more than 2654 mature

miRNAs in humans, around 2000 in murine, have been identified and registered in the miRBase database (55). It is widely accepted that miRNAs regulate at least 60% of human protein-coding genes (56). Their primary function is post-transcriptional gene expression regulation (57) (**Fig. 3**), and miRNAs have been associated with various cellular processes and diseases. Therefore, miRNAs are of significance as possible targets for therapy (58) and as biomarkers for diseases [5-7].

MiRNAs are transcribed either from individual genes or genes clustered together, such as (miR-194-192 cluster) (59). However, it is also possible for some miRNAs to be encoded from distinct genomic loci (60). Genes that encode miRNAs are found in non-coding sequences or introns of either protein-coding genes (known as miR-trons) or non-coding RNA (61). Typically, miRNAs located within introns are expressed in a coordinated manner with their host gene, and often, both the miRNAs and the host gene impact the same signaling pathway (62, 63).

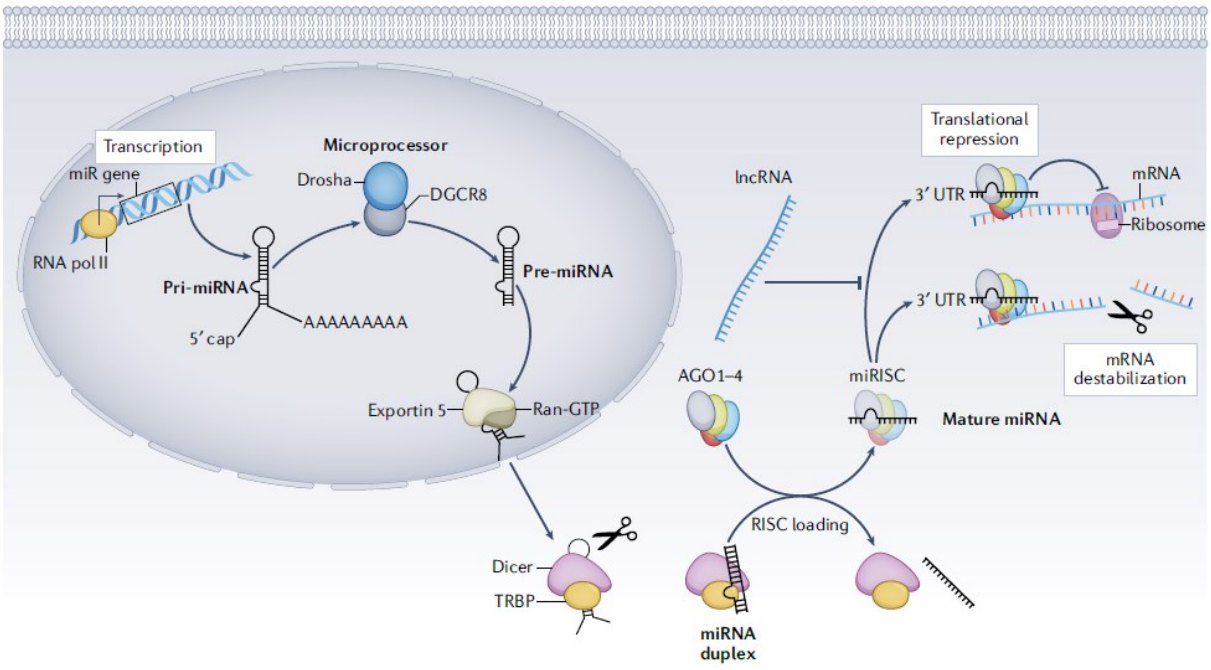

Figure 3. MiRNA biogenesis and action. *In the nucleus, most primary miRNA transcripts (pri-miRNAs) are transcribed by RNA polymerase II (RNA pol II)* (64)*. The microprocessor complex Drosha-DGCR8 cleaves them to generate precursor miRNAs (pre-miRNAs), which are then exported from the nucleus by exportin 5* (65)*. In the cytoplasm, Dicer cleaves the pre-miRNAs to form a miRNA duplex. The duplex interacts with Four Argonaute proteins (AGO1-4) to form the RNA-induced silencing complex (RISC) (66). The miRNA-loaded RISC can further process the miRNA and upload it to its target mRNA. The mRNA–miRNA complex leads to either mRNA destabilization or translational repression (66). Long non-coding RNAs (lncRNAs) can also*

target mature miRNAs, acting as miRNA sponges (66). ***Abbreviations:*** *AGO1-4 - Four Argonaute proteins; DGCR - DiGeorge syndrome critical region 8; miRISC - miRNA- induced silencing complex; mRNA - messenger RNA; RISC - RNA-induced silencing complex; RNA pol II - RNA polymerase II; Ran-GTP - Renin-angiotensin system - related nuclear protein guanosine-5'-triphosphatase; TRBP – Transactivation - responsive RNA - binding protein; 3' UTR - 3' untranslated region. Image adapted from N. Mahtal and colleagues (66).*

In addition, a faulty base-pairing of miRNAs to the 3'UTR of their gene targets (67) enables any specific miRNA to target multiple genes simultaneously. Many miRNA targets enable a single miRNA to selectively target multiple genes in a signal transduction cascade, effectively abolishing their function (68). Moreover, recent findings suggest that miRNAs regulate numerous proteins involved in interconnected signaling pathways (69, 70).

1.2.1. The role of microRNA in kidney diseases

MiRNAs regulate renal function - from blood pressure to fluid and electrolyte balance (59). In mice, inactivation of Dicer (ribonuclease, responsible for processing pre-miRNAs into mature miRNAs) in renin-expressing juxtaglomerular cells leads to loss of these cells, reduced plasma renin, hypotension, and kidney fibrosis (71, 72). Recently, miRNAs have emerged as new diagnostic biomarkers (73) and therapeutic targets (74) with robust stability in urine (75), plasma (76), and tissue (73). MiRNA has autocrine, endocrine, and paracrine effects. It mediates cell-to-cell interaction and can be produced by cells in the form of exosomes or microvesicles. MiRNA can also be bound to plasma proteins and then transported to neighboring and distant cells (66). Different groups of miRNAs are dysregulated in various kidney conditions such as AKI, CKD, DN, and allograft rejection (reviewed in (66)). These differences may reflect variations in the underlying pathophysiology of these conditions. Many novel, high-throughput "omics" technologies have recently made it easier to identify hundreds of potential biomarkers in renal diseases (77). The initial studies were conducted in 2004 and 2005 to identify miRNAs specific to or enriched in the kidney (78, 79). The significance of miRNAs in kidney function was revealed between 2007 and 2008 (80, 81), leading to the implementation of the Human MicroRNA Disease Database (82) and miRNA tissue atlas (83), a subsequent increase in research evidence. This miRNA tissue atlas comprises data obtained by next-generation sequencing and microarray techniques, specifically focusing on the expression of miRNAs in human kidneys. Such databases provide information on miRNAs

linked to AKI, CKD, and healthy donors, all sourced from peer-reviewed studies (84), providing a deeper understanding of miRNA dysregulation in kidney diseases.

The therapeutic potential of miRNAs in kidney disease has been extensively studied in murine models of CKD (reviewed in (85, 86)), but human trials have not yet been implemented. As Liu and colleagues summarized, studies using murine models have shown that anti-miRNA-21 treatment can prevent the development of renal fibrosis (87). This was demonstrated in experimental models of Alport's syndrome (88) and the UUO model (89). In the UUO model, the expression of pro-fibrotic proteins and infiltration of inflammatory macrophages were reduced, ultimately leading to attenuated fibrosis (89). Antagonism of miRNAs was also beneficial in treating streptozotocin-induced DN with miRNA-124 antisense (87, 90). Similarly, miRNA mimics such as miRNA-23b agomir have been found to have beneficial effects on renal fibrosis caused by DN (87, 91).

In clinical cohort studies, several miRNAs are summarized as potential CKD and DN diagnostic markers in human serum and urine (92, 93). Research conducted by J. Li and colleagues found that miR-133, miR-30a, and miR-126 are promising markers for diagnosing CKD with high levels of accuracy, showing sensitivity or specificity above 90% (92).

Due to their nature of having multiple target genes and being involved in various molecular pathways, the functions of miRNAs are not yet fully understood. Therefore, it is crucial to comprehend the miRNA expression patterns in various biological sample types during specific disease stages and their functional role in the development and progression of kidney diseases. This knowledge can be used for diagnostic and therapeutic purposes in the future. High-throughput sequencing of small RNAs has increased the number of registered miRNAs. However, validation of miRNAs in healthy and diseased conditions is still in progress. Meanwhile, several cohort studies have been conducted in CKD patients to ensure miRNAs as a novel diagnostic marker for kidney diseases. However, these studies yielded inconclusive results due to the heterogeneity of patient populations, disease etiology, and tissue origin. Thus, it is essential to systematically review and summarize the existing knowledge of miRNA expression patterns in kidney patients grouped by etiology, tissue of origin, and disease stage. In addition, early-stage studies in miRNAs were primarily done in murine kidney disease models. Therefore, comparing miRNA profiling results from human studies and murine CKD models provides an opportunity to identify differences in miRNA expression between humans and murine animals.

1.2.2. MicroRNAs and TGF-β pathway, fibromiRs

MiRNAs play a dual role in regulating the fibrosis process: they act as downstream effectors of TGF-β-dependent regulation and upstream regulators of TGF-β signaling (59). Animal and human studies confirm that TGF-β1 is a dominant pathogenic factor that drives the progressive form of renal fibrosis (9). Most of the TGF-β family members and the TGF-β-dependent pathway serve as targets for miRNAs, indicating the presence of an autoregulatory feedback loop between TGF-β and miRNAs (**Fig. 4**) (94). It is essential to understand the relationship between TGF-β and miRNA since TGF-β1 is one of the important players in renal fibrosis. In renal fibrosis, several miRNAs, including miR-21 (59) and miR-200 (95), have been investigated and validated for their role in pro- and anti-fibrotic functions (**Fig. 4**).

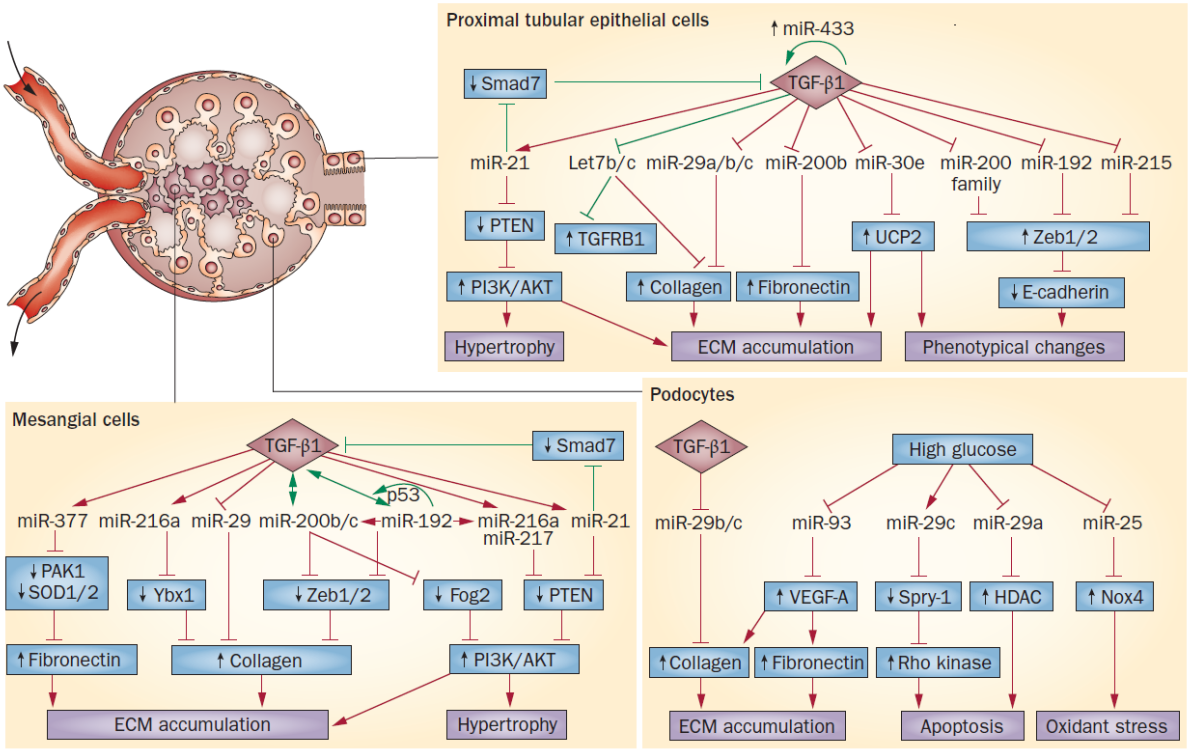

Figure 4. The TGF-β1 regulation in kidney cells. *The diagram illustrates the miRNA-regulatory networks in PTECs, mesangial cells activated by TGF-β1, and the miRNA-regulatory networks in podocytes activated by both TGF-β1 and high glucose. The black arrows indicate upregulated and downregulated expressions, respectively. The green line signifies the miRNA-dependent signaling loops through TGF-β1, which amplifies its signal.* ***Abbreviations:*** *Fog2 - Friend Of GATA 2; HDAC - Histone deacetylase; miRNA - microRNA; Rho kinase - Rho-associated protein kinase; SOD1/2 - Superoxide Dismutase 1/2; Spry-1 - Sprouty homolog 1; TGFBR1 - TGF- β receptor type - 1; Nox4 - NADPH Oxidase 4; PAK1 - P21 Activated Kinase 1; PI3K/AKT - phosphoinositide 3-kinase / protein kinase B; PTEN - Phosphatase And*

Tensin Homolog; p53 - Tumor protein p53; UCP2 - Uncoupling Protein 2; VEGF-A - Vascular Endothelial Growth Factor A; Ybx1 - Y-Box Binding Protein 1; Zeb1/2 - Zinc Finger E-Box Binding Homeobox 1/2. Image adapted from P. Trionfini and colleagues (59).

Additionally, TGF-β induces pro-fibrotic miR-130 in human renal PTECs (96) and miR-199a in the kidneys of hypertensive rats (97). Elevated renal miR-199a-3p can trigger STAT3 activation (98), whereas increased miR-199a-5p was reported in murine and human CKD (99). In DN, several miRNAs, such as miR-133b and miR-199b, which protect against fibrosis, are downregulated (100). The kidney cortex of diabetic Otsuka Long Evans Tokushima Fatty (OLETF) rats showed elevated levels of miR-133b and miR-199b (100). Inhibition of these miRNAs reduced the severity of DN in these rats. In HK-2 cells, upregulation of Sirtuin 1 and alleviation of TGF-β-induced EMT and pro-fibrotic signaling were observed upon the suppression of miR-133b and miR-199b (100).

1.3. PPAR family and molecular mechanism

The PPAR family is one of the four nuclear receptor groups called adopted orphan receptors, which have since been associated with at least one ligand. PPAR family proteins have structural similarities, as they all contain a C-terminus ligand-binding domain (LBD). This domain is responsive to ligand stimulation and regulates the formation of heterodimers with retinoid X receptors (RXR) following activation (101). Unlike others in the nuclear receptor superfamily, PPAR is localized in the nucleus, forming an obligatory complex with RXR as a heterodimer that binds to its cognate Deoxyribonucleic acid (DNA) binding site (102, 103). Upon binding to the ligand, the PPAR/RXR complex undergoes conformational changes in associated transcriptional cofactors, leading to activation of the transcriptional complex. Without a ligand, the heterodimer complex interacts with corepressor (CoR) and histone deacetylases (HDAC) to form a CoR complex, which promotes gene repression. CoR and HDAC keep transcription repressed (102, 103). CoRs are dismissed upon ligand interaction, and transcriptional coactivators are recruited, promoting transactivation (102, 103).

PPAR consists of 3 isoforms (α, βδ, and γ), and each isoform has unique characteristics, such as ligand selectivity, tissue-specific expression, and target genes. PPARα regulates arterial blood pressure and modulates endothelial function as an antioxidant and anti-inflammatory gene expression regulator (104), while PPARβδ is linked to muscle development and oxidative capability (105). PPARγ is ubiquitously expressed and essential in adipogenesis (106). Fatty acids and eicosanoids have the potential to function as PPARγ ligands; however, the specific

ligand(s) that are most significant in physiological contexts are not yet definitively known (107).

The PPARγ gene is located on chromosome 3 (3p25.2) in humans and consists of 9 exons expanding over 100 kb. This gene generates four different variants of PPARγ (γ1, γ2, γ3, and γ4) (108). These isoforms have differential expression across many organs. In both humans and mice, two comparable isoforms of PPARγ have been identified (109). PPARγ1 is present in high quantities in white and brown adipose tissue and, to a lesser extent, in almost all tissues and immune cells, including macrophages. On the other hand, PPARγ2 is primarily found in white and brown adipose tissue.

Activation of PPARγ can be modified by different coactivating or corepressing proteins based on the conformational change of the LBD, which can be triggered by cellular signaling events or small molecules. Several post-translational modifications likely regulate these protein complexes, some of which are still unknown. These post-translational modifications include phosphorylation (110), acetylation (111), glycosylation (112), SUMOylation (113), ubiquitination (114) of proteins, and miRNAs (103). Our project proposed that miRNAs may regulate PPARγ and its ligands. Therefore, we studied miRNA expression in PPARγ agonist-treated primary TECs of mice.

1.3.1. PPARγ in kidney and tubular cell pathophysiology

The PPARγ protein is found in different kidney parts, including interstitial cells, podocytes, tubule segments, juxtaglomerular apparatus, mesangial cells, and renal microvascular endothelial cells (115). It plays a crucial role in maintaining normal kidney function and homeostasis. PPARγ controls the metabolism of lipids, glucose, and minerals in the kidney and regulates systemic blood pressure (116). It has been discovered that the expression of PPARγ isoforms is associated with the circadian rhythm (116), and multiple studies suggest that disrupted circadian rhythms and kidney disease can exacerbate each other, creating a vicious cycle (117). These reports suggest that the function of PPARγ may be more intricate than previously thought and may involve an improvement of both insulin sensitivity and insulin secretion. According to recent research, PPARγ activation can facilitate renin production and thiazolidinediones and PPARγ activators can reduce the hypertensive effects of angiotensin (118). Additionally, researchers reported that aldosterone and mineralocorticoid receptors regulate the expression of PPARγ (119, 120). Aldosterone and angiotensin receptor blockers boost PPARγ activity in adipose tissue, which could explain the protective effect of renin-angiotensin system (RAS) inhibition against developing type 2 diabetes (121).

In addition to the interactions mentioned above, TGF-β is a multifunctional cytokine that induces inflammation, fibrosis, and cell differentiation, while PPARγ activation mitigates these adverse effects in many models (115) , including CKD. Our research group found that PPARγ and TGF-β1 have a crosstalk in TGF-β transgenic mice. We also demonstrated that oral administration of pioglitazone can effectively minimize glomerulosclerosis, tubular injury, and interstitial fibrosis by inhibiting the expression of Early Growth Response-1 (EGR1) and TIMP-1 *in vivo* (22). Other researchers support these results, as rosiglitazone, a PPARγ agonist, attenuated the induction of EMT and interstitial collagen production in UUO mice (122). Moreover, PPARγ activation inhibits EMT and fibrogenesis, preserving the healthy phenotype of PTECs. PPARγ activation increases renal Klotho expression, reduces oxidative stress, and ameliorates age-related nephrosclerosis in apolipoprotein E-null mice (123).

As an extension of the previous project, this thesis explores the anti-fibrotic impact of PPARγ agonist in TGF-β-induced kidney fibrosis models while examining the regulation of pro-fibrotic miRNAs and autophagy markers.

1.4. Early Growth Response Factors in renal fibrosis

EGR1 is a ubiquitous transcription factor that is intricately linked to the processes of inflammation and profibrosis. Early Growth Response genes are part of the ligand-inducible early response genes family and a zinc-finger DNA-binding protein. EGR1 is the positive regulator of the pro-fibrotic process and builds a positive feedback loop with TGF-β (124). Among the several pro-fibrotic transcription factors, EGR1 contributes to fibrosis by directly stimulating collagen synthesis (125) and myofibroblast differentiation (126).

EGR1 expression is low or undetectable in the resting state of cells. However, EGR1 expression is induced by various stimuli such as cytokines, hormones, growth factors, endotoxin, shear stress, mechanical damage, and hypoxia, usually in a rapid and transient manner in different human cell types (127, 128).

EGR1 can upregulate or downregulate the synthesis of various pro-inflammatory and anti-inflammatory protein mediators that bind to complementary motifs on the DNA of the target gene. These mediators play a crucial role in cellular death mechanisms. It is well known that EGR1 is an essential component of the cardiac cell death signaling pathways related to apoptosis, autophagy, mPOS, and ferroptosis (127). Multiple studies have confirmed that EGR1 plays a central role in systemic sclerosis and organ fibrosis, particularly in the liver (129) and lungs (128) (124).

EGR1 is present during kidney development but not in normal adult kidneys (130) is induced in tubular endothelial cells during acute and chronic renal injury (131). Only a few studies have focused on the role of EGR1 in renal fibrosis (132, 133). EGR1 contributes to renal fibrosis through several pathways, for example, promoting mesangial cell proliferation (134), activating the TGF-β signaling pathway (128, 132), and inducing renal TEC transdifferentiation into mesenchymal cells (135). Moreover, the effect of Early Growth Response genes on the fibrotic process in TIF has not been well understood. Our research group has recently investigated the role of Egr1 and Early Growth Response 2 (Egr2) as key players in renal fibrosis (22, 51, 136) and studied their regulation in this thesis on HK-2, primary tubular cells, and TGF-β transgenic mice.

1.5. Autophagy dysfunction in renal fibrosis

Autophagy is essential to kidney homeostasis, function, and structure (137). It is suppressed in aged kidneys, which can accelerate age-related kidney diseases. In AKI, autophagy is induced as a protective mechanism crucial for tubular repair in the recovery phase (138). However, persistent activation of autophagy can promote interstitial fibrosis and contribute to CKD. Studies have demonstrated that TGF-β1 has a dual effect on the regulation of autophagy. Recent research has suggested that TGF-β1 may induce macro-autophagy, resulting in cytoprotective effects (139, 140). Atg5, Atg7, LC3, and Beclin 1 genes were activated by TGF-β1 in renal TECs, leading to autophagosome formation and LC3-II conversion.

LC3-I is the type of LC3 that is found in the cytoplasm, whereas LC3-II is the form that binds to the membranes of autophagosomes. Therefore, a higher LC3-II/I ratio signifies either stimulated autophagy or hindered degradation, resulting in autophagosome buildup with un-degraded contents (141). SQSTM1 (known as p62) is a well-known adaptor protein degraded by autophagy. Therefore, reducing its protein levels indicates more autophagic flux (141).

Autophagy has also been found to regulate the IL-1 family of cytokines, which includes TGF-β1. Autophagy plays a crucial role in preventing the development of interstitial fibrosis in kidney injury by limiting the secretion of TGF-β1. It does so by negatively regulating the production of mature TGF-β1 proteins in renal PTECs (142). Further investigation is needed to understand autophagy's true therapeutic potential and molecular mechanism during kidney fibrosis.

2. OBJECTIVES

2.1. Objective 1 (EMT in HK-2 cells)

The HK-2 cells are often used to study EMT *in vitro*. However, different studies have used different types of cell culture media, which might cause inconsistent experimental results. To address this issue, we conducted a comparative study investigating how different culture media affect the HK-2 cells when exposed to TGF-β1.

Our specific aims were the following:

- Comparison of the morphology of HK-2 cells in different culture media by light microscopy.
- Determination of cell culture medium formulation's effect on the TGF-β1-induced EMT model of HK-2 cells.
- Determining the differential expression of pro- and anti-fibrotic genes and proteins by qRT-PCR, immunoblotting, and localization of pro-fibrotic transcription factors in cells by immunocytochemistry in various cell culture medium formulations.

2.2. Objective 2 (PPARγ agonist in kidney fibrosis)

PPARγ plays a crucial role in maintaining normal kidney function and homeostasis. Recently, our research group studied the anti-fibrotic effect of PPARγ agonist (pioglitazone) in TGF-β transgenic mice by examining pro-fibrotic markers (22). However, we have yet to address the impact of PPARγ agonists on TECs, renal autophagy, and miRNA dysregulation during fibrosis. By highlighting miRNA dysregulation, we aim to elucidate the effect of PPARγ on pro- and anti-fibrotic markers and autophagy in TGF-β-induced kidney tubular cells and tissue from TGF-β transgenic mice.

Our specific aims were the following:

- Administration of pioglitazone to TGF-β transgenic mice to assess pro-fibrotic, anti-fibrotic, and autophagy markers in the kidney using qRT-PCR for messenger RNA (mRNA) and miRNA expression and immunoblotting for protein expression and histology for tissue structure.
- Treatment of primary TECs with pioglitazone, followed by investigating the pro- and anti-fibrotic and autophagy markers using qRT-PCR for mRNA and miRNA expression and immunoblotting for protein expression.

- Detection of the PPARγ's effects on VIM, EGR2, and SQSTM1 protein expression *in vitro* and *in vivo* using immunocytochemistry. Visualize the expression using fluorescent microscopy.
-

2.3. Objective 3 (miRNAs in kidney diseases, meta-analyses)

MiRNAs have emerged as potential markers and therapeutic agents for kidney diseases. However, with over 2000 miRNAs in humans and mice, it is unclear which ones play a key role in kidney diseases. We aimed to identify the most dysregulated miRNAs in human CKD and murine models of CKD, along with their molecular pathways, and to assess the diagnostic accuracy of miRNAs in human CKD from peer-reviewed articles using two different meta-analysis approaches.

Our specific aims were the following:

First systematic review and meta-analysis:

- Determination of the most dysregulated miRNAs in different kidney diseases, biological samples, and stages of CKD patients compared to healthy populations.
- Identification of the most dysregulated miRNAs in the most used murine experimental CKD models and possible overlap between human disease and murine models.
- Gene set enrichment analysis of common target genes, Gene Ontology terms, molecular pathways, and miRNA-target gene interactions of the most dysregulated miRNAs in CKD.

Second systematic review and meta-analysis:

- Assessment of single and panel miRNAs' (combination of several miRNAs) diagnostic accuracy for various kidney diseases and sample types by Receiver operating characteristic (ROC) curve and Area under the curve (AUC).
- Investigation of the diagnostic performance of miRNAs by comparing overt kidney disease groups with healthy individuals and diseased control groups without nephropathy.

3. MATERIALS AND METHODS

The methods section 3.1 has been developed from two thesis-related publications with modifications (143, 144).

3.1. *In vitro* and *in vivo* experiments

3.1.1. HK-2 cell culture

HK-2 cells were purchased from the American Type Cell Collection (ATCC, #CRL-2190). Cells were cultured in T75 flasks in six different growth media (**Fig. 5**) at 37 °C in a humid atmosphere of 95% air and 5% CO2. The medium was refreshed every 48 to 72 hours until the desired confluency. After 3 to 5 days, when cells reached 70–80% confluence, HK-2 cells were trypsinized and passaged at a 1:3 ratio or seeded on 6 or 24-well plates at the desired density for immediate experimental use. HK-2 cells were seeded ~10^5 cells or 3×10^4 per well in 6- or 24-well plates, respectively, cultured in different growth media overnight, and then serum starved for 24 hours. Recombinant human TGF-β1 (10 ng/ml, Sigma-Aldrich) was added to the appropriate wells for 24 hours. Microphotographs of treated and untreated cells in the culture plate wells were taken with a Nikon Coolpix 4500 digital camera attached to a Nikon Eclipse TS100 microscope at 200 × magnification. Cells were then harvested in Trizol (Invitrogen, Thermo, USA) for total RNA isolation according to the manufacturer's protocol or in ice-cold RIPA buffer for protein extraction, as mentioned below.

Medium abbreviations	Formulation
DMEM 2%	DMEM with 1000 mg/L glucose, L-glutamine, sodium bicarbonate (Invitrogen, Carlsbad, CA), and 2% fetal bovine serum (Invitrogen), 50 U/mL penicillin and 50 µg/mL streptomycin (Invitrogen)
DMEM 5%	DMEM with 1000 mg/L glucose, L-glutamine, sodium bicarbonate (Invitrogen, Carlsbad, CA), and 5% fetal bovine serum (Invitrogen), 50 U/mL penicillin and 50 µg/mL streptomycin (Invitrogen)
DMEM 10%	DMEM with 1000 mg/L glucose, L-glutamine, sodium bicarbonate (Invitrogen, Carlsbad, CA), and 10% fetal bovine serum (Invitrogen), 50 U/mL penicillin and 50 µg/mL streptomycin (Invitrogen)
DMEM/F12 10%	DMEM/F12 medium contains a 1:1 mixture of DMEM medium and Ham's F12 medium, With L-glutamine, 15 mM HEPES, sodium bicarbonate (Invitrogen, Carlsbad, CA), and 10% fetal bovine serum (Invitrogen), 50 U/mL penicillin and 50 µg/mL streptomycin (Invitrogen)
PTEC (hormonally defined)	DMEM/F12 (Invitrogen, Carlsbad, CA) supplemented with 2% fetal bovine serum (Invitrogen), 5 µg/mL insulin, 5 µg/mL transferrin, 5 ng/mL selenium, 40 ng/mL hydrocortisone, 5 pg/mL triiodo-1-thyronine, 50 U/mL penicillin and 50 µg/mL streptomycin (Invitrogen)
KSFM	Keratinocyte Serum-Free Growth Medium (Invitrogen, Carlsbad, CA) supplemented with 0.05 mg/ml Bovine Pituitary Extract, 5 ng/ml Human Recombinant epidermal growth factor (Invitrogen, Carlsbad, CA), 50 U/mL penicillin and 50 µg/mL streptomycin (Invitrogen)

Figure 5. Cell culture media and their formulation *(143).*

3.1.2. Primary Tubular Epithelial Cell Isolation and Cell Culture

A 4-week-old C57B1/6J male mouse was euthanized, and both kidneys were quickly removed after median laparotomy under aseptic conditions. The kidneys were placed on a 10 cm cell culture dish containing an ice-cold sterile Hanks' Balanced Salt Solution buffer under a laminar flow box. The kidneys were de-capsulated and cut into several slices, and the medulla was excised. Chopped small cortical fragments were digested in Dulbecco's Modified Eagle Medium: Nutrient Mixture /F12 (DMEM/F12) containing 1 mg/mL collagenase type-II for 20 minutes at 37 °C with vortexing every 10 minutes. The digested cortex was washed through a series of brass sieves with 100-60-40 µm mesh diameters. Tubules were collected from the 40 µm nylon mesh. The collected cells were resuspended in a selective PTEC medium (detailed in **Fig. 5**). The isolated mouse primary TECs were cultured in tissue culture flasks coated with 1% gelatin in a humidified atmosphere with 5% CO2 at 37 °C for 14 days. The purity of TEC cultures was then validated by immunoblot and immunocytochemistry. Only the TECs culture expressing epithelial marker E-cadherin without mesenchymal markers VIM and α-SMA was passed into a new flask and used for further experiments.

3.1.3. Primary Tubular Epithelial Cell Culture treated with PPARγ agonist

Primary TECs with passage numbers 6 to 8 were seeded at a density of 1×10^5 cells or 3×10^4 cells per well on 1% gelatin-coated 6-well and 24-well plates, respectively. On the following day, the medium was changed to serum-free DMEM/F12 medium, and the cells were subjected to pre-treatment with 5 µM pioglitazone in 0.1% dimethyl sulfoxide or 0.1% dimethyl sulfoxide alone (controls). After 24 hours of serum starvation, recombinant human TGF-β1 (10 ng/mL, Sigma-Aldrich) was added to the respective wells and incubated for 24 hours (n = 3–4/group).

3.1.4. Animal experiments

Ten-week-old male TGF-β1 transgenic mice on C57Bl6/J genetic background (B6-Alb/TGF-β1(Cys^{223,225}Ser), obtained initially from Snorri S. Thorgeirsson at the National Cancer Institute, USA and backcrossed in our laboratory (12, 51) and wild-type C57Bl6/J males of the same age (controls, CTL, n = 6) were kept in a standard specific pathogen-free environment at the Semmelweis University NET GMO Animal Facility (Budapest, Hungary). Transgenic mice have higher plasma TGF-β1 levels due to hepatic production of full-length active TGF-β1, which causes, among other effects, progressive kidney fibrosis (12). Our

research group's previous publication describes the plasma TGF-β1 levels from blood samples and proteinuria (urinary protein to creatinine ratio) (51). All mice were kept on a 10/14-hour light/dark cycle and had unlimited access to rodent feed and drinking water. Isoflurane anesthesia was used for blood sampling and euthanasia. The Animal Ethics Committee of Semmelweis University approved all animal procedures in advance (PE/EA/948-4/2018). Transgenic mice were separated into two groups: one received standard rodent chow (TGF, n = 6), and the other received pioglitazone-containing rodent chow (TGF + Pio, n = 6) for chronic treatment (20 mg/kg/day, adjusted to average food consumption). The mice were euthanized with 5% isoflurane after 6 weeks of the treatment period and perfused with 4 °C physiological saline using an intracardiac cannula until blood was washed out of the kidneys. The kidneys were collected and cut to be frozen in liquid nitrogen or fixed in a 4% buffered formalin solution.

3.1.5. RNA isolation and Quantitative RT-PCR Analysis

Total RNA from Trizol (Invitrogen, Thermo, Waltham, MA, USA) samples were extracted according to the manufacturer's protocol. RNA concentration and purity were verified on a Nanodrop 2000 (Thermo, USA) and then reverse transcribed using the High-Capacity cDNA kit (Applied Biosystems/Life Technologies, Carlsbad, CA, USA) for mRNA and miRCURY LNA RT Kit (Qiagen, USA) for miRNA. Each PCR reaction with specific primers was performed on a Bio-Rad CFX96 thermal cycler (Bio-Rad Hungary, Budapest, Hungary) in duplicates using the SensiFast SYBR Green PCR Master Mix (Bioline, Germany) for mRNA and miRCURY LNA SYBR Green PCR Kit (Qiagen, USA) for miRNA. The specificity and effectivity of PCR reactions were verified by melting curve analysis. Target gene expression was normalized to glyceraldehyde-3-phosphate dehydrogenase (GAPDH) mRNA (for HK-2 cells) or 18S ribosomal RNA (rRNA) (for mouse samples) and U6 snRNA for miRNA expression using the $2^{-\Delta\Delta Ct}$ formula and expressed as fold expression relative to a control sample. Each gene expression is presented as mean and standard deviation (mean ± SD). Appropriate positive and negative controls were included in each PCR experiment to verify the results and avoid false positive signals due to contamination. Only miRNA primers are listed below. Human and mouse primers are detailed in corresponding publications (143, 144).

miRNA primer sequences (5' – 3') used for quantitative PCR:

mmu-miR-199a-3p *5'ACAGUAGUCUGCACAUUGGUUA*

mmu-miR-199a-5p *5'CCCAGUGUUCAGACUACCUGUUC*

mmu-miR-21-5p *5'UAGCUUAUCAGACUGAUGUUGA*

mmu-miR-130a-5p *5'GCUCUUUUCACAUUGUGCUACU*

3.1.6. Immunoblot

HK-2 and primary TECs were lysed in ice-cold RIPA buffer containing a "Complete Mini" protease inhibitor cocktail (Roche, Mannheim, Germany). Protein concentration was determined using BCA assay (Thermo Scientific, Waltham, MA, USA). Equal amounts (20 µg) of protein were loaded in 2 x Laemmli buffer on 12% or 15% SDS-polyacrylamide gels. A 3 mm^3 kidney cortex was homogenized for mice kidney tissue in ice-cold RIPA lysis buffer. Equal protein amounts (60 µg cortex) were loaded with Laemmli buffer (Bio-Rad) on 12% and 15% SDS-polyacrylamide gels. Separated samples were transferred to nitrocellulose membranes by wet method, blocked with 5% skim milk, and incubated with primary antibodies overnight at 4 °C. The primary antibodies used in the study have been listed in the corresponding publications (143, 144). After serial washing in Tris-buffered saline with 0.1% Tween® 20 Detergent, membranes were incubated with the appropriate HRP-conjugated secondary antibodies for one hour at room temperature. Blots were visualized with an enhanced chemiluminescence detection kit (Thermo). Tubulin or GAPDH were used as loading controls. Image Studio Lite 5.2 (Li-Cor Biosciences, Lincoln, NE, USA) software was used to examine and evaluate data.

3.1.7. Immunocytochemistry

HK-2 cells (10,000/well) were seeded on glass coverslips in a 24-well plate. After 24 h treatment with 10 ng/ml TGF-β1 in serum-free medium, cells were washed and fixed in methanol (−20 °C) for 15 min on ice, then permeabilized with 0.25% Triton-X for 10 min. Non-specific secondary antibody binding was blocked using 2% donkey serum for 30 min. Cells were incubated overnight at 4 °C with primary antibodies or PBS for negative controls (excluding primary antibodies). Next, the cells were incubated with donkey anti-rabbit IgG-A594 (1:200) (Jackson Immunoresearch) at room temperature for 1 hour in the dark. Coverslips were mounted with Vectashield containing DAPI (Vector Laboratories, Burlingame, CA, USA). The protein expression of EGR1 and TGF-β was assessed using immunofluorescence (**see subchapter 3.1.6**). Cells were visualized and photographed under UV light using a Leica DMR-HC microscope at 400 × magnification. Primary antibody specificity was checked and evaluated on immunoblots.

Primary TECs at a density of 3×10^4 cells per well were grown on 1% gelatin-coated glass coverslips in 24-well plates. Other steps followed, as mentioned in the HK-2 experiment section. Immunostaining reactivity of the cells for EGR2, EGR1, and VIM was evaluated in a single-blinded fashion (unaware of the treatment groups) by calculating the average signal intensity of each stained area using ImageJ v1.53 and expressed as arbitrary units (a.u.). SQSTM1 staining was evaluated by calculating the percentage of positive cytoplasmic area with ImageJ.

3.1.8. Renal Histology and Immunohistochemistry

Formalin-fixed, paraffin-embedded kidney slices were stained with Masson's trichrome. The degree of glomerulosclerosis and tubulointerstitial damage was measured blinded using a semi-quantitative scale. The arithmetic mean of 100 evaluated glomeruli, the glomerulosclerosis index of each animal was determined by light microscopy at 400× magnification as follows: 0: healthy morphology, 1: attachment to Bowman's capsule, mesangial expansion in less than 25% of glomerular area, 2: mesangial expansion in 25-50% of glomerular area, 3: mesangial expansion and capillary obliteration in 50-75% of glomerular area, 4: sclerosis with complete capillary obliteration in the whole glomerulus.

Tubulointerstitial damage was scored at 100× magnification as follows: for tubular dilatation, 0: none, 1: dilated tubule; for tubular atrophy, 0: none, 1: signs of atrophy, 2: apoptosis and desquamation of cells; for hyaline deposition, 0: none, 1: hyaline deposition; interstitial infiltration of mononuclear cells, 0: none, 1: infiltration of mononuclear cells; for interstitial fibrosis, 0: none, 1: mild, 2: severe.

SQSTM1 immunofluorescent staining of paraffin-embedded sections was performed using citrate buffer pH 6.0 for heat-induced antigen retrieval and overnight incubation with the primary antibody, followed by Alexa Fluor-594-conjugated anti-rabbit IgG (**see subchapter 3.1.6**). ImageJ v1.53 software (NIH, Bethesda, MD, USA) was used to evaluate the SQSTM1-positive stained area at a magnification of 400 for each slide.

3.1.9. Statistical analysis

Experimental data are presented as mean ± SD. Statistical analysis was performed using IBM SPSS Statistics for Windows, Version 28.0. Armonk, NY: The IBM Corp. Shapiro-Wilk test was performed to analyze the normal distribution of the data. For the HK-2 experiments, pairwise comparisons were conducted using the independent samples Kruskal-Wallis and

Mann-Whitney U test and Bonferroni multiple comparison corrections, as indicated. Pearson's correlation was used to test the relationship between continuous and discrete variables. For the primary TECs and TGF-β transgenic mice experiments, One-Way ANOVA and Holm–Sidak post hoc tests were used. The significance level was $p < 0.05$ at the 95% confidence level.

3.2. Systematic review and meta-analysis

The methods section 3.2 has been developed from two thesis-related manuscripts (submitted) with modifications.

Methods were specified in a protocol registered with the PROSPERO International Prospective Register of Systematic Reviews (CRD42021283763 and CRD42021282785). The PRISMA 2020 guideline (145) and the Cochrane Handbook (version 6.2) (146) were used as references throughout the meta-analyses. We systematically searched Embase, Web of Science (WoS), PubMed, Scopus, and CENTRAL databases without restrictions until June 12, 2023, for the first meta-analysis and until November 26, 2022, for the second meta-analysis.

3.2.1. Eligibility criteria

First systematic review and meta-analysis: The PECO framework was applied as follows: the population (P) included patients and murine experimental models for which assays on hypothesis-free whole miRNA profiling were performed; the exposed group (E) included CKD patients regardless of stage or etiology or murine CKD models irrespective of type; the control group (C) had: healthy or sham controls, respectively; the outcome (O) was the identification of dysregulated mature miRNAs in CKD patients in comparison to healthy controls.

Second systematic review and meta-analysis: To define our clinical question and eligibility criteria, we applied the PIRD framework as follows: the population (P) consisted of individuals with (case group) and without CKD (healthy and diseased control groups); the index test (I) was miRNA detection performed by qRT-PCR; the reference test (R) was clinical diagnosis confirmed by biopsy or laboratory parameters; the diagnosis (D) was CKD. Studies were considered eligible if they met the following criteria: (1). The diagnostic accuracy of miRNA for CKD was provided; (2) all patients with CKD were diagnosed by the gold standards in diagnostics (biopsy or laboratory); (3) AUC, ROC curve, sensitivity (SEN) and specificity (SPE) were provided; (4) observational and interventional studies were included.

3.2.2. Statistical analysis: meta-analysis

First meta-analysis: To identify the most dysregulated miRNA signatures that are consistently up- or downregulated across all studies, we used the robust rank aggregation (RRA) (147, 148) and the vote-counting method (149). The RRA method assigns a p-value to each element in the aggregated list, indicating how much higher it ranks than a null model with random ordering. After Bonferroni p-value correction, an adjusted p-value lower than 0.05 was considered significant. As a sensitivity analysis, we calculated the essential components of the vote-counting method (149) based on the number of appearances and opposite presences of miRNAs. Subgroup analysis was conducted based on the types of biological samples, diseases, and stages. We used a heat map to visualize ranking similarities between individual studies and miRNAs (150). The enrichment analysis was performed on Gene Ontology (GO) terms, KEGG and REACTOME (151) pathways set from the Molecular Signatures Database (MSigDB) (152) and PFAM (miRNA-protein interaction) utilizing DIANA-miRPath v4.0 (153). miRNA targets were identified by two different algorithms experimentally validated tools: miRTarBase (v.8) (154) and – *in silico* target prediction tools: TargetScan (v.8.0) using default settings (155). The Minimum Information About a Microarray Experiment (MIAME) for array and Minimum Information for Publication of Quantitative Real-time PCR Experiments (MIQE) (156) and Syrcle Rob tools (157) for animal studies were used to assess the study quality.

Second meta-analysis: In terms of clinical applicability, data were pooled, considering the following moderators: (1) comparison of CKD patients with healthy and diseased controls, (2) individual kidney diseases, (3) biological sample types, (4) single miRNA or panel miRNAs, and (5) ethnicity. We analyzed the most frequent miRNAs in the included studies separately. The statistical analysis was performed using the R software (version 4.1.2.) (158). Statistical significance was defined as a p-value less than 0.05. We collected AUC values and computed their standard deviation using the confidence interval or the method of Hanley and colleagues (159) when the confidence interval was unavailable. For rigorous pooled AUC (pAUC) values, we considered the correlations between sample errors and random effects corresponding to the miRNAs present in the same study by a multivariate mixed-effect model supplemented with the robust approach (160). Univariate and multivariate analyses of AUC values were performed to identify the effect of moderator variables. In addition, we applied well-known methods (161-163) to obtain pooled SEN and SPE. To address the mentioned correlation, we randomly selected SEN and SPE; we chose only one miRNA from each study and then calculated pooled SEN and SPE. In the ROC plot visualization, the size of the prediction region provides insight

into heterogeneity. In the case of the meta-analysis of specific miRNAs, we performed classical inverse variance AUC meta-analysis due to the lack of the mentioned correlations. In these cases, the heterogeneity was calculated by I^2. We created AUC funnel plots showing all available data to assess publication bias. Similarly, as above, we performed Egger's test after randomly selecting one result from each study. Studies reporting only CKD without a specific diagnosis were excluded from the meta-analysis to avoid selection bias.

4. RESULTS

In section 4.1, there is a peer-reviewed publication available (143).

4.1. Results 1 (EMT in HK-2 cells)

While introducing the TGF-β1-induced EMT model in the HK-2 cell line, we noticed that the expression of pro- and anti-fibrotic genes and proteins differed when different cell culture media were used. Subsequently, we investigated the effect of six different cell culture medium formulations on the expression of pro- and antifibrotic markers (143).

First, we observed the effect of six culture medium formulations (**ingredients are shown in Fig. 5**) on cell morphology (**Fig. 6**). As a result, cells without TGF-β1 showed epithelial morphology, whereas cells treated with TGF-β1 (10 ng/ml) for 24-hour were elongated in all culture media. However, HK-2 cells cultured in DMEM 5% FBS appeared round-shaped and polygonal, but cells in KFSM looked smaller and did not divide as much as cells cultured in FBS-supplemented media.

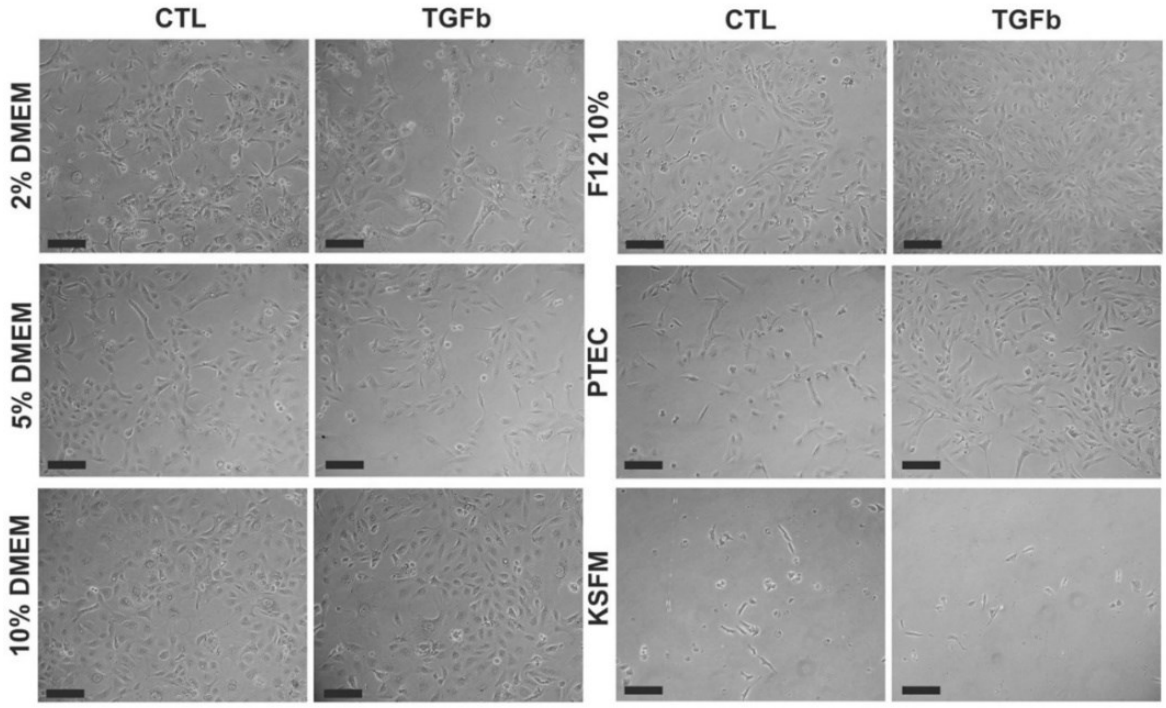

Figure 6. Effect of different medium formulations on HK-2 cell morphology. *Figure shown by control (CTL) and TGF-β1-treated (TGFb) groups. Light microscopy, 200 × magnification; scale bar represents 100 μm (143).*

In TGF-β-induced HK-2 cells, the *TGFB1* gene, protein, and mesenchymal markers were highly expressed (**Fig. 7**). At the mRNA level, the EMT-related changes were consistent across all culture media. However, the VIM protein expression was elevated in all media except DMEM 5% FBS by immunoblotting (**Fig. 8**). TGF-β1 partially induced the mRNA expression of *FN* in PTEC 2%, DMEM F12 10% and KFSM (**Fig. 8a**) and the protein expression in almost all media except DMEM/F12 10% and KFSM.

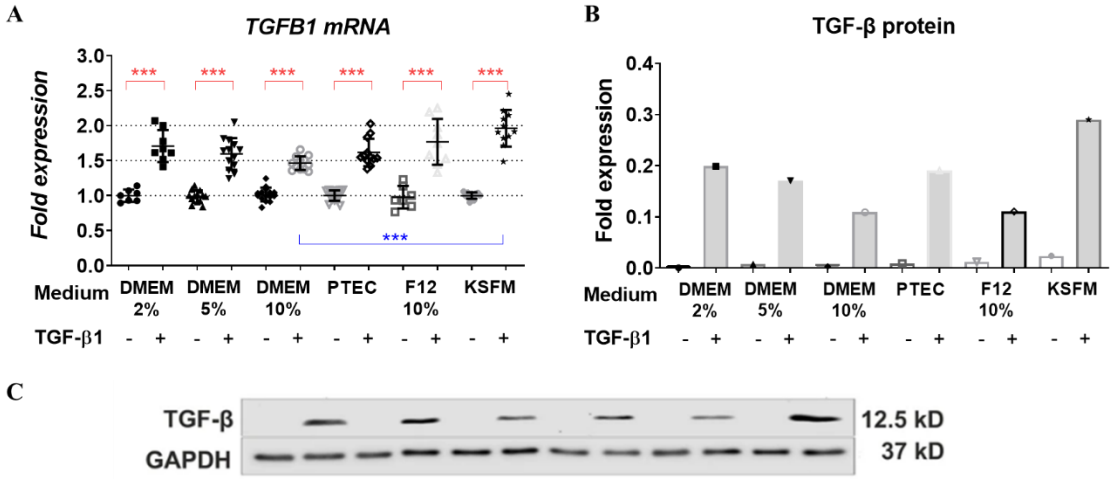

Figure 7. TGFB1 mRNA and protein (*TGF-β*) expression of HK-2 cells in different medium formulations. ***A.*** *QRT-PCR results of TGF-β1-induced effects on TGFB1 mRNA expression in HK-2 cells cultured in different medium formulations for 24 h. The gene expression of TGFB1 was normalized to GAPDH and indicated as fold expression relative to the respective controls (mean ± SD). Significant differences between the control vs. TGFb groups (n = 7–16/group) are marked in red, and TGFb vs. TGFb groups between culture media are marked in blue; p < 0.05*, p < 0.01** and p < 0.001***. Independent samples - Kruskal-Wallis and Mann-Whitney U test.* ***B.*** **TGF-β1** *protein expression is shown for each group; GAPDH was used as a loading control.* ***C.*** *Representative immunoblot of TGF-β1 and GAPDH. The order of stripes is the same as in Fig. 7A.* ***Abbreviations:*** *TGFB1 - Transforming growth factor mRNA, TGF-β1 - Transforming growth factor beta protein, CTL - Control group, TGFb - Transforming growth factor beta-1 (10 ng/ml)-treated group (143).*

CTGF, *COL4A1*, and EGR2 expressions were significantly elevated in the EMT model (**Fig. 9A, 9B, and 9C**), whereas *PPARG* decreased in all culture media (**Fig. 9D**). Interestingly, medium formulations had a substantial impact on pro-fibrotic *EGR1* expression. TGF-β1

treatment significantly increased *EGR1* mRNA expression only in DMEM 5% and DMEM/F12 10% media but decreased *EGR1* in PTEC 2% and DMEM 10% (**Fig. 9E**).

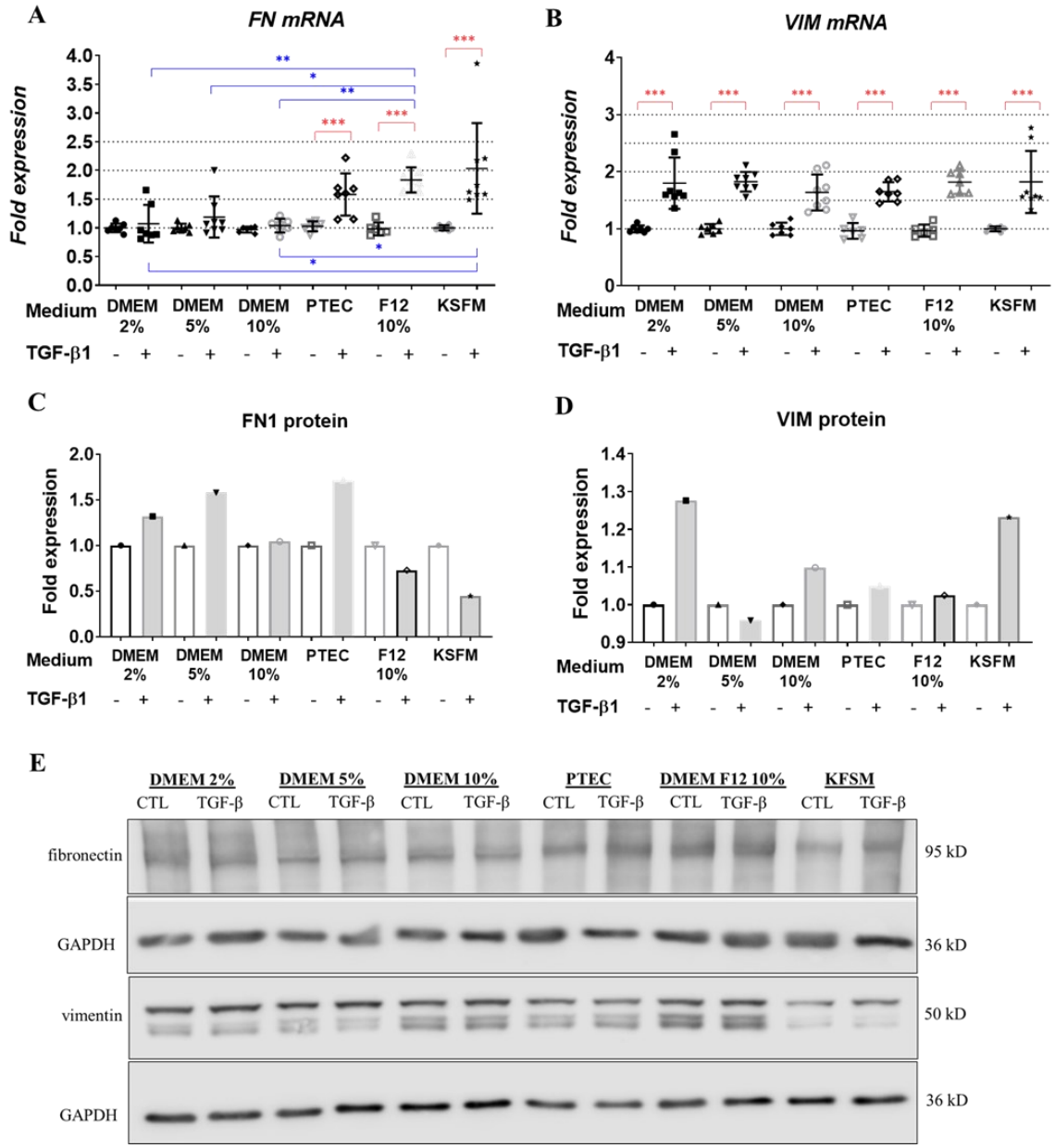

Figure 8. Gene and protein expressions of mesenchymal markers. *Gene expression of CTL and TGF-β1-treated cells in each culture medium is expressed as fold expression relative to the corresponding controls. Expression of each gene was normalized to GAPDH, and mean expression levels with standard deviation (± SD) are shown* ***A.*** *FN (n = 7–8/group),* ***B.*** *VIM (n = 7–8/group). Significant differences within the groups are marked in red: p < 0.05*, p < 0.01**, and p < 0.001***. Inter-group differences are marked in blue; p < 0.05*, p < 0.01** and p < 0.001***. Independent samples - Kruskal-Wallis and Mann-Whitney U test.* ***Immunoblot results of mesenchymal markers*** *(**C:** FN1 protein and **D:** VIM protein) in CTL and TGFb treated HK-2 cells in the six culture medium formulations. GAPDH was used as a*

loading control. The mean expression for each culture medium group is shown relative to the corresponding controls. ***E:*** *representative immunoblot.* ***Abbreviations:*** *CTL – Control group; TGFb – Transforming growth factor-β1 (10 ng/ml)-treated group; FN – Fibronectin; VIM - Vimentin (143).*

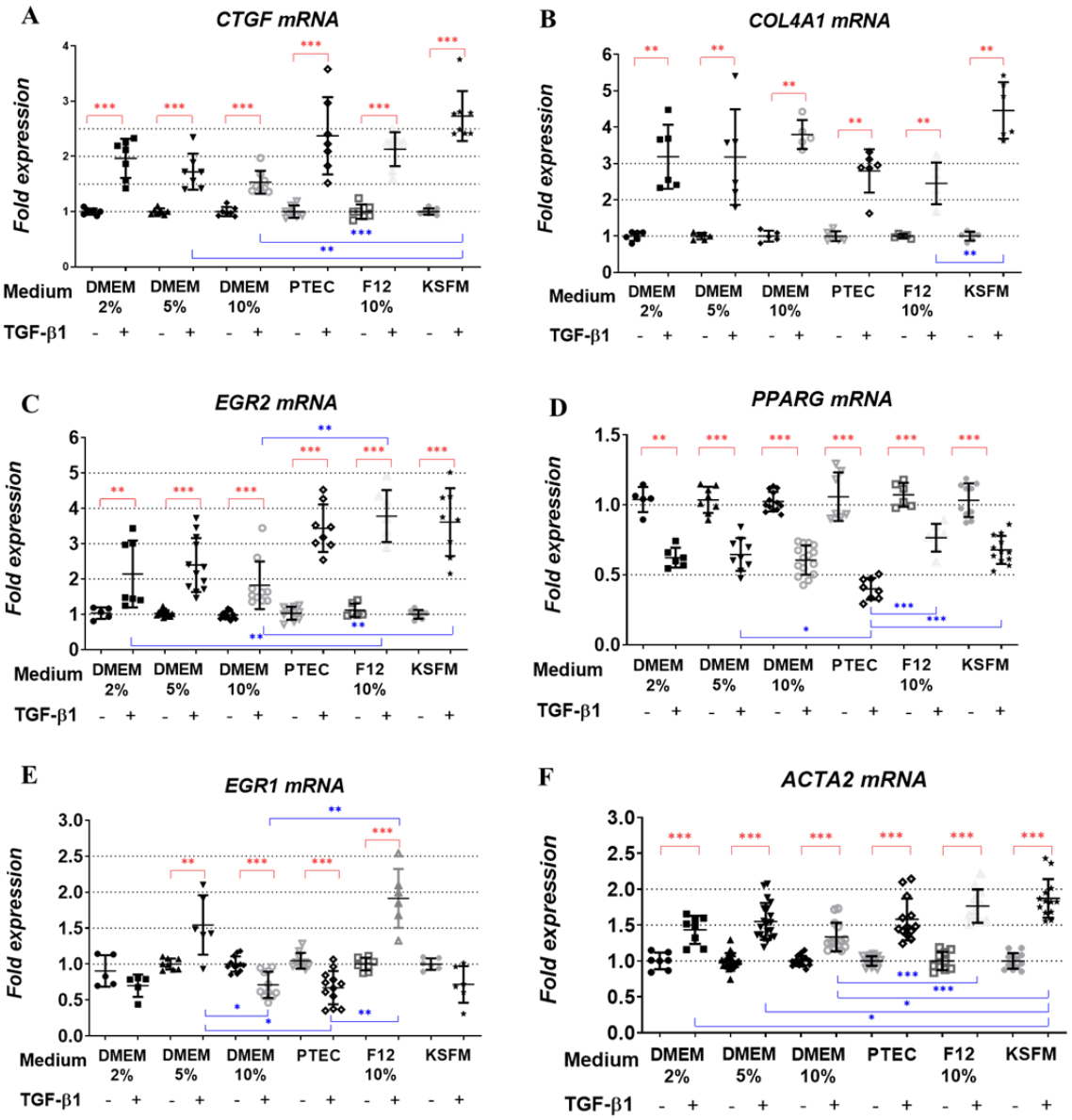

Figure 9. Gene expression pattern of transcription factors in various culture medium formulations. *Gene expression of control (CTL) and TGF-β1-treated HK-2 cells in each culture medium are expressed as fold expression relative to the corresponding controls as follows:* ***A. CTGF*** *(n = 7–8/group),* ***B.*** *COL4A1 (n = 5-6/group),* ***C.*** *EGR2 (n = 5–14/group),* ***D.*** *PPARG (n = 5–13/group),* ***E.*** *EGR1 (n = 5–12/group),* ***F.*** *ACTA2 (n-7–24/group). Expression of each gene was normalized to GAPDH and shown as mean ± SD. Significant differences within the groups are marked in red: *p < 0.05, **p < 0.01, and ***p < 0.001. Inter-group differences*

*are marked in blue; *p < 0.05, **p < 0.01 and ***p < 0.001. Independent samples- Kruskal-Wallis and Mann-Whitney U test (143).*

Among the inflammatory markers, *IL6* mRNA was not induced in TGF-β1-treated HK-2 cells cultured in PTEC 2% medium in addition to the DMEM 2% (**Fig. 10A**). The expression of the complement C3 protein-coding gene, *C3*, decreased in KSFM and increased in DMEM 5% but did not change in any other media upon TGF-β1 treatment (**Fig. 10B**).

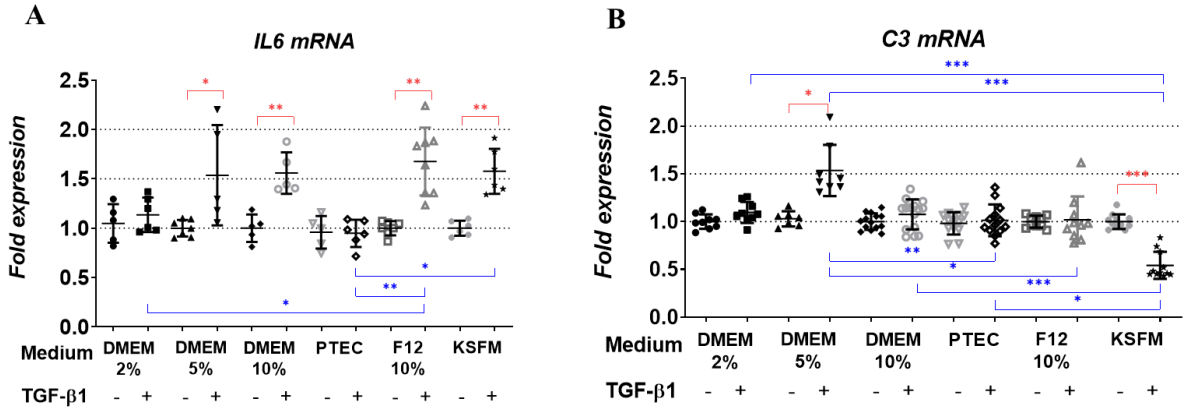

Figure 10. Cell culture medium-dependent expression of inflammatory genes*. Gene expression of control (CTL) and TGF-β1-treated HK-2 cells in each culture medium is expressed as fold expression relative to the corresponding controls as follows:* ***A****. IL6 (n = 5–7),* ***B****. C3 (n = 7–11/group). Gene expression was normalized to GAPDH and shown as mean ± SD. Significant differences within the groups are marked in red: *p ≤ 0.05, **p ≤ 0.01, and ***p ≤ 0.001. Inter-group differences are marked in blue; *p ≤ 0.05, **p ≤ 0.01 and ***p ≤ 0.001. Independent samples - Kruskal-Wallis and Mann-Whitney U test (143).*

Based on the differential expression of mRNAs in culture medium formulations, we investigated the expression pattern of EGR1 in TGF-β-induced HK-2 cells by immunofluorescence. TGF-β1 induced EGR1 translocation to the nucleus indicating transcriptional activation in DMEM F12 10% and KFSM media (**Fig. 11A**). Cells grown in other media (DMEM 2%, 5%, 10%, and PTEC 2%) showed only cytoplasmic overexpression of EGR1 (**Fig. 11A**). Still, by both gene expression and immunoblot analysis, we observed TGF-β1 protein expression induced by TGF-β1 treatment independent of the culture medium used (**Fig. 11B**).

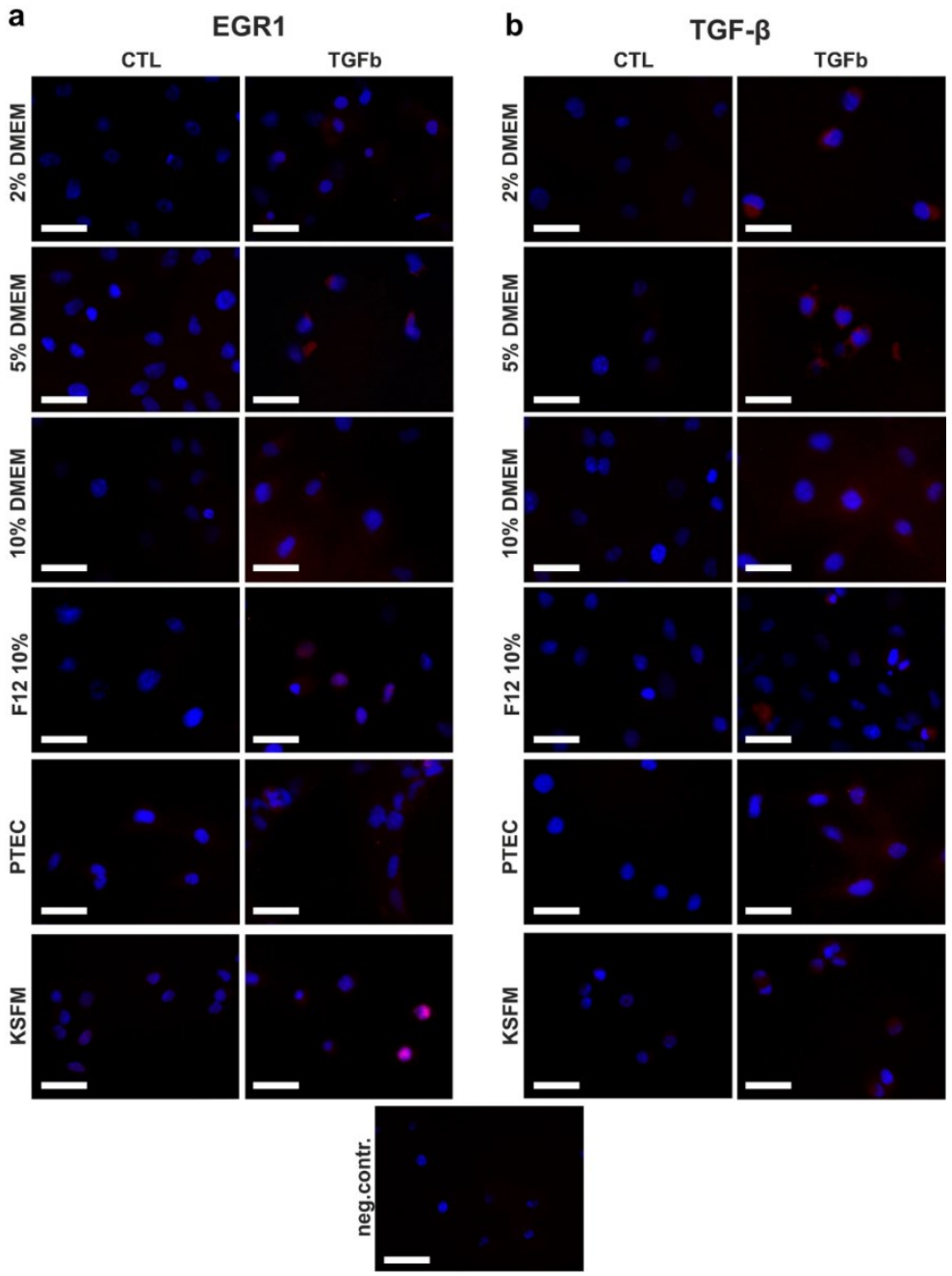

Figure 11. EGR1 and TGF-β1 immunocytochemistry of TGF-β1-induced HK-2 cells. *EGR1* ***(A)*** *and TGF-β1 (****B****) protein expression of control and TGF-β1-treated (10 ng/ml for 24 h) cells in different medium formulations. Immunofluorescence, 400 × magnification. Neg. Contr.: representative photograph of the negative control sample (omitting the primary antibodies). The scale bar represents 50 μm. Red staining: EGR1 or TGF-β1 1; blue staining: nuclei (DAPI). Magenta: double staining (143).*

4.2. Results 2 (PPARγ agonist in kidney fibrosis)

In section 4.2, there is a peer-reviewed publication available (144).

4.2.1. The effect of PPARγ agonist on the fibrotic process

In previous years, our research team has shown that pioglitazone effectively decreased the development of TGF-β-induced glomerulosclerosis and TIF *in vivo* (22). Therefore, our objective was to investigate the impact of pioglitazone on EMT and fibrogenesis *in vitro* using primary mouse renal TECs. *In vitro*, TGF-β1 induction resulted in increased expression of pro-fibrotic *Tgfb1* and *Ctgf* mRNA and TGF-β1 protein (**Fig. 12A–C)**. A two-fold rise in *Col1a1* is observed (**Fig. 12D**). Pioglitazone therapy effectively inhibited all these inductions of pro-fibrotic gene expression. The data presented here corroborate our research team's prior *in vivo* findings (22).

In addition, TGF-β1 increased the expression of the pro-fibrotic *Runx1* transcription factor (**Fig. 12E**) and the matrix-degrading *Mmp2* (**Fig. 12F**), dramatically reduced by pioglitazone therapy. While TGF-β1 did not enhance the mRNA expression of the *Mmp2* inhibitor *Timp2* (**Fig. 12G**), pioglitazone decreased its expression to lower levels than the control. TGF-β1 also stimulated the EMT in primary TECs, as seen by increased levels of *Acta2* mRNA and VIM protein expression (**Fig. 12H, J**). Conversely, pioglitazone reduced the expression of both transcripts to levels comparable to the control.

Interestingly, the nearly 50% reduction in *Pparg* expression upon TGF-β1 administration was not influenced by pioglitazone treatment *in vitro* (**Fig. 12I**). In addition, we noticed that pioglitazone therapy had a beneficial effect on the expression of *Egr1* and *Stat3* mRNA in primary TECs (**Fig. 13A, B**), which aligns with our prior findings *in vivo (22)*.

Given the significant involvement of EGR2 in the development of kidney fibrosis (51), we aimed to examine the impact of pioglitazone on the expression of Egr2 induced by TGF-β, both *in vitro* and *in vivo*. The application of TGF-β1 to primary mouse TECs resulted in a four-fold increase in *Egr2* expression, which was inhibited by the administration of pioglitazone (**Fig. 14A**). The cells showed minimal levels of EGR2 immunostaining in untreated controls. However, with TGF-β1 treatment, there was a considerable increase in EGR2 expression with nuclear localization. In contrast, pioglitazone treatment reduced the up-regulation of TGF-β1-induced EGR2 expression (**Fig. 14B**).

We observed similar protective effects of chronic pioglitazone treatment *in vivo*. Untreated TGF-β transgenic mice showed a significant *Egr2* mRNA (**Fig. 14C**) and protein overexpression compared to wild-type controls (**Fig. 14D**), significantly reduced to control

levels by pioglitazone treatment. Pioglitazone inhibited further fibrotic responses in mouse kidneys. The extent of TGF-β-induced glomerulosclerosis (**Fig. 14E and G**) was significantly reduced by pioglitazone. However, chronic pioglitazone treatment completely reversed tubulointerstitial damage induced by TGF-β (**Fig. 14F and G**).

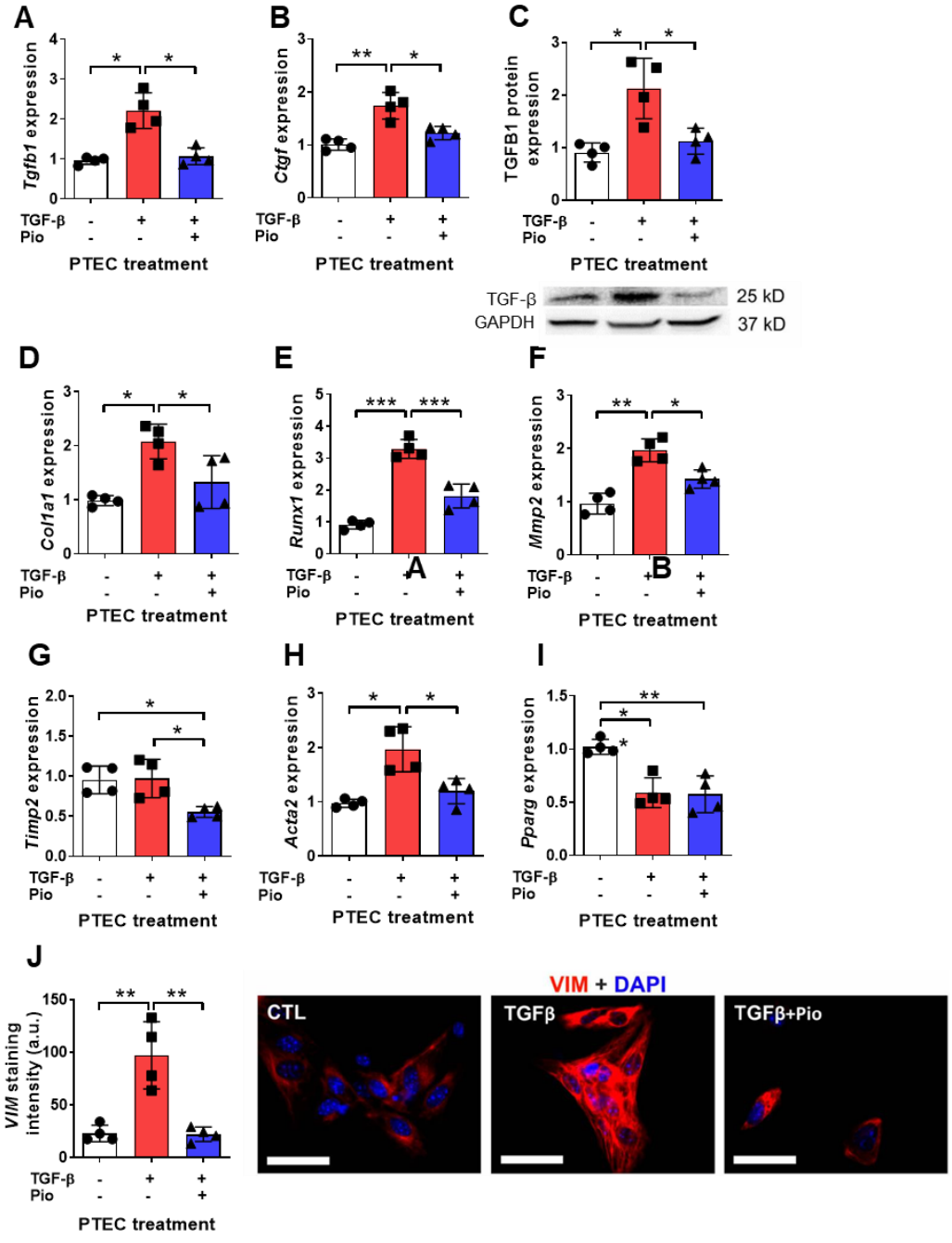

Figure 12. The effect of pioglitazone on the fibrotic response and EMT of primary murine TECs. *Bar charts represent PTECs treated with TGF-β1 for 24 h (10 ng/mL) and pioglitazone (5 μM) (n = 4/group): expression of mRNAs is shown in* ***(A)*** *Tgfb1,* ***(B)*** *Ctgf,* ***(D)*** *collagen-1 (Col1a1),* ***(E)*** *Runx1,* ***(F)*** *Mmp2,* ***(G)*** *Timp2,* ***(H)*** *α-SMA (Acta2),* ***(I)*** *PPARγ (Pparg). Proteins are shown in* ***(C)*** *TGF-β1 and* ***(J)*** *vimentin (VIM). Target gene expressions were normalized to*

*18S rRNA. VIM staining intensity in arbitrary units (a.u.) was calculated using ImageJ v1.53 (VIM: red; nuclear staining (DAPI, blue); 400× magnification, white scale bars represent 20 µm). Data represented as mean ± SD, One-way ANOVA, and Holm–Sidak post hoc test: *: p < 0.05; **: p < 0.01; ***: p < 0.001 (144).*

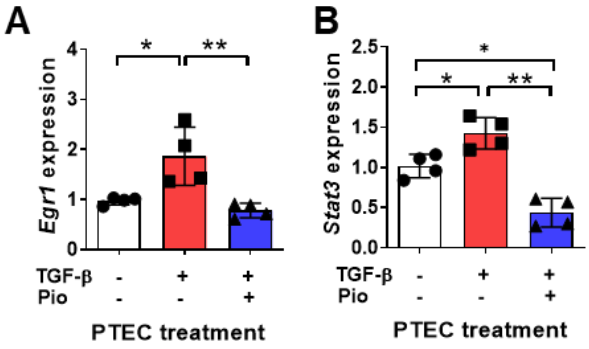

Figure 13. Pioglitazone inhibits TGF-β1-induced EGR1 and STAT3 transcription in primary TECs. *The mRNA expression of Egr1* ***(A)*** *and Stat3* ***(B)*** *was significantly induced by 24 h TGF-β1 treatment (10 ng/mL), but they restored to or maintained less than control levels by 5 µM pioglitazone (n = 4/group). Data are presented as mean ± SD, One-way ANOVA, and Holm–Sidak post hoc test, *: p < 0.05; **: p < 0.01 (144).*

Therefore, the expression of the clusterin (Clu) gene, which serves as an indicator of tubular damage, was considerably increased in transgenic mice that did not receive treatment. However, in mice treated with pioglitazone, the expression of the Clu gene remained at the same level as in the control group (**Fig. 14H**). The administration of pioglitazone eliminated the increased expression of *Mmp2* and *Timp2* genes in TGF-β transgenic mice, similar to the findings in primary TECs. Additionally, pioglitazone therapy significantly suppressed the up-regulation of the *Runx1* transcription factor (**Fig. 15A–C**). In contrast to primary TECs, pioglitazone therapy effectively restored the renal *Pparg* expression, significantly reduced by TGF-β1 *in vivo* (**Fig. 15D**).

Figure 14. The effect of TGF-β and pioglitazone on the renal pro-fibrotic EGR2 response in

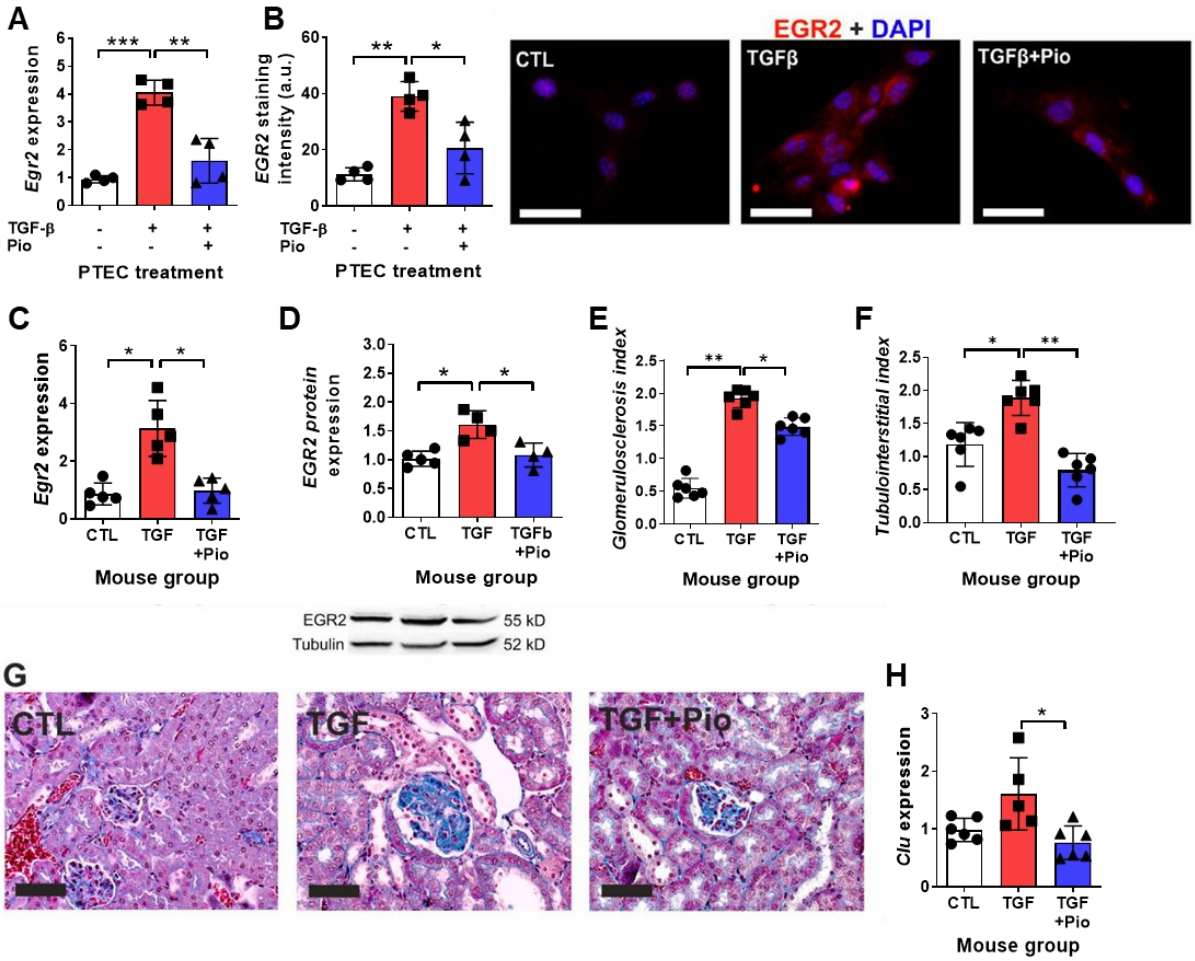

vitro and in vivo. *A-B charts represent PTECs treated with TGF-β1 for 24 h (10 ng/mL) and pioglitazone (5 μM) (n = 4/group): expression of mRNA or protein shown in* ***(A)*** *Egr2,* ***(B)*** *EGR2 protein. A-H charts represent mouse groups (n = 6/group): CTL: wild-type controls, TGF: un-treated TGF-β transgenic mice; TGF + Pio: pioglitazone-treated (20 mg/kg/day) TGF-β transgenic mice:* ***(C)*** *Egr2 mRNA,* ***(D)*** *EGR2 protein,* ***(H)*** *Clu mRNA. Mouse kidney immunohistochemistry is shown in* ***(E)*** *glomerulosclerosis index,* ***(F)*** *tubulointerstitial index,* ***(G)*** *dilatation, and epithelial cell desquamation. Target gene expressions were normalized to 18S rRNA. EGR2 staining intensity in arbitrary units (a.u.) was calculated using ImageJ v1.53 (EGR2: red; nuclear staining (DAPI, blue); co-localization: purple; 400× magnification, white scale bars represent 20 μm). Representative photomicrographs of Masson's trichrome-stained mouse kidneys were taken at 400× magnification (black scale bars represent 50 μm). Data are presented as mean ± SD, One-way ANOVA, and Holm–Sidak post hoc test, *: $p < 0.05$; **: $p < 0.01$; ***: $p < 0.001$ (144).*

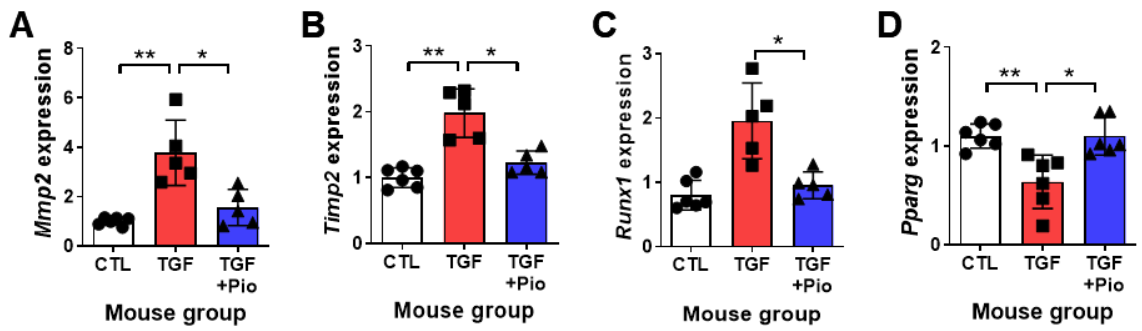

Figure 15. Pioglitazone reverses the dysregulated renal gene expression of fibrosis-related factors in TGF-β transgenic mice. *Charts represent mouse groups (n = 6/group): CTL: wild-type controls, TGF: un-treated TGF-β transgenic mice; TGF + Pio: pioglitazone-treated (20 mg/kg/day) TGF-β transgenic mice:* ***(A)*** *Mmp2,* ***(B)*** *Timp2,* ***(C)*** *Runx1,* ***(D)*** *Pparg. The expression of target genes was normalized to 18S rRNA. Data are presented as mean ± SD, One-way ANOVA, and Holm–Sidak post hoc test, *: $p < 0.05$; **: $p < 0.01$ (144).*

The anti-inflammatory effect of pioglitazone was also explored. In mouse primary TECs, pioglitazone administration decreased TGF-β1 inducted *Ccl2*, *Lgals3*, and pro-inflammatory cytokine *Il6* mRNA overexpression. TGF-β1 suppressed *C3* mRNA expression and was even further reduced by pioglitazone in primary TECs **(Fig. 16D**). Pioglitazone alleviated TGF-β1 induced mice renal *Ccl2*, *Lgals3*, and *Il6* ((**Fig. 16E-G)**. To investigate the potential regulation of C3 by TGF-β and pioglitazone in primary TECs and mice kidneys, we also studied the possible contribution of local renal C3 to tubulointerstitial inflammation and fibrosis. While the expression of renal *C3* was increased in TGF-β transgenic animals (**Fig. 16H**), it is doubtful that this shift can be attributable to modifications in tubular cells since they exhibited a decreasing tendency *in vitro* (**Fig. 16D**).

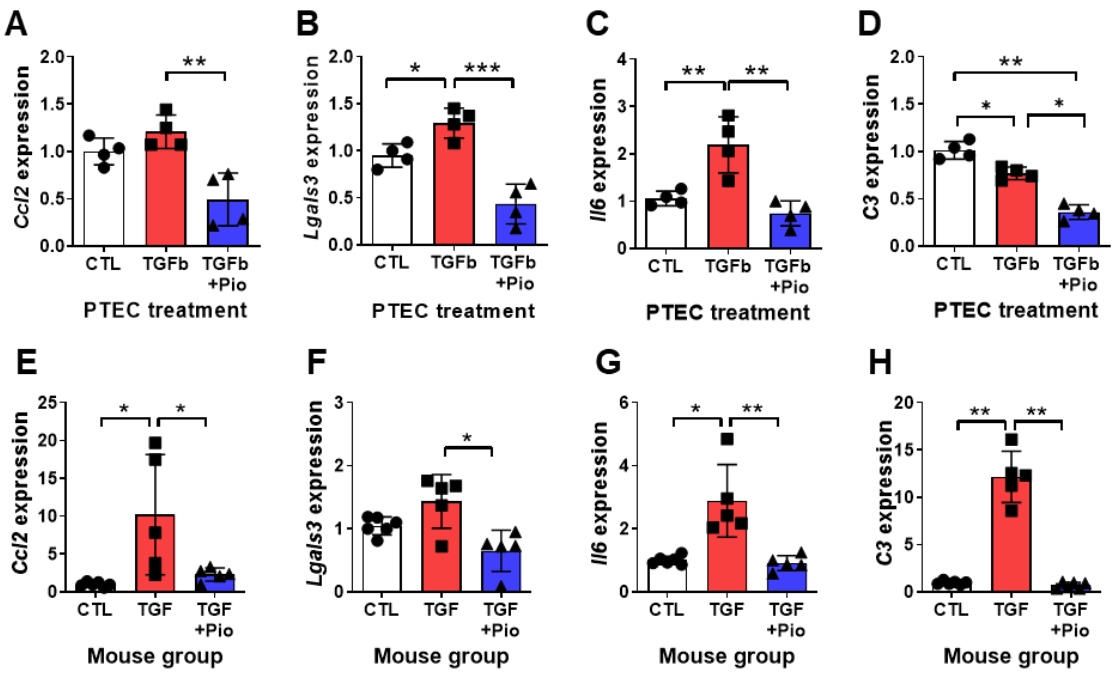

Figure 16. Pioglitazone inhibited the TGF-β1-induced inflammatory response in vitro and in vivo. *Charts A-D represent PTEC treatment groups (n = 4/group; TGF-β: 10 ng/mL; Pio: 5 μM pioglitazone):* ***(A)*** *Ccl2,* ***(B)*** *Lgals3,* ***(C)*** *Il6 and* ***(D)*** *C3 mRNA. Charts E-H represent mouse groups (n = 6/group): CTL: wild-type controls, TGF: untreated TGF-β transgenic mice; TGF + Pio: pioglitazone-treated (20 mg/kg/day) TGF-β transgenic mice:* ***(E)*** *Ccl2,* ***(F)*** *Lgals3,* ***(G)*** *Il6, and* ***(H)*** *C3 mRNA expression. Target gene expressions were normalized to 18S rRNA. Data are presented as mean ± SD, One-way ANOVA, and Holm–Sidak post hoc, *: $p < 0.05$; **: $p < 0.01$; ***: $p < 0.001$ (144).*

4.2.2. PPARγ agonist and "fibromiRs"

Both miR-199a-3p and miR-199a-5p can regulate TGF-β-mediated pathological renal processes, as shown in studies (97-99). The treatment with TGF-β1 significantly enhanced the expression of both miR-199a-3p and miR-199a-5p in primary TECs. However, this effect was suppressed by pioglitazone, as shown in **Fig. 17A and B**. In line with these findings observed *in vitro*, the kidneys of untreated TGF-β transgenic mice showed a four-fold increase in miR-199a-3p expression and a three-fold increase in miR-199a-5p expression compared to the kidneys of control mice. However, when these mice were treated with pioglitazone for a long time, the levels of miR-199a-3p and miR-199a-5p were effectively reduced to those in the kidneys of control mice (**Fig. 17D and E**). Consistent with previous findings on human kidney cells (96), our experiments confirmed that the expression of miR-130a was significantly up-regulated in our primary murine TECs after TGF-β1 treatment (**Fig. 17C**) and also in the

kidneys of TGF-β transgenic mice (**Fig. 17F**). However, this up-regulation was effectively suppressed by pioglitazone treatment. The renal miR-21-5p, expressed at a much higher level in TGF-β transgenic than in wild-type mice, returned to normal levels after five weeks of oral administration of pioglitazone (**Fig. 17G**). This finding further confirms the effectiveness of pioglitazone therapy against the pro-fibrotic effects of TGF-β *in vivo* (**Fig. 15**).

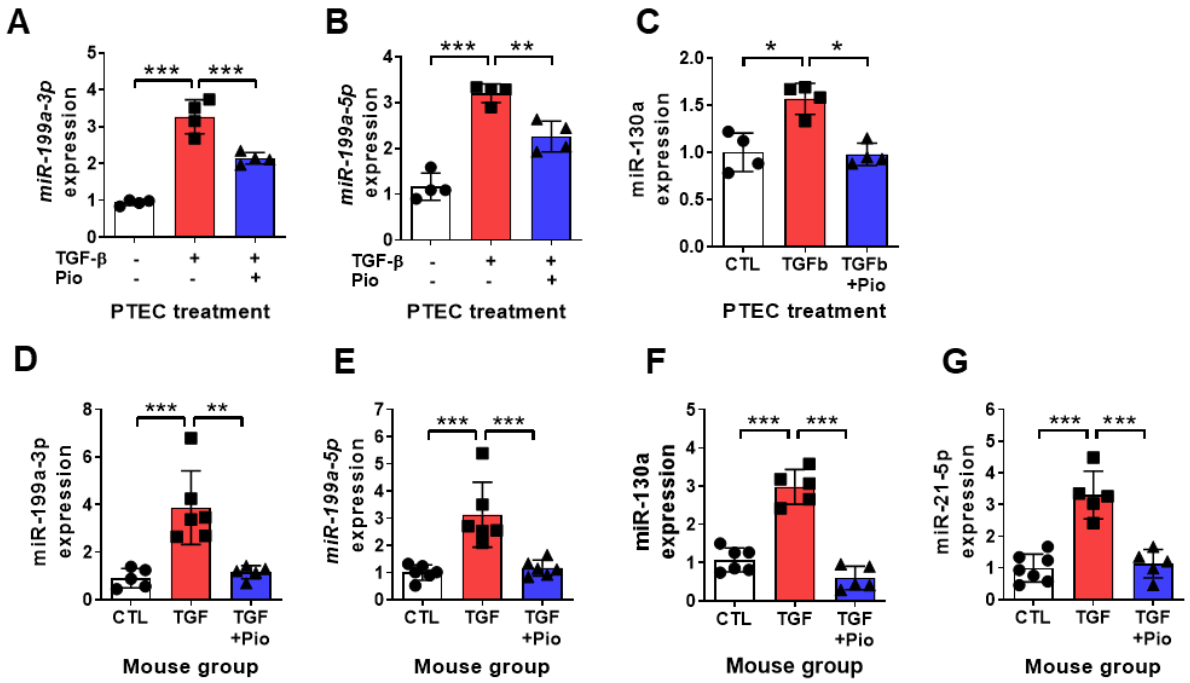

Figure 17. Pioglitazone attenuates the TGF-β induced dysregulation of pro-fibrotic miRNAs in vitro and in vivo*. Charts A-C represent primary TEC treatment groups (n = 4/group; TGFβ: 10 ng/mL; Pio: 5 μM pioglitazone): **(A)** miR-199a-3p, **(B)** miR-199a-5p and **(C)** miR-130a. Charts D-G represent mouse groups (n = 6/group): CTL: wild-type controls, TGF: untreated TGF-β transgenic mice; TGF + Pio: pioglitazone-treated (20 mg/kg/day, p.o.) TGF-β transgenic mice: **(D, E)** miR-199a, **(F)** miR-130a, and **(G)** miR-21-5p. Target miRNA expressions were normalized to U6 snRNA. Data are presented as mean ± SD, One-way ANOVA, and Holm–Sidak post hoc test, *: $p < 0.05$; **: $p < 0.01$; ***: $p < 0.001$ (144).*

4.2.3. PPARγ agonist improves autophagy dysfunction

To evaluate the impact of pioglitazone on impaired autophagy in renal tubules, both *in vitro* and *in vivo*, we measured the levels of LC3 and SQSTM1. The expression of LC3 was increased in primary TECs when exposed to human recombinant TGF-β1, as shown in **Fig. 18A and B**. However, despite the observed increase, autophagy degradation was not stimulated, as shown by the decreased LC3-II/I ratio (**Fig. 18C**) and the accumulation of SQSTM1 (**Fig.**

18D). The immunostaining results provided further evidence by demonstrating a significant buildup of SQSTM1 protein in cells treated with TGF-β1, which was subsequently eliminated with pioglitazone treatment (**Fig. 18E**).

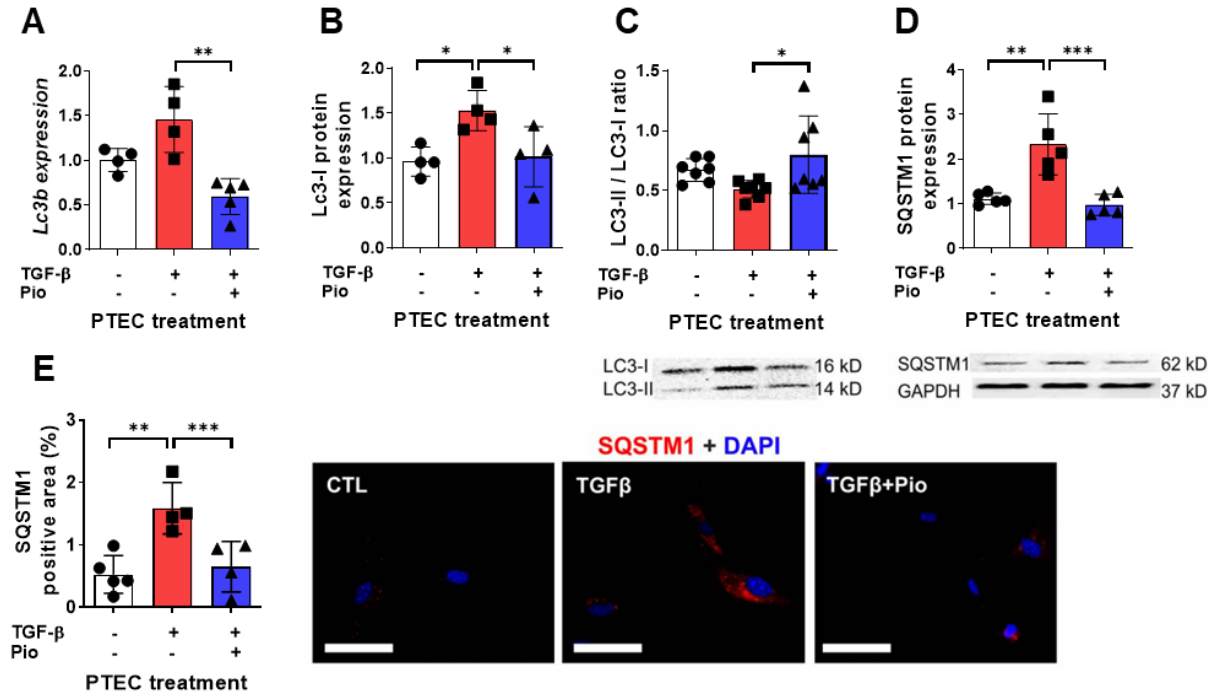

Figure 18. Pioglitazone protects primary tubular epithelial cells (TEC) from TGF-β-induced autophagy dysfunction in vitro. *Charts represent primary TEC treatment groups. (n = 4/group; TGF-β1: 10 ng/mL; Pio: 5 µM pioglitazone):* ***(A)*** *Lc3b mRNA,* ***(B)*** *LC3-I protein,* ***(C)*** *LC3-II/LC3-I ratio,* ***(D, E)*** *SQSTM1 protein. Target gene expressions were normalized to 18S rRNA. SQSTM1 staining was evaluated as the percentage of positively stained cytoplasmic area using ImageJ v1.53 (SQSTM1: red; nuclear staining (DAPI, blue), 400× magnification, white scale bars represent 20 µm). Data are presented as mean ± SD, One-way ANOVA, and Holm–Sidak post hoc test, *: $p < 0.05$; **: $p < 0.01$; ***: $p < 0.001$ (144).*

Moreover, the kidneys of TGF-β transgenic mice demonstrated increased LC3b and Sqstm1 expression levels. Additionally, there was a decrease in the LC3-II/I ratio and a significant accumulation of SQSTM1 (**Fig. 19A-E**). This indicates that the increase in gene expression did not result in an enhanced rate of autophagy degradation. On the other hand, long-term administration of pioglitazone restored the impaired autophagy induced by TGF-β. This was evident from the increased LC3-II/I ratio and decreased accumulation of SQSTM1. Significantly, SQSTM1 was mostly found in the renal tubular epithelium (**Fig. 19E**), which confirms our *in vitro* findings.

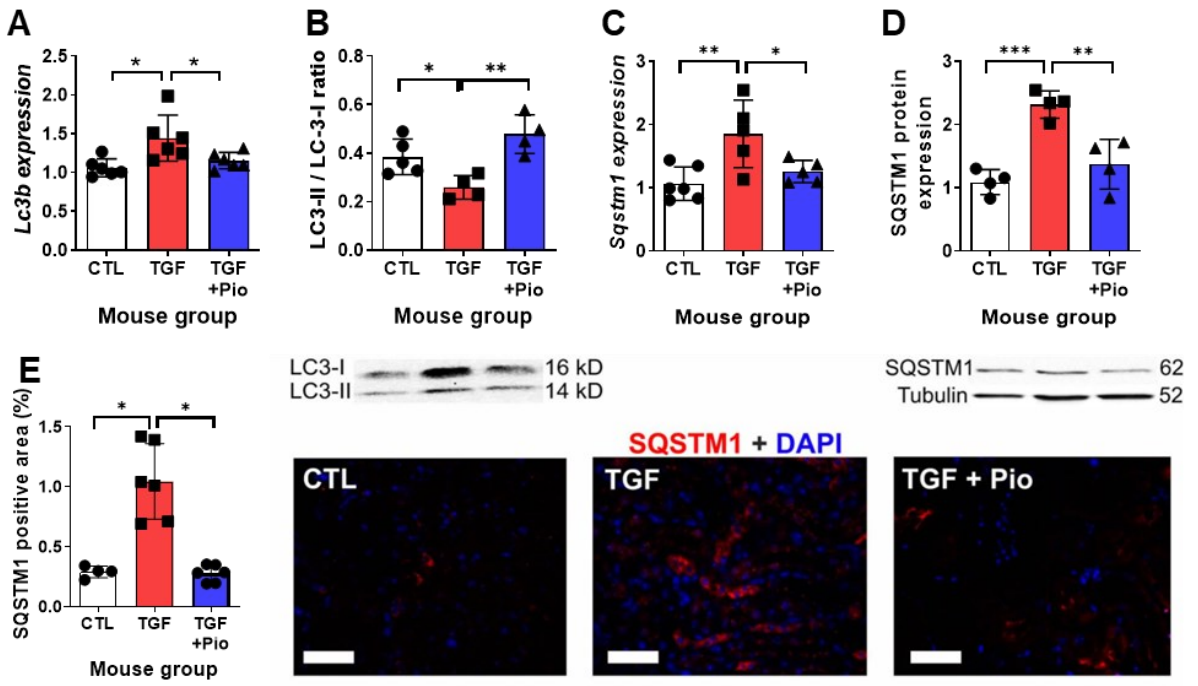

Figure 19. Pioglitazone reversed renal autophagy dysfunction induced by TGF-β in mice. *Charts represent mouse groups (n = 6/group): CTL: wild-type controls, TGF: un-treated TGF-β transgenic mice; TGF + Pio: pioglitazone-treated (20 mg/kg/day) TGF-β transgenic mice:* ***(A)*** *Lc3b mRNA,* ***(B)*** *LC3-II/LC3-I protein ratio,* ***(C)*** *Sqstm1 mRNA,* ***(D)*** *SQSTM1 protein and* ***(E)*** *SQSTM1 accumulation in kidney tubules. Target gene expressions were normalized to 18S rRNA. SQSTM1 staining was evaluated as the percentage of a positively stained tubular area using ImageJ v1.53 (SQSTM1: red; nuclear stain DAPI: blue 400× magnification, white scale bars represent 50 µm). Data are presented as mean ± SD, One-way ANOVA, and Holm–Sidak post hoc test, *: $p < 0.05$; **: $p < 0.01$; ***: $p < 0.001$ (144).*

4.3. Results 3 (miRNA in kidney diseases, meta-analysis)

Two systematic reviews and meta-analyses are contained in Section 4.3, one published (164) and one unpublished (accepted in BMC Nephrology).

First systematic review and meta-analysis:

38 human (762 cases, 671 controls) and 12 murine (70 cases, 66 controls) eligible studies were analyzed. The most dysregulated miRNAs in human CKD and murine model of CKD are listed in **Table 1**. Additionally, early CKD stages depicted up-regulated urinary miR-27b-3p and circulating miR-122-5p. Enrichment analysis revealed apoptosis, TNF-α signaling via NF-kB, G2/M checkpoint, EMT, TGF-β signaling, hypoxia, and cholesterol homeostasis known to be involved in CKD pathogenesis as the most affected pathways in both species (**Fig. 20**).

Table 1. The CKD miRNA signature for humans and murine was obtained through Robust Rank Aggregation. ** - Bonferroni adjusted p-value (p<0.1 considered significant),* ***Abbreviations:*** *miRNA - microRNA, N – number (unpublished).*

CKD patients			
miRNA	**p-value***	**N. of studies**	**Sample type**
Downregulated			
hsa-miR-181a-5p	1.6E-02	5	urine
hsa-miR-451a	9.7E-03	6	blood
hsa-miR-106b-5p	2.8E-02	5	
hsa-miR-486-5p	-6.0E-06	12	kidney biopsy
hsa-miR-486-3p	1.4E-05	8	
hsa-miR-451a	4.9E-03	7	
Upregulated			
hsa-miR-27a-3p	3.1E-02	6	urine
hsa-miR-1260b	2.4E-02	5	blood
hsa-miR-155-5p	3.5E-03	6	kidney biopsy
hsa-miR-21-5p	1.8E-02	7	
Murine experimental models of CKD			
miRNA	**p-value***		**Sample type**
Downregulated			
mmu-miR-20a-5p	6.7E-04	4	kidney tissue
mmu-miR-709	1.8E-03	4	
mmu-miR-429-3p	3.5E-02	4	
Upregulated			
mmu-miR-21a-5p	2.8E-03	5	kidney tissue
mmu-miR-223-3p	3.0E-03	4	
mmu-miR-342-3p	3.7E-03	4	
mmu-miR-214-3p	1.8E-02	4	
mmu-miR-199a-5p	4.6E-02	4	

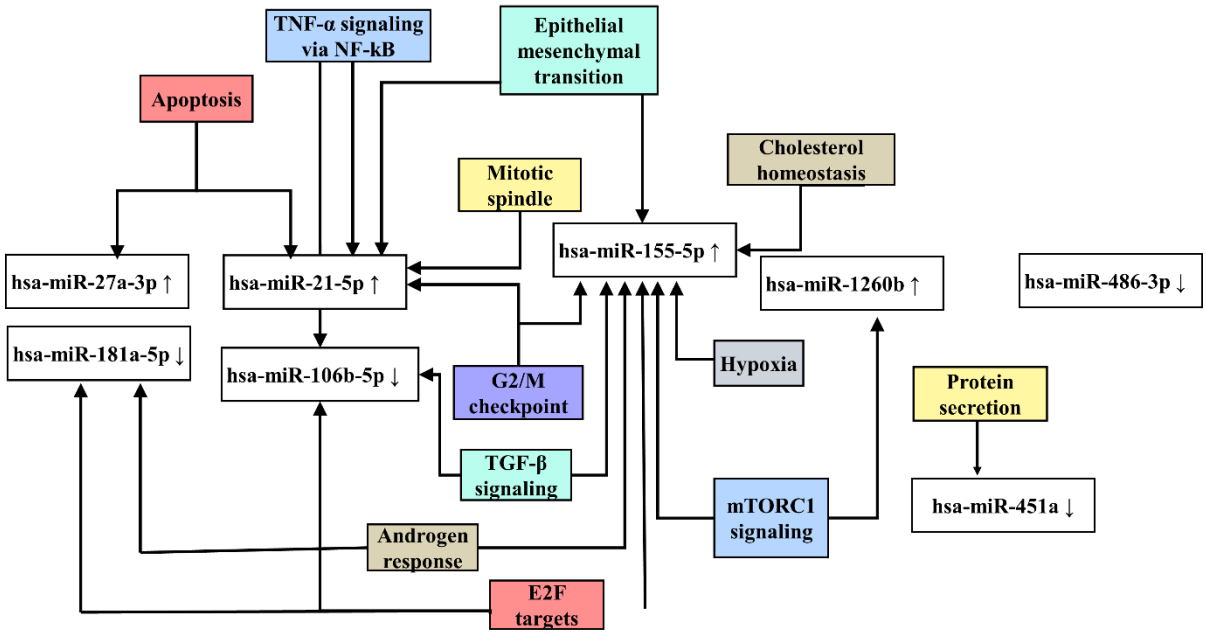

Figure 20. Pathway union. *The scheme was created from the DIANA-miRPath v4.0 (153) analysis for the pathway union of MSigDB hallmark gene sets of significantly dysregulated miRNA in human CKD. MSigDB pathway union represents well-defined biological states or processes from GSEA software.* ***Abbreviations:*** *E2F – E2F transcription factor; mTORC1 - Mechanistic Target of Rapamycin Kinase; G2/M checkpoint -; Gap2 phase and Mitosis checkpoint; TNF-α - Tumor necrosis factor α; NF-κB - Nuclear factor κB (unpublished).*

Second systematic review and meta-analysis:

Eighty-seven articles (from 2013 to 2022) reported 238 single and 34 panel miRNA results, which were included in the analysis. We analyzed data from 8351 CKD patients, 2989 healthy individuals, and 4331 diseased controls. Among single miRNAs, pooled SEN was 0.82, and SPE was 0.81 for DN vs. diabetes mellitus (DM). SEN and SPE were 0.91 and 0.89 for DN vs. healthy control, respectively (**Fig. 21A**). MiR-192 was the most frequently reported in DN, with pAUC of 0.91 and SEN and SPE of 0.89 and 0.89, respectively, compared to healthy controls (**Fig. 22A**). Panel miRNAs outperformed single miRNAs (pAUC of 0.86 vs 0.79, $p<0.05$). SEN and SPE of panel miRNAs were 0.89 and 0.73 in DN vs. DM, respectively. In lupus nephritis (LN) vs. systemic lupus erythematosus (SLE), the SEN and SPE of single miRNAs were 0.84 and 0.81, respectively (**Fig. 21B**). Urinary miRNAs tended to be more effective than blood miRNAs ($p=0.06$).

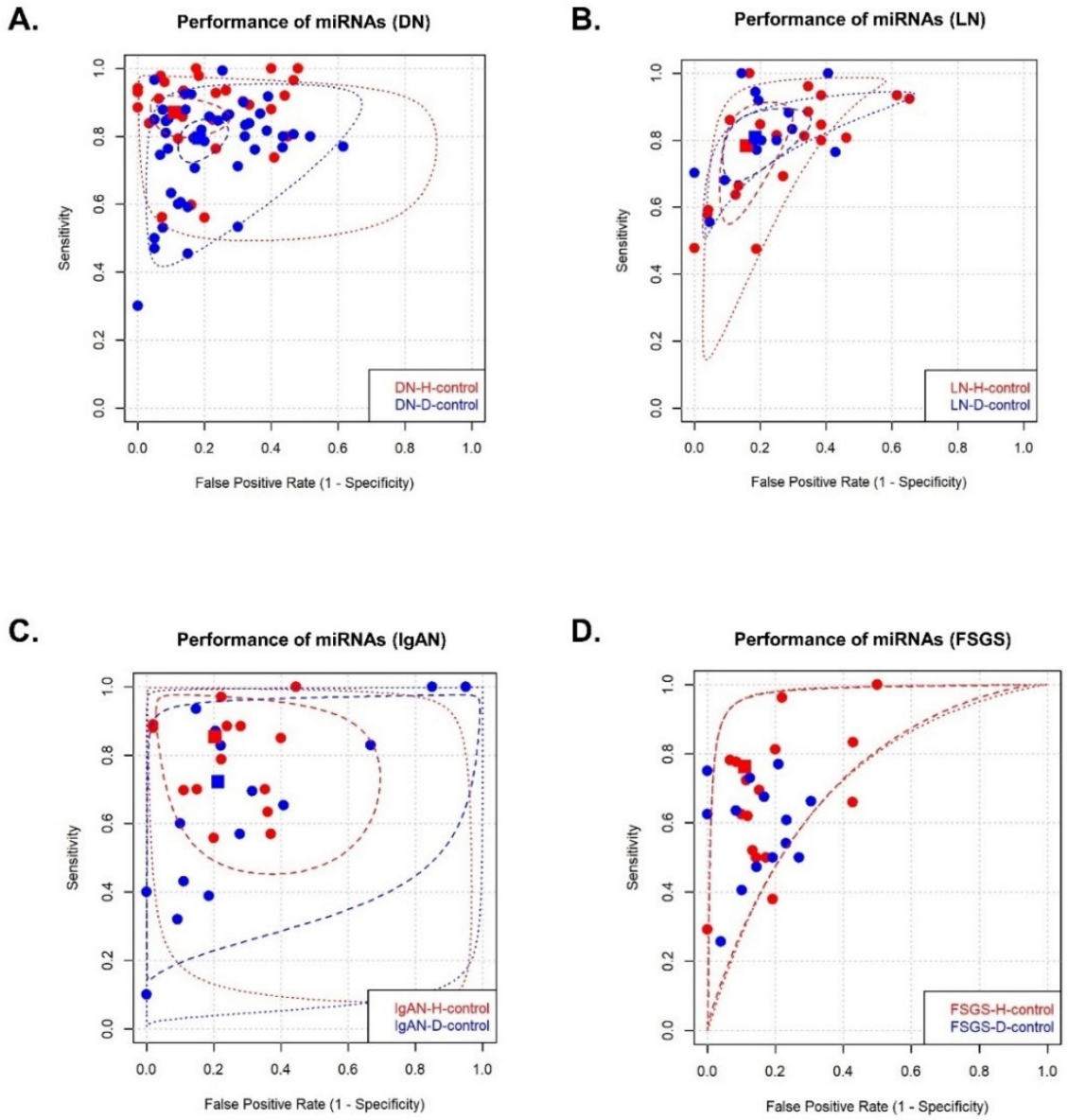

Figure 21. The pooled sensitivity and specificity of single miRNAs in CKDs. *The pooled SEN and SPE results in DN compared to T2DM patients were 0.82 (95% CI; 0.76-0.87) and 0.81 (95% CI; 0.74-0.86) for single miRNAs* ***(A)****. When LN patients were compared to SLE, the pooled SEN was 0.84 (95% CI; 0.74-0.91), and the SPE was 0.81 (95% CI; 0.72-0.88)* ***(B)****.* ***(C)*** *and* ***(D)*** *show the pooled analysis from IgAN and FSGS.* ***Abbreviations:*** *LN - Lupus nephritis; DN - Diabetic nephropathy; FSGS - Focal segmental glomerulosclerosis; IgAN - IgA nephropathy; SLE – systemic lupus erythematosus; T2DM - Type 2 diabetes mellitus; H-control - Healthy control; D-control - Diseased control (unpublished).*

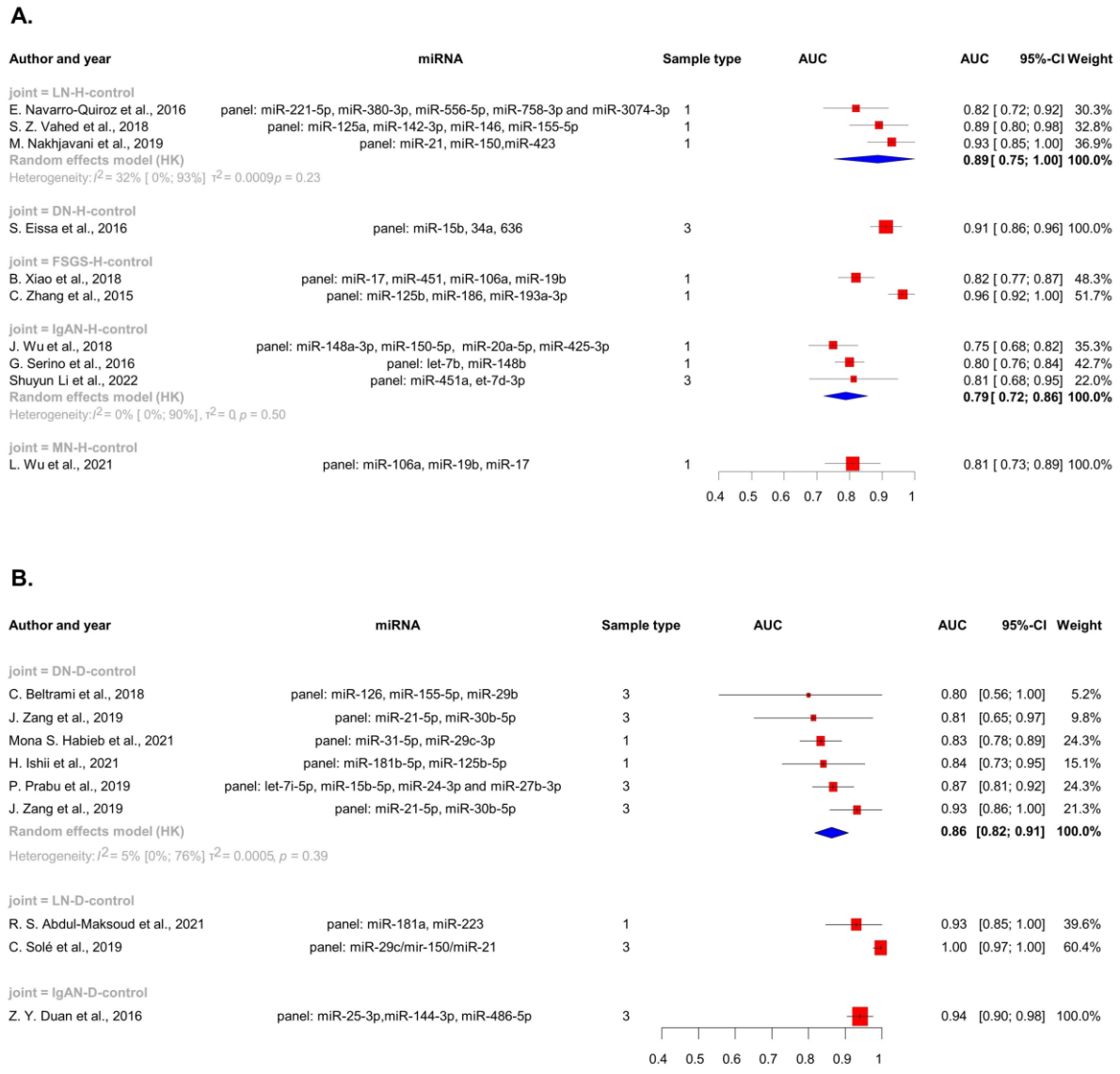

Figure 22. The pooled AUC values of panel miRNAs in CKD comparison with A. Healthy and B. Diseased control groups. *In the DN with healthy control, only AUC values for a panel of miR-15b, miR-34a, and miR-636 were reported (0.91, 95% CI; 0.86-0.96) (**A**). The pAUC of panel miRNAs in IgAN vs healthy controls was 0.79 (95% CI; 0.72-0.86) (**A**). The pAUC of DN vs. DM was 0.86 (95% CI; 0.82-0.91) for panel miRNAs (**B**). Among the individual studies, panel miR-21 and miR-30-b-5p showed higher AUC in DN than DM patients, 0.93 (95% CI; 0.86-1.0) (**B**). LN patients with SLE control groups had a higher AUC than the other kidney diseases, e.g., panel miR-29c, miR-150, and miR-21 had 1.00 (95% CI; 0.97-1.00) (B).* ***Abbreviations:*** *LN - Lupus nephritis; DM - diabetes mellitus; DN - Diabetic nephropathy; FSGS - Focal segmental glomerulosclerosis; IgAN - IgA nephropathy; SLE - systemic lupus erythematosus; MN - Membranous nephropathy; H-control - Healthy control; D-control - Diseased control (unpublished).*

5. DISCUSSION

5.1.Discussion 1 (EMT in HK-2 cells)

The HK-2 cell is widely used to study EMT in kidney tubules *in vitro*. However, different cell culture media have been used in published studies (165-167), which can lead to inconsistent experimental results. Therefore, we conducted a comparative study to investigate how different culture medium formulations affect cell behavior upon TGF-β1 administration, including cell morphology, gene expression pattern, and protein expression pattern. This is the first study to compare HK-2 cell morphology and expression patterns in different culture medium formulations.

In general, our research found that TGF-β1 induced EMT in all the culture media we used. We also discovered that HK-2 cells cultured in serum-free and DMEM 2% medium had a slower growth rate and smaller cell size than those cultured in other media. Interestingly, our study showed that cells grown in media with a higher proportion of FBS (10%) appeared enlarged, but we did not find any evidence suggesting a connection between PTECs size and FBS concentration. Another study reported increased size, similar to human pancreatic cancer spheres, when FBS was present (168). Further research is needed to understand the effects of FBS on cell growth and size. We also observed that cells grown in a hormonally defined medium looked more flattened and elongated. The slower growth rate of cells in the DMEM 2% medium was predictable since FBS is the main component of culture media supporting cell growth (169, 170).

Our study found that the gene expression of classic EMT markers *ACTA2, TGFB*, *VIM*, and *CTGF* was significantly increased in TGF-β1-induced HK-2 cells, irrespective of the culture medium used. This suggests that any of the tested medium formulations can be used to investigate the expression changes of these genes in a TGF-β1-induced system. This finding supports previously published research (171). The EMT model used in this study induced the expression of some mesenchymal markers such as α-SMA, VIM and FN. However, there were some differences between protein and mRNA expression results. Khundmiri and colleagues noted that protein expression in HK-2 cells could differ from mRNA expression in human kidney and primary PTECs due to the low percentage (26%) of proximal tubule-specific transcripts detected in the HK-2 cell line, as obtained from RNA-Sequencing (172).

The differential expression of genes and proteins may be explained by the lack of serum in the serum-free medium or interactions with other additives in the culture medium. Among these additives, EGF is a mitogen that aids cell proliferation, but its combination with TGF-β may cause primary PTECs hypertrophy and excessive accumulation of extracellular matrix

proteins (173). This could be the reason behind the higher expression of *COL4A1* in the KFSM medium supplemented with EGF compared to other media used in our study.

PPARγ is a nuclear receptor superfamily member shown to improve renal fibrogenesis (22, 122). Studies have found that PPARG is downregulated in fibrosis, and PPARγ agonists can potentially treat fibrotic diseases (22, 174, 175). Our findings support these studies, as we observed a significant decrease in *PPARG* expression in all medium formulations tested when exposed to TGF-β1 (**Fig. 9D**).

The EGR1 and EGR2 are believed to be essential for fibrosis in kidney diseases (126, 128, 176-178). In a previous study, we found evidence of a PPARG-EGR1 connection in TGF-β-induced renal fibrosis (22). Interestingly, EGR1 expression varied in response to TGF-β1 stimulation depending on the culture medium used. Despite increased TGF-β mRNA and protein expression and reduced PPARG in all media, we observed nuclear translocation of EGR1 only in two culture media tested. This suggests that EGR1's transcriptional activity may be influenced by the culture medium used. In contrast, EGR2 expression was significantly and similarly induced by TGF-β1 in all media investigated.

Interestingly, inflammatory mediators IL-6 and C3 expression depend on the type of cell culture media used. The kidney proximal tubular cells are exposed to various cytokines from glomerular filtration, and they synthesize complement proteins, including C3 and factors B and H (179, 180). Our study found that C3 production depended on the serum content of the medium, particularly in DMEM and DMEM/F12-based formulations. TGF-β induced C3 overexpression only in DMEM with 5% FBS medium. Previous research has shown that C3 decreases upon TGF-β1 in primary PTECs in a serum-free medium supplemented with hormones and EGF (181). This supports our observation as C3 was downregulated by 50% in the serum-free KSFM. The differences in FBS-supplemented media require further investigation.

It is essential to acknowledge the limitations of using cultured HK-2 cells as a model of the proximal tubule. These cells do not fully replicate the natural expression of apical/basal membrane transporters and metabolizing enzymes in the kidneys. *In vivo*, renal proximal tubular cells display metabolic zonation with different enzyme machinery and transporters along proximal tubule segments S1, S2, and S3 (182, 183). HK-2 cells may only represent one of these segments. Despite these limitations, HK-2 cells are widely used in translational research (184).

To gain a more detailed understanding of the effect of different medium formulations in HK-2 cells, it is necessary to investigate the long-term effect of TGF-β1-induced gene and

protein expression and regulation. Furthermore, future studies should investigate the effect of individual additives, hormones, growth factors, and insulin, e.g., on the TGF-β-induced EMT model in HK-2 cells.

5.1.Discussion 2 (PPARγ agonist in kidney fibrosis)

We have demonstrated that pioglitazone, a PPARγ agonist, can protect renal tubular cells from TGF-β1-induced pro-fibrotic response (Fig. 24). This protection was observed in both *in vitro* and *in vivo* settings. Pioglitazone ameliorated autophagy dysfunction, reduced pro-fibrotic miRNAs and EGR2, and inhibited inflammation. Notably, our study is the first to show that pioglitazone can prevent a significant increase in EGR2 expression induced by TGF-β1 in both mouse primary TECs and TGF-β transgenic mouse kidneys. Pioglitazone modulation was associated with reduced nuclear localization (shuttling) of EGR2.

The EGR2 protein is similar to EGR1 in structure and function, but they have distinct roles and are not interchangeable. EGR2 is critical in peripheral nerve myelination, adipogenesis, and immune tolerance (185). Its involvement in kidney fibrosis has been recently discovered (51). When TGF-β is present, EGR1 is quickly and transiently upregulated, which triggers the stimulation of EGR2 gene expression. Both EGR1 and EGR2 directly enhance collagen gene expression (185). *In vitro*, EGR2 overexpression induces the fibrotic response, while EGR2 silencing *in vitro* and *in vivo* inhibits the response. Additionally, EGR1 enhances renal collagen transcription and induces autophagy-related LC3B expression in pulmonary disease (186).

Some miRNAs with abnormal expression have also been associated with fibrosis progression (referred to as fibromiRs) and were postulated as potential therapeutic targets. The miR-199a-5p and -3p can be generated from miR-199a-1 and -2 precursors, and both can influence the TGF-β pathway. For instance, miR-199a-5p was reported to inhibit ER stress in renal IRI (187) and to down-regulate PPARγ, exacerbating renal interstitial fibrosis in rats with hyperuricemia (97). Elevated miR-199a-5p has also been reported in mouse and human CKD, underscoring its potential importance (99). On the other hand, PPARγ might regulate the expression of miR-199a-5p by influencing the processing or stability of pre-miR-199a at the post-transcriptional level (188). Other studies suggested miR-199a-3p to play a role in fibrosis development by regulating TGF-β signaling. Yang and colleagues showed that p53 increased renal miR-199a-3p expression, leading to STAT3 activation in UUO mice (98). In rats, subtotal nephrectomy induced renal miR-199a-3p overexpression (189). In renal TECs, miR-199a-3p expression was significantly elevated upon TGF-β1 treatment, and overexpression of miR-

199a-3p influenced collagen synthesis (190). Our experiments revealed that both miR-199a-5p and miR-199a-3p were similarly increased in TGF-β-treated primary TECs and the kidneys of TGF-β-overexpressing mice, but the PPARγ agonist pioglitazone alleviated the dysregulation of miR-199a-3p and miR-199a-5p.

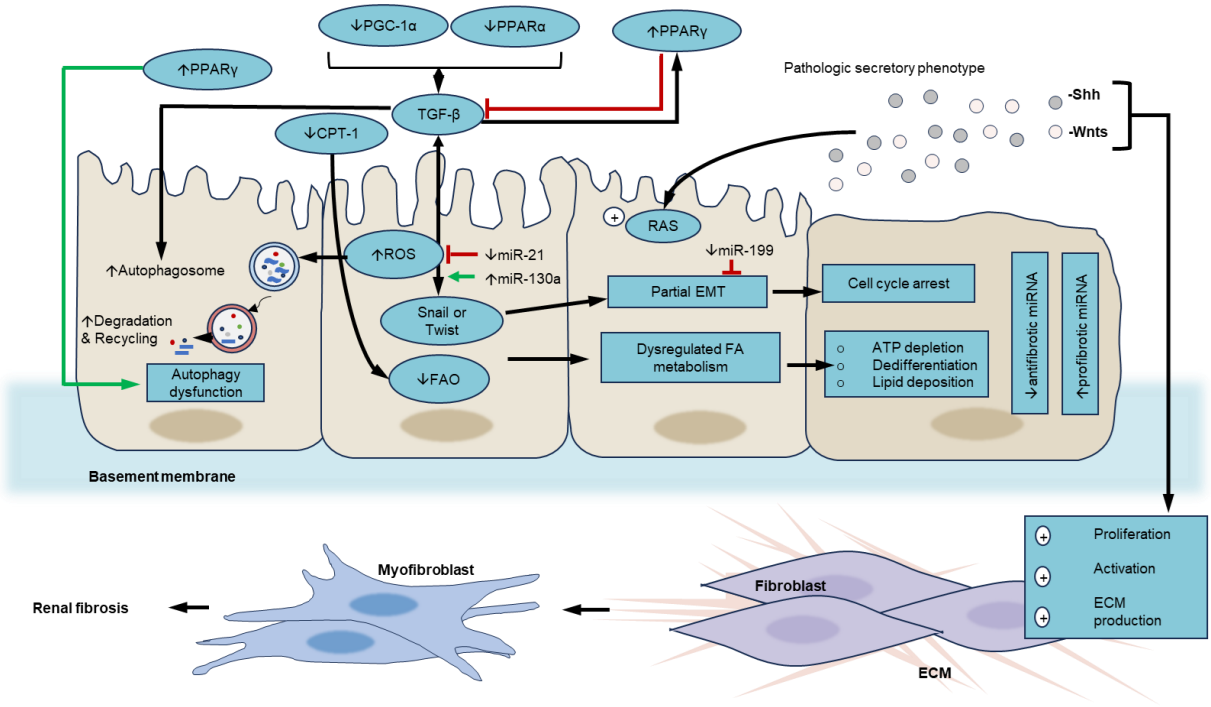

Figure 24. Proposed tubular cells respond to pro-fibrotic factors, leading to the development of kidney fibrosis. *The figure shows possible tubular cell responses to TGF-β overexpression, such as inflammation, autophagy dysfunction, and the expression of both anti- and pro-fibrotic miRNAs, in addition to the known tubular cell responses, such as overexpression of RAS, decreased FAO, cell cycle arrest and ECM production. PPARγ agonists can modulate these responses during kidney fibrosis. PPARγ agents are known to have off-target effects, but we propose a crosstalk between PPARγ and TGF-β expression during kidney fibrosis based on our PPARγ agonist results in vitro and in vivo models.* ***Abbreviations****: CPT-1 - Carnitine palmitoyltransferase 1α; ECM - Extracellular matrix; EMT - Epithelial to mesenchymal transition; FA - Fatty acid; FAO - Fatty acid oxidation; PGC-1α - PPARγ coactivator; ROS - Reactive oxygen species; Snail - Snail family zinc finger 1; RAS - Renin-angiotensin system; Shh - Sonic hedgehog signaling ligands; Wnts - Wnt/β-catenin signaling ligands. Image modified from D. Zhou and Y. Liu (39).*

TargetScan analysis suggests that PGC-1α coding genes *PPARGC1B, EGR1, FN1,* and *RUNX1* are among the miR-199a-3p target genes, and they are highly conserved (191).

However, the only *RUNX1* binding that was experimentally validated in the miRTarBase database (154), *EGR1, FN1,* and *PPARGC1B,* must be validated in further studies. During TGF-β1 overexpression, the levels of *RUNX1, EGR1*, miR-130a, and miR-199a-3p/5p increased in primary TECs and kidney tissue from TGF-β transgenic mice in our study. On the other hand, in administering a PPARγ agonist, all of them returned to the control group expression levels. This might explain the relationship between these genes, miRNAs, and PPARγ during renal fibrosis. However, we did not investigate the expression of *PPARGC1B* in our study, and researchers need to address this aspect further.

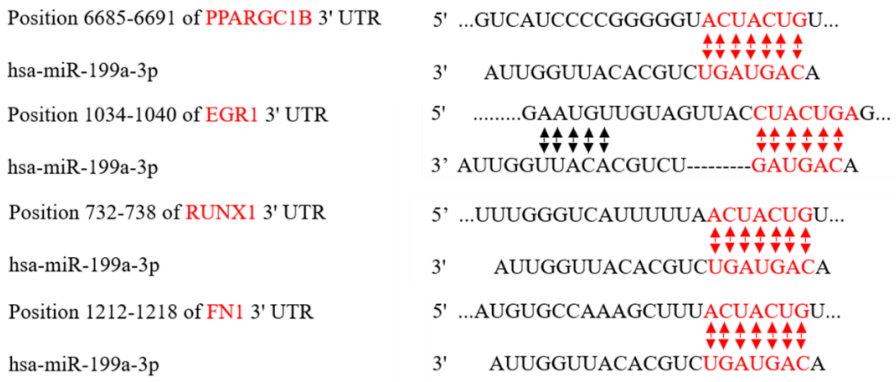

Figure 25. The conserved binding sites between miR-199a-3p and target genes 3'UTR. Abbreviations*: PPARGC1B - PGC-1α coding gene; EGR1 - Early growth response 1; FN1 - Fibronectin 1; RUNX1 - Runt-related transcription factor 1 (data retrieved from TargetScan (v.8.0) (155), unpublished).*

For instance, the inhibition of miR-130a-3p protected against renal fibrosis *in vitro* through the TGF-β1/Smad pathway (96). Our research team has previously reviewed that TGF-β1 decreases PPARγ mRNA via induction of the miR-130a/301b cluster in human and murine pulmonary artery smooth muscle cells (30). Additionally, PPARγ inhibits miR-130a expression in cardiac cells, and pioglitazone mitigates doxorubicin-induced cardiotoxicity via miR-130a (192). Corroborating these studies, we observed that five-week treatment with the PPARγ agonist pioglitazone reduced miR-130a expression to control levels in mice with TGF-β-induced kidney fibrosis. In addition, as previously demonstrated in HK-2 cells (193), the ability of pioglitazone to reduce miR-21 was also expressed in our mouse kidneys.

Studies have demonstrated that TGF-β1 has a dual effect on the regulation of autophagy (194). Persistent activation of autophagy can promote interstitial fibrosis and contribute to CKD. On the other hand, autophagy functions as a cytoprotective mechanism by negatively regulating mature TGF-β1 in renal PTECs (142).

In the kidney, PTECs exhibit relatively low levels of autophagy function, which TGF-β can induce (195). Mature TGF-β is degraded by the autophagic pathway when stimulated by TGF-β and auto-induction (196). Defective autophagy can worsen renal fibrosis, as seen in a rat model of UUO, where the administration of the autophagy inhibitor 3-MA enhanced tubular apoptosis and interstitial fibrosis (196, 197). Deletion of the autophagic protein beclin-1 in mice increased type-1 collagen deposition in the kidneys (195). LC3-deficient and beclin-1-deficient mice subjected to UUO also showed increased collagen deposition and TGF-β1 protein levels (196). Despite the transcriptional upregulation of autophagy-related genes, our experiments indicate that tubular SQSTM1 protein levels remained elevated, suggesting dysfunctional degradation via autophagy upon TGF-β induction in both primary TECs and the kidneys of TGF-β transgenic mice.

Several studies have verified the association between PPARγ and the pathways associated with autophagy. PPARγ agonists in bronchial epithelial cells have been shown to enhance the expression of autophagy-related proteins, including beclin-1 and LC3-II/I, while reducing the buildup of SQSTM1. These findings indicate that PPARγ can enhance autophagy (198). Our data confirm that the PPARγ agonist pioglitazone (a clinically proven anti-diabetic medication) has shown efficacy in decreasing the tubular buildup of SQSTM1. Furthermore, it restored the impaired autophagy caused by TGF-β both *in vitro* and *in vivo*.

The pathogenesis of kidney fibrosis can also be initiated or worsened by inflammation through multiple pathways, regulated by a complex interaction of different factors involving cytokines, chemokines, and adhesion molecules. CCL2 levels significantly correlated with the progression of interstitial fibrosis in human CKD patients (199). Suppression of IL-6 in TECs hampered interstitial fibrosis and tubular atrophy. Conversely, chronic administration of IL-6 enhanced the fibrotic process (34). Extracellular galectin-3 can modulate significant interactions between epithelial cells and the extracellular matrix (200), and the absence of galectin-3 protects against renal myofibroblast accumulation and activation in the UUO kidney fibrosis model (33). Additionally, studies suggest that functionally active C3 proteins and C3aR are expressed in PTECs and play an essential role in the pathogenesis of kidney fibrosis (201, 202). In our study, fibrotic kidneys and TGF-β-treated TECs exerted up-regulation of pro-inflammatory transcripts Il6, Ccl2, and Lgals3, successfully attenuated by pioglitazone treatment. Previous studies reported the anti-inflammatory actions of pioglitazone in coronary arteriosclerosis by reducing the expression of CCL2 receptor (CCR2) (203) as well as in traumatic brain injury by modulating the PPARγ/NF-κB/IL-6 pathway (204). As part of its anti-inflammatory effect, pioglitazone attenuated the renal C3 overexpression in our TGF-β

transgenic mice. Moreover, short-term pioglitazone administration exerted anti-inflammatory effects in DN patients as well (205).

5.2.Discussion 3 (miRNA in kidney diseases, meta-analyses)

First systematic review and meta-analysis:

The first meta-analysis was the new method to summarize hypothesis-free miRNA profiling studies by disease, sample type, and stages that might reveal novel miRNAs and avoid miRNA selection bias. To overcome the potential effects of various platforms and sample sizes, we implemented RRA (147, 148) and vote-counting (149) methods for statistical analysis. Overall, RRA and vote-counting results were consistent, and four up- and six down-regulated miRNAs in CKD patients and five up- and three down-regulated miRNAs in murine CKD models were identified. The enrichment analysis of top dysregulated miRNAs revealed their involvement in various pathways. These pathways are known to be associated with the pathogenesis of CKD (**Fig. 20**) (206-208).

In our study, miR-21a-5p, miR-223-3p, and miR-214-3p were up-regulated in murine experimental CKD, while miR-21-5p was up-regulated in CKD patients. These findings are consistent with a previous meta-analysis of kidney fibrosis (209). In the meta-analysis of DN, three up-regulated and two down-regulated miRNAs were previously reported, but only miR-21-5p overlapped with our analysis (210). A meta-analysis of LN patients identified five meta-signatures in kidney tissue, 9 in blood, and 5 in urine samples, but only miR-1260b, miR-21-5p, and miR-155 corroborate our results (211). Our study focused only on hypothesis-free miRNA profiling studies that included healthy controls, which might explain the differences in top-listed miRNAs compared to previous studies.

Second systematic review and meta-analysis:

Our objective was to assess the accuracy of single and panel miRNAs in diagnosing kidney diseases using various sample types. After a meta-analysis, we found that panel miRNAs more effectively detect kidney diseases than single miRNAs. Furthermore, the overall diagnostic performance of miRNAs, the pAUC, was better when comparing kidney disease patients to healthy controls rather than diseased controls. In addition, urinary miRNAs tended to exhibit higher diagnostic accuracy with an overall pAUC of 0.86 compared to blood samples with an overall pAUC of 0.82.

Previous studies are in agreement with our finding that the diagnostic accuracy of the panel of miRNAs is superior to that of single miRNAs (212). We also considered specific

kidney diseases and conducted separate analyses for healthy and diseased control groups while considering the correlation between results from the same population. In addition, we performed a pooled analysis for AUC values from each study to determine overall diagnostic accuracy, eliminating the possibility of threshold effects.

We found that certain panels of miRNAs had higher overall AUC when comparing DN, LN, or FSGS to healthy controls. These panels include miR-15b, miR-34a, miR-636 for DN, miR-21, miR-150, miR-423 for LN and miR-125b, miR-186, miR-193a-3p for FSGS. For disease control studies, panels of miRNAs, such as miR-21 and miR-30-b-5p, had better overall AUC differentiating between DN vs. T2DM patients. Similarly, panels of miR-29c, miR-150, and miR-21 effectively distinguished LN from SLE patients. Another study by J. Li and colleagues also identified specific miRNA panels that were superior for CKD, such as miR-27b-3p and miR-1228-3p for DN, miR-21, miR-150, and miR-29c for LN, miR-106a-5p, and miR-30a-5p for mesangial proliferative glomerulonephritis (212).

In comparison, our findings may differ slightly from those of J. Li and colleagues, it is essential to note that our analysis included separate controls for healthy and diseased individuals with various kidney diseases. Multiple studies on cancer have also shown that a miRNA panel is a more effective diagnostic marker than a single miRNA (213). For instance, Bhaskaran V and colleagues reported that several miRNAs showed a clustered expression pattern in glioblastoma, even if not encoded in the same genetic locus (214). Moreover, they focused on targeting several miRNAs simultaneously; as a result, co-expressed miRNAs allow repression of epigenetic oncogenic signaling pathways and have more profound therapeutic effects than single miRNA therapy (214). In nephrology, it might also be helpful to consider the expression of miRNA clusters and test a miRNA panel for diagnostic purposes.

6. CONCLUSIONS

Our study concludes that the behavior of HK-2 cells during TGF-β1-induced *in vitro* EMT can be affected by cell culture medium formulations. Although TGF-β1 triggers EMT in all investigated culture medium formulations in HK-2 cells, the activation of EGR1 and the inflammatory response varies. Therefore, it is crucial to carefully select cell culture medium formulations and explain the expression of EMT and pro- and anti-fibrotic markers in TGF-β1-induced HK-2 cells, as it should not be ignored in translational research.

Taken together with results from the second experimental study, we propose that pioglitazone treatment can rescue the dysfunctional autophagic activity in TGF-β1 induced renal fibrosis and facilitate the clearance of damaged cellular organelles, restoring cellular function. This effect and the decreased expression of fibromiRs and pro-inflammatory molecules (**Fig. 16-17**) likely account for the potential anti-fibrotic, anti-inflammatory, and protective effects of PPAR agonists in CKD, which are highly relevant according to clinical therapy.

Two meta-analysis approaches showed us the importance of miRNA dysregulation in CKD and their usage as diagnostic biomarkers. In addition, dysregulated miRNAs could be specific to disease, biological samples, and disease stages in CKD patients. From the diagnostic accuracy analyses, miRNAs could differentiate CKD patients, healthy individuals, and disease patients without overt CKD. The panel miRNAs were more compelling to diagnose CKD patients than single miRNAs. However, the fewer published articles in this field complicated the meta-analysis approach and did not provide the possibility to synthesize data on each kidney disease.

Novelty of the thesis:

- Highlighting the variety of cell culture medium-related biases in the TGF-β-induced EMT model *in vitro*.
- miR-199-3p and miR-199-5p are involved in TGF-β-induced kidney fibrosis *in vitro* and *in vivo*. The antifibrotic effect of PPARγ might be related to miR-199 and its target genes.
- Using systematic review and meta-analysis approaches to identify most dysregulated miRNAs from studies focused on hypothesis-free assays and identifying targeted molecular pathways are relatively new methods in translational nephrology.

7. SUMMARY

CKD is a significant health challenge that affects 13.4 percent of the global adult population (3). It is a leading cause of mortality (4), and patients often face irreversible structural and functional losses in their kidneys. However, recent research has shed light on several promising avenues for tackling kidney fibrosis. These include exploring TGF-β-induced renal fibrosis models, which have helped researchers gain a deeper understanding of the molecular basis of this condition. Dysregulation of autophagy and miRNAs also appear to play critical roles in kidney injury besides well-known fibrotic and inflammatory processes, and further study in this area may yield new insights into the development of diagnostic markers and therapeutic agents. In addition to novel therapeutic approaches, repurposing existing medications is a timeless strategy for enhancing health outcomes — for example, the anti-diabetic PPARγ agonist pioglitazone is known to have anti-fibrotic effects.

In this thesis, we elucidated four separate projects focused on different aspects of kidney fibrosis: **1)** human PTECs response to the pro-fibrotic cytokine, TGF-β1, and variety of cell culture medium can influence the understanding of the fibrotic mechanisms *in vitro*; **2)** in addition to the previously known anti-fibrotic effect of pioglitazone *in vivo* from our research group, anti-fibrotic and -inflammatory effects were validated in TEC, *in vitro*. Additionally, there was miRNA dysregulation and autophagy dysfunction in TGF-β-induced kidney fibrosis. The administration of pioglitazone attenuated these processes; **3)** using systematic review and meta-analysis approaches, the most dysregulated miRNAs in human and murine models of CKD and diagnostic performance of miRNA in human CKDs were determined. The panel miRNAs had better diagnostic performance than single miRNAs in any biological sample type.

The following conclusions were drawn from our studies: **1)** In translational research, experimental factors, such as culture medium variability, can lead to inconclusive results, especially in the TGF-β-induced EMT model in HK-2 cells; **2)** Pioglitazone has an anti-fibrotic effect and has the potential to regulate miRNA and macroautophagy function. Our *in vitro* and *in vivo* kidney fibrosis model results may indicate that we can repurpose pioglitazone to treat CKD. However, adverse reactions due to the activation of PPARγ, such as fluid retention, are a concern in the clinic. Understanding the molecular mechanism of PPARγ in CKD can increase the chance of developing targeted agents with fewer adverse reactions in the future; **3)** Lastly, miRNA dysregulation is common during CKD. These miRNAs have the potential to be used as biomarkers in CKD.

8. REFERENCES

1. Chertow GM, Marsden PA, Skorecki K, Luyckx V, Taal MW, Yu ASL. Brenner & Rector's the kidney: Elsevier; 2019.

2. Rosenberg M. Overview of the management of chronic kidney disease in adults. UpToDate, Wolters Kluwer 2024 (Accessed on July 26, 2024).

3. Hill NR, Fatoba ST, Oke JL, Hirst JA, O'Callaghan CA, Lasserson DS, Hobbs FD. Global Prevalence of Chronic Kidney Disease - A Systematic Review and Meta-Analysis. PLoS One. 2016;11(7):e0158765.

4. Collaborators GBDCoD. Global, regional, and national age-sex specific mortality for 264 causes of death, 1980-2016: a systematic analysis for the Global Burden of Disease Study 2016. Lancet. 2017;390(10100):1151-1210.

5. Foreman KJ, Marquez N, Dolgert A, Fukutaki K, Fullman N, McGaughey M, Pletcher MA, Smith AE, Tang K, Yuan CW, Brown JC, Friedman J, He J, Heuton KR, Holmberg M, Patel DJ, Reidy P, Carter A, Cercy K, Chapin A, Douwes-Schultz D, Frank T, Goettsch F, Liu PY, Nandakumar V, Reitsma MB, Reuter V, Sadat N, Sorensen RJD, Srinivasan V, Updike RL, York H, Lopez AD, Lozano R, Lim SS, Mokdad AH, Vollset SE, Murray CJL. Forecasting life expectancy, years of life lost, and all-cause and cause-specific mortality for 250 causes of death: reference and alternative scenarios for 2016-40 for 195 countries and territories. Lancet. 2018;392(10159):2052-2090.

6. Kidney Disease: Improving Global Outcomes (KDIGO) CKD Work Group. KDIGO 2024 Clinical Practice Guideline for the Evaluation and Management of Chronic Kidney Disease. Kidney Int. 2024;105(4S):S117-S314.

7. Bidin MZ, Shah AM, Stanslas J, Seong CLT. Blood and urine biomarkers in chronic kidney disease: An update. Clin Chim Acta. 2019;495:239-250.

8. Rysz J, Gluba-Brzozka A, Franczyk B, Jablonowski Z, Cialkowska-Rysz A. Novel Biomarkers in the Diagnosis of Chronic Kidney Disease and the Prediction of Its Outcome. Int J Mol Sci. 2017;18(8).

9. Meng X-m, Nikolic-Paterson DJ, Lan HY. TGF-β: the master regulator of fibrosis. Nature Reviews Nephrology. 2016;12(6):325-338.

10. Ma T-T, Meng X-M. TGF-β/Smad and Renal Fibrosis. In: Liu B-C, Lan H-Y, Lv L-L, editors. Renal Fibrosis: Mechanisms and Therapies. Singapore: Springer Singapore; 2019. p. 347-364.

11. Yu L, Border WA, Huang Y, Noble NA. TGF-beta isoforms in renal fibrogenesis. Kidney Int. 2003;64(3):844-856.

12. Sanderson N, Factor V, Nagy P, Kopp J, Kondaiah P, Wakefield L, Roberts AB, Sporn MB, Thorgeirsson SS. Hepatic expression of mature transforming growth factor beta 1 in transgenic mice results in multiple tissue lesions. Proc Natl Acad Sci U S A. 1995;92(7):2572-2576.

13. Böttinger EP, Bitzer M. TGF-beta signaling in renal disease. J Am Soc Nephrol. 2002;13(10):2600-2610.

14. López-Hernández FJ, López-Novoa JM. Role of TGF-β in chronic kidney disease: an integration of tubular, glomerular and vascular effects. Cell Tissue Res. 2012;347(1):141-154.

15. Wanner N, Bechtel-Walz W. Epigenetics of kidney disease. Cell Tissue Res. 2017;369(1):75-92.

16. Kanwar YS, Sun L, Xie P, Liu FY, Chen S. A glimpse of various pathogenetic mechanisms of diabetic nephropathy. Annu Rev Pathol. 2011;6:395-423.

17. Gewin LS. Renal fibrosis: Primacy of the proximal tubule. Matrix Biology. 2018;68-69:248-262.

18. Edeling M, Ragi G, Huang S, Pavenstadt H, Susztak K. Developmental signalling pathways in renal fibrosis: the roles of Notch, Wnt and Hedgehog. Nat Rev Nephrol. 2016;12(7):426-439.

19. Peng Z, Wang H, Zheng J, Wang J, Xiang Y, Liu C, Ji M, Liu H, Pan L, Qin X, Qu X. Is the proximal tubule the focus of tubulointerstitial fibrosis? Heliyon. 2023;9(2):e13508.

20. Mitrofanova A, Merscher S, Fornoni A. Kidney lipid dysmetabolism and lipid droplet accumulation in chronic kidney disease. Nat Rev Nephrol. 2023;19(10):629-645.

21. Agarwal R, Saha C, Battiwala M, Vasavada N, Curley T, Chase SD, Sachs N, Semret MH. A pilot randomized controlled trial of renal protection with pioglitazone in diabetic nephropathy. Kidney Int. 2005;68(1):285-292.

22. Németh Á, Mózes MM, Calvier L, Hansmann G, Kökény G. The PPARγ agonist pioglitazone prevents TGF-β induced renal fibrosis by repressing EGR-1 and STAT3. BMC Nephrol. 2019;20(1):245.

23. Dihazi H, Dihazi GH, Bibi A, Eltoweissy M, Mueller CA, Asif AR, Rubel D, Vasko R, Mueller GA. Secretion of ERP57 is important for extracellular matrix accumulation and progression of renal fibrosis, and is an early sign of disease onset. J Cell Sci. 2013;126(Pt 16):3649-3663.

24. Li Q, Chen C, Chen X, Han M, Li J. Dexmedetomidine attenuates renal fibrosis via α2-adrenergic receptor-dependent inhibition of cellular senescence after renal ischemia/reperfusion. Life sciences. 2018;207:1-8.

25. Matsui F, Meldrum KK. The role of the Janus kinase family/signal transducer and activator of transcription signaling pathway in fibrotic renal disease. The Journal of surgical research. 2012;178(1):339-345.
26. Huang JS, Guh JY, Hung WC, Yang ML, Lai YH, Chen HC, Chuang LY. Role of the Janus kinase (JAK)/signal transducters and activators of transcription (STAT) cascade in advanced glycation end-product-induced cellular mitogenesis in NRK-49F cells. The Biochemical journal. 1999;342(Pt 1):231-238.
27. Nakajima H, Takenaka M, Kaimori JY, Hamano T, Iwatani H, Sugaya T, Ito T, Hori M, Imai E. Activation of the signal transducer and activator of transcription signaling pathway in renal proximal tubular cells by albumin. J Am Soc Nephrol. 2004;15(2):276-285.
28. Kuratsune M, Masaki T, Hirai T, Kiribayashi K, Yokoyama Y, Arakawa T, Yorioka N, Kohno N. Signal transducer and activator of transcription 3 involvement in the development of renal interstitial fibrosis after unilateral ureteral obstruction. Nephrology (Carlton). 2007;12(6):565-571.
29. Ogata H, Chinen T, Yoshida T, Kinjyo I, Takaesu G, Shiraishi H, Iida M, Kobayashi T, Yoshimura A. Loss of SOCS3 in the liver promotes fibrosis by enhancing STAT3-mediated TGF-beta1 production. Oncogene. 2006;25(17):2520-2530.
30. Calvier L, Chouvarine P, Legchenko E, Hoffmann N, Geldner J, Borchert P, Jonigk D, Mozes MM, Hansmann G. PPARgamma Links BMP2 and TGFbeta1 Pathways in Vascular Smooth Muscle Cells, Regulating Cell Proliferation and Glucose Metabolism. Cell Metab. 2017;25(5):1118-1134 e1117.
31. Yang X, Lin Y, Shi Y, Li B, Liu W, Yin W, Dang Y, Chu Y, Fan J, He R. FAP Promotes Immunosuppression by Cancer-Associated Fibroblasts in the Tumor Microenvironment via STAT3-CCL2 Signaling. Cancer research. 2016;76(14):4124-4135.
32. Lv LL, Feng Y, Wen Y, Wu WJ, Ni HF, Li ZL, Zhou LT, Wang B, Zhang JD, Crowley SD, Liu BC. Exosomal CCL2 from Tubular Epithelial Cells Is Critical for Albumin-Induced Tubulointerstitial Inflammation. J Am Soc Nephrol. 2018;29(3):919-935.
33. Henderson NC, Mackinnon AC, Farnworth SL, Kipari T, Haslett C, Iredale JP, Liu FT, Hughes J, Sethi T. Galectin-3 expression and secretion links macrophages to the promotion of renal fibrosis. Am J Pathol. 2008;172(2):288-298.
34. Ranganathan P, Jayakumar C, Ramesh G. Proximal tubule-specific overexpression of netrin-1 suppresses acute kidney injury-induced interstitial fibrosis and glomerulosclerosis through suppression of IL-6/STAT3 signaling. Am J Physiol Renal Physiol. 2013;304(8):F1054-1065.

35. Tang Z, Lu B, Hatch E, Sacks SH, Sheerin NS. C3a mediates epithelial-to-mesenchymal transition in proteinuric nephropathy. J Am Soc Nephrol. 2009;20(3):593-603.
36. Bao L, Wang Y, Haas M, Quigg RJ. Distinct roles for C3a and C5a in complement-induced tubulointerstitial injury. Kidney Int. 2011;80(5):524-534.
37. Zhou T, Luo M, Cai W, Zhou S, Feng D, Xu C, Wang H. Runt-Related Transcription Factor 1 (RUNX1) Promotes TGF-β-Induced Renal Tubular Epithelial-to-Mesenchymal Transition (EMT) and Renal Fibrosis through the PI3K Subunit p110δ. EBioMedicine. 2018;31:217-225.
38. Zeng L-F, Xiao Y, Sun L. A Glimpse of the Mechanisms Related to Renal Fibrosis in Diabetic Nephropathy. In: Liu B-C, Lan H-Y, Lv L-L, editors. Renal Fibrosis: Mechanisms and Therapies. Singapore: Springer Singapore; 2019. p. 49-79.
39. Zhou D, Liu Y. Renal fibrosis in 2015: Understanding the mechanisms of kidney fibrosis. Nat Rev Nephrol. 2016;12(2):68-70.
40. Kramann R, DiRocco DP, Humphreys BD. Understanding the origin, activation and regulation of matrix-producing myofibroblasts for treatment of fibrotic disease. J Pathol. 2013;231(3):273-289.
41. Humphreys BD, Lin SL, Kobayashi A, Hudson TE, Nowlin BT, Bonventre JV, Valerius MT, McMahon AP, Duffield JS. Fate tracing reveals the pericyte and not epithelial origin of myofibroblasts in kidney fibrosis. Am J Pathol. 2010;176(1):85-97.
42. Humphreys BD. Mechanisms of Renal Fibrosis. Annu Rev Physiol. 2018;80:309-326.
43. Kalluri R, Weinberg RA. The basics of epithelial-mesenchymal transition. J Clin Invest. 2009;119(6):1420-1428.
44. Zeisberg M, Neilson EG. Biomarkers for epithelial-mesenchymal transitions. J Clin Invest. 2009;119(6):1429-1437.
45. Tian YC, Phillips AO. TGF-beta1-mediated inhibition of HK-2 cell migration. Journal of the American Society of Nephrology.14(3):631-640.
46. Wang Z, Divanyan A, Jourd'heuil FL, Goldman RD, Ridge KM, Jourd'heuil D, Lopez-Soler RI. Vimentin expression is required for the development of EMT-related renal fibrosis following unilateral ureteral obstruction in mice. Am J Physiol Renal Physiol. 2018;315(4):F769-F780.
47. Zhou M, Ma H, Lin H, Qin J. Induction of epithelial-to-mesenchymal transition in proximal tubular epithelial cells on microfluidic devices. Biomaterials. 2014;35(5):1390-1401.

48. Le Clef N, Verhulst A, D'Haese PC, Vervaet BA. Unilateral Renal Ischemia-Reperfusion as a Robust Model for Acute to Chronic Kidney Injury in Mice. PLoS One. 2016;11(3):e0152153.
49. Luo W, Tang S, Xiao X, Luo S, Yang Z, Huang W, Tang S. Translation Animal Models of Diabetic Kidney Disease: Biochemical and Histological Phenotypes, Advantages and Limitations. Diabetes Metab Syndr Obes. 2023;16:1297-1321.
50. Liang J, Liu Y. Animal Models of Kidney Disease: Challenges and Perspectives. Kidney360. 2023;4(10):1479-1493.
51. Kökény G, Németh Á, Kopp JB, Chen W, Oler AJ, Manzéger A, Rosivall L, Mózes MM. Susceptibility to kidney fibrosis in mice is associated with early growth response-2 protein and tissue inhibitor of metalloproteinase-1 expression. Kidney Int. 2022;102(2):337-354.
52. Hosszu A, Kaucsar T, Seeliger E, Fekete A. Animal Models of Renal Pathophysiology and Disease. Methods Mol Biol. 2021;2216:27-44.
53. He X, Zhang T, Tolosa M, Goru SK, Chen X, Misra PS, Robinson LA, Yuen DA. A new, easily generated mouse model of diabetic kidney fibrosis. Scientific Reports. 2019;9(1):12549.
54. Lee RC, Feinbaum RL, Ambros V. The C. elegans heterochronic gene lin-4 encodes small RNAs with antisense complementarity to lin-14. Cell. 1993;75(5):843-854.
55. Kozomara A, Birgaoanu M, Griffiths-Jones S. miRBase: from microRNA sequences to function. Nucleic Acids Res. 2019;47(D1):D155-D162.
56. Bartel DP. MicroRNAs: target recognition and regulatory functions. Cell. 2009;136(2):215-233.
57. Filipowicz W, Jaskiewicz L, Kolb FA, Pillai RS. Post-transcriptional gene silencing by siRNAs and miRNAs. Curr Opin Struct Biol. 2005;15(3):331-341.
58. Sridharan K, Gogtay NJ. Therapeutic nucleic acids: current clinical status. Br J Clin Pharmacol. 2016;82(3):659-672.
59. Trionfini P, Benigni A, Remuzzi G. MicroRNAs in kidney physiology and disease. Nat Rev Nephrol. 2015;11(1):23-33.
60. Kriegel AJ, Liu Y, Fang Y, Ding X, Liang M. The miR-29 family: genomics, cell biology, and relevance to renal and cardiovascular injury. Physiol Genomics. 2012;44(4):237-244.
61. Krol J, Loedige I, Filipowicz W. The widespread regulation of microRNA biogenesis, function and decay. Nat Rev Genet. 2010;11(9):597-610.

62. Baskerville S, Bartel DP. Microarray profiling of microRNAs reveals frequent coexpression with neighboring miRNAs and host genes. Rna. 2005;11(3):241-247.
63. Kato M, Wang L, Putta S, Wang M, Yuan H, Sun G, Lanting L, Todorov I, Rossi JJ, Natarajan R. Post-transcriptional up-regulation of Tsc-22 by Ybx1, a target of miR-216a, mediates TGF-{beta}-induced collagen expression in kidney cells. J Biol Chem. 2010;285(44):34004-34015.
64. Lee Y, Kim M, Han J, Yeom KH, Lee S, Baek SH, Kim VN. MicroRNA genes are transcribed by RNA polymerase II. Embo j. 2004;23(20):4051-4060.
65. Bohnsack MT, Czaplinski K, Gorlich D. Exportin 5 is a RanGTP-dependent dsRNA-binding protein that mediates nuclear export of pre-miRNAs. Rna. 2004;10(2):185-191.
66. Mahtal N, Lenoir O, Tinel C, Anglicheau D, Tharaux P-L. MicroRNAs in kidney injury and disease. Nature Reviews Nephrology. 2022;18(10):643-662.
67. Brennecke J, Stark A, Russell RB, Cohen SM. Principles of microRNA-target recognition. PLoS Biol. 2005;3(3):e85.
68. Small EM, Olson EN. Pervasive roles of microRNAs in cardiovascular biology. Nature. 2011;469(7330):336-342.
69. Chau BN, Xin C, Hartner J, Ren S, Castano AP, Linn G, Li J, Tran PT, Kaimal V, Huang X, Chang AN, Li S, Kalra A, Grafals M, Portilla D, MacKenna DA, Orkin SH, Duffield JS. MicroRNA-21 promotes fibrosis of the kidney by silencing metabolic pathways. Sci Transl Med. 2012;4(121):121ra118.
70. Denby L, Ramdas V, Lu R, Conway BR, Grant JS, Dickinson B, Aurora AB, McClure JD, Kipgen D, Delles C, van Rooij E, Baker AH. MicroRNA-214 antagonism protects against renal fibrosis. J Am Soc Nephrol. 2014;25(1):65-80.
71. Lorenzen JM, Haller H, Thum T. MicroRNAs as mediators and therapeutic targets in chronic kidney disease. Nature Reviews Nephrology. 2011;7(5):286-294.
72. Sequeira-Lopez ML, Weatherford ET, Borges GR, Monteagudo MC, Pentz ES, Harfe BD, Carretero O, Sigmund CD, Gomez RA. The microRNA-processing enzyme dicer maintains juxtaglomerular cells. J Am Soc Nephrol. 2010;21(3):460-467.
73. Xi Y, Nakajima G Fau - Gavin E, Gavin E Fau - Morris CG, Morris Cg Fau - Kudo K, Kudo K Fau - Hayashi K, Hayashi K Fau - Ju J, Ju J. Systematic analysis of microRNA expression of RNA extracted from fresh frozen and formalin-fixed paraffin-embedded samples. (1355-8382 (Print)).

74. Zankar S, Trentin-Sonoda M, Viñas JL, Rodriguez RA, Bailey A, Allan D, Burns KD. Therapeutic effects of micro-RNAs in preclinical studies of acute kidney injury: a systematic review and meta-analysis. Scientific Reports. 2021;11(1):9100.

75. Mall C, Rocke DM, Durbin-Johnson B, Weiss RH. Stability of miRNA in human urine supports its biomarker potential. Biomark Med. 2013;7(4):623-631.

76. Mitchell PS, Parkin RK, Kroh EM, Fritz BR, Wyman SK, Pogosova-Agadjanyan EL, Peterson A, Noteboom J, O'Briant KC, Allen A, Lin DW, Urban N, Drescher CW, Knudsen BS, Stirewalt DL, Gentleman R, Vessella RL, Nelson PS, Martin DB, Tewari M. Circulating microRNAs as stable blood-based markers for cancer detection. Proc Natl Acad Sci U S A. 2008;105(30):10513-10518.

77. Zurbig P, Dihazi H, Metzger J, Thongboonkerd V, Vlahou A. Urine proteomics in kidney and urogenital diseases: Moving towards clinical applications. Proteomics Clin Appl. 2011;5(5-6):256-268.

78. Sun Y, Koo S, White N, Peralta E, Esau C, Dean NM, Perera RJ. Development of a micro-array to detect human and mouse microRNAs and characterization of expression in human organs. Nucleic Acids Res. 2004;32(22):e188.

79. Naraba H, Iwai N. Assessment of the microRNA system in salt-sensitive hypertension. Hypertens Res. 2005;28(10):819-826.

80. Kato M, Zhang J, Wang M, Lanting L, Yuan H, Rossi JJ, Natarajan R. MicroRNA-192 in diabetic kidney glomeruli and its function in TGF-beta-induced collagen expression via inhibition of E-box repressors. Proc Natl Acad Sci U S A. 2007;104(9):3432-3437.

81. Harvey SJ, Jarad G, Cunningham J, Goldberg S, Schermer B, Harfe BD, McManus MT, Benzing T, Miner JH. Podocyte-specific deletion of dicer alters cytoskeletal dynamics and causes glomerular disease. J Am Soc Nephrol. 2008;19(11):2150-2158.

82. Huang Z, Shi J, Gao Y, Cui C, Zhang S, Li J, Zhou Y, Cui Q. HMDD v3.0: a database for experimentally supported human microRNA-disease associations. Nucleic Acids Res. 2019;47(D1):D1013-d1017.

83. Keller A, Gröger L, Tschernig T, Solomon J, Laham O, Schaum N, Wagner V, Kern F, Schmartz GP, Li Y, Borcherding A, Meier C, Wyss-Coray T, Meese E, Fehlmann T, Ludwig N. miRNATissueAtlas2: an update to the human miRNA tissue atlas. Nucleic Acids Res. 2022;50(D1):D211-d221.

84. Lv L-Z. The urinary RNA atlas of patients with chronic kidney disease. Scientific Reports. 2023;13(1):19084.

85. Gomez IG, Nakagawa N, Duffield JS. MicroRNAs as novel therapeutic targets to treat kidney injury and fibrosis. Am J Physiol Renal Physiol. 2016;310(10):F931-944.
86. Gluba-Sagr A, Franczyk B, Rysz-Górzyńska M, Ławiński J, Rysz J. The Role of miRNA in Renal Fibrosis Leading to Chronic Kidney Disease. Biomedicines. 2023;11(9).
87. Liu F, Zhuang S. New Therapies for the Treatment of Renal Fibrosis. In: Liu B-C, Lan H-Y, Lv L-L, editors. Renal Fibrosis: Mechanisms and Therapies. Singapore: Springer Singapore; 2019. p. 625-659.
88. Gomez IG, MacKenna DA, Johnson BG, Kaimal V, Roach AM, Ren S, Nakagawa N, Xin C, Newitt R, Pandya S, Xia TH, Liu X, Borza DB, Grafals M, Shankland SJ, Himmelfarb J, Portilla D, Liu S, Chau BN, Duffield JS. Anti-microRNA-21 oligonucleotides prevent Alport nephropathy progression by stimulating metabolic pathways. J Clin Invest. 2015;125(1):141-156.
89. Zarjou A, Yang S Fau - Abraham E, Abraham E Fau - Agarwal A, Agarwal A Fau - Liu G, Liu G. Identification of a microRNA signature in renal fibrosis: role of miR-21. Am J Physiol Renal Physiol. October 2011;301(4): F793–F801.
90. Li D, Lu Z, Jia J, Zheng Z, Lin S. MiR-124 is Related to Podocytic Adhesive Capacity Damage in STZ-Induced Uninephrectomized Diabetic Rats. Kidney and Blood Pressure Research. 2013;37(4-5):422-431.
91. Zhao B, Li H, Liu J, Han P, Zhang C, Bai H, Yuan X, Wang X, Li L, Ma H, Jin X, Chu Y. MicroRNA-23b Targets Ras GTPase-Activating Protein SH3 Domain-Binding Protein 2 to Alleviate Fibrosis and Albuminuria in Diabetic Nephropathy. J Am Soc Nephrol. 2016;27(9):2597-2608.
92. Li J, Ma L, Yu H, Yao Y, Xu Z, Lin W, Wang L, Wang X, Yang H. MicroRNAs as Potential Biomarkers for the Diagnosis of Chronic Kidney Disease: A Systematic Review and Meta-Analysis. Front Med (Lausanne). 2021;8:782561.
93. Assmann TS, Recamonde-Mendoza M, de Souza BM, Bauer AC, Crispim D. MicroRNAs and diabetic kidney disease: Systematic review and bioinformatic analysis. Mol Cell Endocrinol. 2018;477:90-102.
94. Butz H, Rácz K, Hunyady L, Patócs A. Crosstalk between TGF-β signaling and the microRNA machinery. Trends Pharmacol Sci. 2012;33(7):382-393.
95. Li R, Chung AC, Yu X, Lan HY. MicroRNAs in Diabetic Kidney Disease. Int J Endocrinol. 2014;2014:593956.

96. Ai K, Zhu X, Kang Y, Li H, Zhang L. miR-130a-3p inhibition protects against renal fibrosis in vitro via the TGF-beta1/Smad pathway by targeting SnoN. Experimental and molecular pathology. 2020;112:104358.
97. Du P, Chen M, Deng C, Zhu C. microRNA-199a downregulation alleviates hyperuricemic nephropathy via the PPARgamma/beta-catenin axis. Journal of receptor and signal transduction research. 2022;42(4):373-381.
98. Yang R, Xu X, Li H, Chen J, Xiang X, Dong Z, Zhang D. p53 induces miR199a-3p to suppress SOCS7 for STAT3 activation and renal fibrosis in UUO. Sci Rep. 2017;7:43409.
99. Deng L, Xu G, Huang Q. Comprehensive analyses of the microRNA-messenger RNA-transcription factor regulatory network in mouse and human renal fibrosis. Frontiers in genetics. 2022;13:925097.
100. Sun Z, Ma Y, Chen F, Wang S, Chen B, Shi J. miR-133b and miR-199b knockdown attenuate TGF-beta1-induced epithelial to mesenchymal transition and renal fibrosis by targeting SIRT1 in diabetic nephropathy. Eur J Pharmacol. 2018;837:96-104.
101. Kersten S, Desvergne B, Wahli W. Roles of PPARs in health and disease. Nature. 2000;405(6785):421-424.
102. Rigano D, Sirignano C, Taglialatela-Scafati O. The potential of natural products for targeting PPARα. Acta Pharm Sin B. 2017;7(4):427-438.
103. Seiri P, Abi A, Soukhtanloo M. PPAR-γ: Its ligand and its regulation by microRNAs. J Cell Biochem. 2019;120(7):10893-10908.
104. Diep QN, Amiri F, Touyz RM, Cohn JS, Endemann D, Neves MF, Schiffrin EL. PPARalpha activator effects on Ang II-induced vascular oxidative stress and inflammation. Hypertension. 2002;40(6):866-871.
105. Luquet S, Lopez-Soriano J, Holst D, Fredenrich A, Melki J, Rassoulzadegan M, Grimaldi PA. Peroxisome proliferator-activated receptor delta controls muscle development and oxidative capability. FASEB J. 2003;17(15):2299-2301.
106. Barak Y, Nelson MC, Ong ES, Jones YZ, Ruiz-Lozano P, Chien KR, Koder A, Evans RM. PPAR gamma is required for placental, cardiac, and adipose tissue development. Mol Cell. 1999;4(4):585-595.
107. Schupp M, Lazar MA. Endogenous ligands for nuclear receptors: digging deeper. J Biol Chem. 2010;285(52):40409-40415.
108. Fajas L, Auboeuf D, Raspé E, Schoonjans K, Lefebvre A-M, Saladin R, Najib J, Laville M, Fruchart J-C, Deeb S, Vidal-Puig A, Flier J, Briggs MR, Staels B, Vidal H, Auwerx J. The

Organization, Promoter Analysis, and Expression of the Human PPARγ Gene*. Journal of Biological Chemistry. 1997;272(30):18779-18789.
109. Sauer S. Ligands for the Nuclear Peroxisome Proliferator-Activated Receptor Gamma. Trends Pharmacol Sci. 2015;36(10):688-704.
110. Hu E, Kim JB, Sarraf P, Spiegelman BM. Inhibition of adipogenesis through MAP kinase-mediated phosphorylation of PPARγ. Science. 1996;274(5295):2100-2103.
111. Qiang L, Wang L, Kon N, Zhao W, Lee S, Zhang Y, Rosenbaum M, Zhao Y, Gu W, Farmer SR, Accili D. Brown remodeling of white adipose tissue by SirT1-dependent deacetylation of Pparγ. Cell. 2012;150(3):620-632.
112. Ji S, Park SY, Roth J, Kim HS, Cho JW. O-GlcNAc modification of PPARγ reduces its transcriptional activity. Biochemical and Biophysical Research Communications. 2012;417(4):1158-1163.
113. Ohshima T, Koga H, Shimotahno K. Transcriptional activity of peroxisome proliferator-activated receptor γ is modulated by SUMO-1 modification. Journal of Biological Chemistry. 2004;279(28):29551-29557.
114. Kilroy GE, Zhang X, Floyd ZE. PPAR-γ AF-2 domain functions as a component of a ubiquitin-dependent degradation signal. Obesity. 2009;17(4):665-673.
115. Kökény G, Calvier L, Hansmann G. PPARγ and TGFβ-Major Regulators of Metabolism, Inflammation, and Fibrosis in the Lungs and Kidneys. Int J Mol Sci. 2021;22(19).
116. Corrales P, Izquierdo-Lahuerta A, Medina-Gómez G. Maintenance of Kidney Metabolic Homeostasis by PPAR Gamma. Int J Mol Sci. 2018;19(7).
117. Mohandas R, Douma LG, Scindia Y, Gumz ML. Circadian rhythms and renal pathophysiology. J Clin Invest. 2022;132(3).
118. Diep QN, El Mabrouk M, Cohn JS, Endemann D, Amiri F, Virdis A, Neves MF, Schiffrin EL. Structure, endothelial function, cell growth, and inflammation in blood vessels of angiotensin II-infused rats: role of peroxisome proliferator-activated receptor-gamma. Circulation. 2002;105(19):2296-2302.
119. Guo C, Ricchiuti V, Lian BQ, Yao TM, Coutinho P, Romero JR, Li J, Williams GH, Adler GK. Mineralocorticoid receptor blockade reverses obesity-related changes in expression of adiponectin, peroxisome proliferator-activated receptor-gamma, and proinflammatory adipokines. Circulation. 2008;117(17):2253-2261.
120. Caprio M, Fève B, Claës A, Viengchareun S, Lombès M, Zennaro MC. Pivotal role of the mineralocorticoid receptor in corticosteroid-induced adipogenesis. Faseb j. 2007;21(9):2185-2194.

121. Scheen AJ. Renin-angiotensin system inhibition prevents type 2 diabetes mellitus. Part 2. Overview of physiological and biochemical mechanisms. Diabetes Metab. 2004;30(6):498-505.
122. Zhao M, Chen Y, Ding G, Xu Y, Bai M, Zhang Y, Jia Z, Huang S, Zhang A. Renal tubular epithelium-targeted peroxisome proliferator-activated receptor-γ maintains the epithelial phenotype and antagonizes renal fibrogenesis. Oncotarget. 2016;7(40):64690-64701.
123. Shen D, Li H, Zhou R, Liu MJ, Yu H, Wu DF. Pioglitazone attenuates aging-related disorders in aged apolipoprotein E deficient mice. Exp Gerontol. 2018;102:101-108.
124. Shen L, Yin H, Sun L, Zhang Z, Jin Y, Cao S, Fu Q, Fan C, Bao C, Lu L, Zhan Y, Xu X, Chen X, Yan Q. Iguratimod attenuated fibrosis in systemic sclerosis via targeting early growth response 1 expression. Arthritis Res Ther. 2023;25(1):151.
125. Chen SJ, Ning H, Ishida W, Sodin-Semrl S, Takagawa S, Mori Y, Varga J. The early-immediate gene EGR-1 is induced by transforming growth factor-beta and mediates stimulation of collagen gene expression. J Biol Chem. 2006;281(30):21183-21197.
126. Bhattacharyya S, Fang F, Tourtellotte W, Varga J. Egr-1: new conductor for the tissue repair orchestra directs harmony (regeneration) or cacophony (fibrosis). J Pathol. 2013;229(2):286-297.
127. Xie Y, Li Y, Chen J, Ding H, Zhang X. Early growth response-1: Key mediators of cell death and novel targets for cardiovascular disease therapy. Front Cardiovasc Med. 2023;10:1162662.
128. Bhattacharyya S, Wu M, Fang F, Tourtellotte W, Feghali-Bostwick C, Varga J. Early growth response transcription factors: Key mediators of fibrosis and novel targets for anti-fibrotic therapy. Matrix Biology. 2011;30(4):235-242.
129. Wei M, Zhang Y, Zhang H, Huang Z, Miao H, Zhang T, Lu B, Ji L. HMGB1 induced endothelial to mesenchymal transition in liver fibrosis: The key regulation of early growth response factor 1. Biochim Biophys Acta Gen Subj. 2022;1866(10):130202.
130. Chen J, Chen Y, Olivero A, Chen X. Identification and Validation of Potential Biomarkers and Their Functions in Acute Kidney Injury. Frontiers in genetics. 2020;11:411.
131. Jeong K, Je J, Dusabimana T, Kim H, Park SW. Early Growth Response 1 Contributes to Renal IR Injury by Inducing Proximal Tubular Cell Apoptosis. Int J Mol Sci. 2023;24(18).
132. Xu P, Zhan H, Zhang R, Xu XJ, Zhang Y, Le Y, Bi JG. Early growth response factor 1 upregulates pro-fibrotic genes through activation of TGF-β1/Smad pathway via transcriptional regulation of PAR1 in high-glucose treated HK-2 cells. Mol Cell Endocrinol. 2023;572:111953.

133. Nakamura H, Isaka Y, Tsujie M, Rupprecht HD, Akagi Y, Ueda N, Imai E, Hori M. Introduction of DNA enzyme for Egr-1 into tubulointerstitial fibroblasts by electroporation reduced interstitial α-smooth muscle actin expression and fibrosis in unilateral ureteral obstruction (UUO) rats. Gene therapy. 2002;9(8):495-502.
134. Carl M, Akagi Y, Weidner S, Isaka Y, Imai E, Rupprecht HD. Specific inhibition of Egr-1 prevents mesangial cell hypercellularity in experimental nephritis. Kidney Int. 2003;63(4):1302-1312.
135. Yang YL, Hu F, Xue M, Jia YJ, Zheng ZJ, Li Y, Xue YM. Early growth response protein-1 upregulates long noncoding RNA Arid2-IR to promote extracellular matrix production in diabetic kidney disease. Am J Physiol Cell Physiol. 2019;316(3):C340-c352.
136. Mózes MM, Szoleczky P, Rosivall L, Kökény G. Sustained hyperosmolarity increses TGF-ß1 and Egr-1 expression in the rat renal medulla. BMC Nephrol. 2017;18(1):209.
137. Tang C, Livingston MJ, Liu Z, Dong Z. Autophagy in kidney homeostasis and disease. Nature Reviews Nephrology. 2020;16(9):489-508.
138. Kimura T, Takabatake Y, Takahashi A, Kaimori JY, Matsui I, Namba T, Kitamura H, Niimura F, Matsusaka T, Soga T, Rakugi H, Isaka Y. Autophagy protects the proximal tubule from degeneration and acute ischemic injury. J Am Soc Nephrol. 2011;22(5):902-913.
139. Yang X, Wang H, Tu Y, Li Y, Zou Y, Li G, Wang L, Zhong X. WNT1-inducible signaling protein-1 mediates TGF-β1-induced renal fibrosis in tubular epithelial cells and unilateral ureteral obstruction mouse models via autophagy. J Cell Physiol. 2020;235(3):2009-2022.
140. Kaushal GP, Chandrashekar K, Juncos LA, Shah SV. Autophagy Function and Regulation in Kidney Disease. Biomolecules. 2020;10(1).
141. Huber TB, Edelstein CL, Hartleben B, Inoki K, Jiang M, Koya D, Kume S, Lieberthal W, Pallet N, Quiroga A, Ravichandran K, Susztak K, Yoshida S, Dong Z. Emerging role of autophagy in kidney function, diseases and aging. Autophagy. 2012;8(7):1009-1031.
142. Sureshbabu A, Muhsin SA, Choi ME. TGF-β signaling in the kidney: profibrotic and protective effects. Am J Physiol Renal Physiol. 2016;310(7):F596-f606.
143. Garmaa G, Manzéger A, Haghighi S, Kökény G. HK-2 cell response to TGF-β highly depends on cell culture medium formulations. Histochemistry and Cell Biology. 2024;161(1):69-79.
144. Manzéger A, Garmaa G, Mózes MM, Hansmann G, Kökény G. Pioglitazone Protects Tubular Epithelial Cells during Kidney Fibrosis by Attenuating miRNA Dysregulation and Autophagy Dysfunction Induced by TGF-β. Int J Mol Sci. 2023;24(21).

145. Page MJ, McKenzie JE, Bossuyt PM, Boutron I, Hoffmann TC, Mulrow CD, Shamseer L, Tetzlaff JM, Akl EA, Brennan SE, Chou R, Glanville J, Grimshaw JM, Hrobjartsson A, Lalu MM, Li T, Loder EW, Mayo-Wilson E, McDonald S, McGuinness LA, Stewart LA, Thomas J, Tricco AC, Welch VA, Whiting P, Moher D. The PRISMA 2020 statement: an updated guideline for reporting systematic reviews. BMJ. 2021;372:n71.
146. Higgins JPT TJ, Chandler J, Cumpston M, Li T, Page MJ, Welch VA. Cochrane Handbook for Systematic Reviews of Interventions version 6.2 (updated February 2021) Cochrane, 2021 [Available from: www.training.cochrane.org/handbook.
147. Kolde R, Laur S, Adler P, Vilo J. Robust rank aggregation for gene list integration and meta-analysis. Bioinformatics. 2012;28(4):573-580.
148. Vosa U, Kolde R, Vilo J, Metspalu A, Annilo T. Comprehensive meta-analysis of microRNA expression using a robust rank aggregation approach. Methods Mol Biol. 2014;1182:361-373.
149. Griffith OL, Melck A Fau - Jones SJM, Jones Sj Fau - Wiseman SM, Wiseman SM. Meta-analysis and meta-review of thyroid cancer gene expression profiling studies identifies important diagnostic biomarkers. Journal of Clinical Oncology. 2006;24(31).
150. Tang K, Xu H. Prognostic value of meta-signature miRNAs in renal cell carcinoma: an integrated miRNA expression profiling analysis. Sci Rep. 2015;5:10272.
151. Gillespie M, Jassal B, Stephan R, Milacic M, Rothfels K, Senff-Ribeiro A, Griss J, Sevilla C, Matthews L, Gong C, Deng C, Varusai T, Ragueneau E, Haider Y, May B, Shamovsky V, Weiser J, Brunson T, Sanati N, Beckman L, Shao X, Fabregat A, Sidiropoulos K, Murillo J, Viteri G, Cook J, Shorser S, Bader G, Demir E, Sander C, Haw R, Wu G, Stein L, Hermjakob H, D'Eustachio P. The reactome pathway knowledgebase 2022. Nucleic Acids Res. 2022;50(D1):D687-D692.
152. Liberzon A, Birger C, Thorvaldsdóttir H, Ghandi M, Mesirov Jill P, Tamayo P. The Molecular Signatures Database Hallmark Gene Set Collection. Cell Systems. 2015;1(6):417-425.
153. Tastsoglou S, Skoufos G, Miliotis M, Karagkouni D, Koutsoukos I, Karavangeli A, Kardaras FS, Hatzigeorgiou Artemis G. DIANA-miRPath v4.0: expanding target-based miRNA functional analysis in cell-type and tissue contexts. Nucleic Acids Research. 2023;51(W1):W154-W159.
154. Huang HY, Lin YC, Li J, Huang KY, Shrestha S, Hong HC, Tang Y, Chen YG, Jin CN, Yu Y, Xu JT, Li YM, Cai XX, Zhou ZY, Chen XH, Pei YY, Hu L, Su JJ, Cui SD, Wang F, Xie YY, Ding SY, Luo MF, Chou CH, Chang NW, Chen KW, Cheng YH, Wan XH, Hsu WL, Lee

TY, Wei FX, Huang HD. miRTarBase 2020: updates to the experimentally validated microRNA-target interaction database. Nucleic Acids Res. 2020;48(D1):D148-D154.
155. McGeary SE, Lin KS, Shi CY, Pham TM, Bisaria N, Kelley GM, Bartel DP. The biochemical basis of microRNA targeting efficacy. Science. 2019;366(6472).
156. Bustin SA, Benes V, Garson JA, Hellemans J, Huggett J, Kubista M, Mueller R, Nolan T, Pfaffl MW, Shipley GL, Vandesompele J, Wittwer CT. The MIQE guidelines: minimum information for publication of quantitative real-time PCR experiments. Clin Chem. 2009;55(4):611-622.
157. Hooijmans CR, Rovers MM, de Vries RB, Leenaars M, Ritskes-Hoitinga M, Langendam MW. SYRCLE's risk of bias tool for animal studies. BMC Med Res Methodol. 2014;14:43.
158. Freeman SC, Kerby CR, Patel A, Cooper NJ, Quinn T, Sutton AJ. Development of an interactive web-based tool to conduct and interrogate meta-analysis of diagnostic test accuracy studies: MetaDTA. BMC Med Res Methodol. 2019;19(1):81.
159. Hanley JA, McNeil BJ. The meaning and use of the area under a receiver operating characteristic (ROC) curve. Radiology. 1982;143(1):29-36.
160. Pustejovsky JE, Tipton E. Meta-analysis with Robust Variance Estimation: Expanding the Range of Working Models. Prev Sci. 2022;23(3):425-438.
161. Reitsma JB, Glas AS, Rutjes AW, Scholten RJ, Bossuyt PM, Zwinderman AH. Bivariate analysis of sensitivity and specificity produces informative summary measures in diagnostic reviews. J Clin Epidemiol. 2005;58(10):982-990.
162. Chu H, Cole SR. Bivariate meta-analysis of sensitivity and specificity with sparse data: a generalized linear mixed model approach. J Clin Epidemiol. 2006;59(12):1331-1332; author reply 1332-1333.
163. Harbord RM, Deeks JJ, Egger M, Whiting P, Sterne JA. A unification of models for meta-analysis of diagnostic accuracy studies. Biostatistics. 2007;8(2):239-251.
164. Garmaa G, Bunduc S, Kói T, Hegyi P, Csupor D, Ganbat D, Dembrovszky F, Meznerics FA, Nasirzadeh A, Barbagallo C, Kökény G. A Systematic Review and Meta-Analysis of microRNA Profiling Studies in Chronic Kidney Diseases. Non-Coding RNA [Internet]. 2024; 10(3).
165. Bozic M, de Rooij J Fau - Parisi E, Parisi E Fau - Ortega MR, Ortega Mr Fau - Fernandez E, Fernandez E Fau - Valdivielso JM, Valdivielso JM. Glutamatergic signaling maintains the epithelial phenotype of proximal tubular cells. J Am Soc Nephrol.22(6):1099-1111.

166. Bozic M, Caus MA-O, Rodrigues-Diez RA-O, Pedraza NA-O, Ruiz-Ortega M, Garí E, Gallel P, Panadés MJ, Martinez A, Fernández E, Valdivielso JM. Protective role of renal proximal tubular alpha-synuclein in the pathogenesis of kidney fibrosis. Nat Commun. 2020 Apr 23;11(1):1943.
167. Li H, Ruan XZ, Powis SH, Fernando R, Mon WY, Wheeler DC, Moorhead JF, Varghese Z. EPA and DHA reduce LPS-induced inflammation responses in HK-2 cells: evidence for a PPAR-gamma-dependent mechanism. Kidney Int. 2005;67(3):867-874.
168. Sasaki N, Toyoda M, Hasegawa F, Fujiwara M, Gomi F, Ishiwata T. Fetal bovine serum enlarges the size of human pancreatic cancer spheres accompanied by an increase in the expression of cancer stem cell markers. Biochem Biophys Res Commun. 2019;514(1):112-117.
169. Yao T, Asayama Y. Human Preimplantation Embryo Culture Media: Past, Present, and Future. Journal of Mammalian Ova Research. 2016;33(1):17-34, 18.
170. Puck TT, Cieciura SJ, Robinson A. Genetics of somatic mammalian cells. III. Long-term cultivation of euploid cells from human and animal subjects. J Exp Med. 1958;108(6):945-956.
171. Brennan EP, Morine MJ, Walsh DW, Roxburgh SA, Lindenmeyer MT, Brazil DP, Gaora PO, Roche HM, Sadlier DM, Cohen CD, Consortium G, Godson C, Martin F. Next-generation sequencing identifies TGF-beta1-associated gene expression profiles in renal epithelial cells reiterated in human diabetic nephropathy. Biochim Biophys Acta. 2012;1822(4):589-599.
172. Khundmiri SJ, Chen L, Lederer ED, Yang CR, Knepper MA. Transcriptomes of Major Proximal Tubule Cell Culture Models. J Am Soc Nephrol. 2021;32(1):86-97.
173. Franch HA, Shay JW, Alpern RJ, Preisig PA. Involvement of pRB family in TGF beta-dependent epithelial cell hypertrophy. J Cell Biol. 1995;129(1):245-254.
174. Kökény G, Calvier L Fau - Legchenko E, Legchenko E Fau - Chouvarine P, Chouvarine P Fau - Mózes MM, Mózes Mm Fau - Hansmann G, Hansmann G. PPARγ is a gatekeeper for extracellular matrix and vascular cell homeostasis: beneficial role in pulmonary hypertension and renal/cardiac/pulmonary fibrosis. Curr Opin Nephrol Hypertens. 2020;29(2):171-179.
175. Ghallab A, Seddek A. PPARG as therapeutic target for antifibrotic therapy. EXCLI J. 2020;19:227-229.
176. Ho LC, Sung JM, Shen YT, Jheng HF, Chen SH, Tsai PJ, Tsai YS. Egr-1 deficiency protects from renal inflammation and fibrosis. J Mol Med (Berl). 2016;94(8):933-942.

177. Sun S, Ning X, Zhai Y, Du R, Lu Y, He L, Li R, Wu W, Sun W, Wang H. Egr-1 mediates chronic hypoxia-induced renal interstitial fibrosis via the PKC/ERK pathway. Am J Nephrol. 2014;39(5):436-448.

178. Vollmann EH, Cao L, Amatucci A, Reynolds T, Hamann S, Dalkilic-Liddle I, Cameron TO, Hossbach M, Kauffman KJ, Mir FF, Anderson DG, Novobrantseva T, Koteliansky V, Kisseleva T, Brenner D, Duffield J, Burkly LC. Identification of Novel Fibrosis Modifiers by In Vivo siRNA Silencing. Mol Ther Nucleic Acids. 2017;7:314-323.

179. Gerritsma JS, Gerritsen AF, De Ley M, van Es LA, Daha MR. Interferon-gamma induces biosynthesis of complement components C2, C4 and factor H by human proximal tubular epithelial cells. Cytokine. 1997;9(4):276-283.

180. Peake PW, O'Grady S, Pussell BA, Charlesworth JA. C3a is made by proximal tubular HK-2 cells and activates them via the C3a receptor. Kidney Int. 1999;56(5):1729-1736.

181. Gerritsma JSJ, van Kooten C, Gerritsen AF, van Es LA, Daha MR. Transforming growth factor-β1 regulates chemokine and complement production by human proximal tubular epithelial cells. Kidney International. 1998;53(3):609-616.

182. Sanchez-Romero N, Schophuizen CM, Gimenez I, Masereeuw R. In vitro systems to study nephropharmacology: 2D versus 3D models. Eur J Pharmacol. 2016;790:36-45.

183. Lee JW, Chou CL, Knepper MA. Deep Sequencing in Microdissected Renal Tubules Identifies Nephron Segment-Specific Transcriptomes. J Am Soc Nephrol. 2015;26(11):2669-2677.

184. Valdés A, Lucio-Cazaña FJ, Castro-Puyana M, García-Pastor C, Fiehn O, Marina ML. Comprehensive metabolomic study of the response of HK-2 cells to hyperglycemic hypoxic diabetic-like milieu. Sci Rep. 2021;11(1):5058.

185. Fang F, Ooka K, Bhattacharyya S, Wei J, Wu M, Du P, Lin S, Del Galdo F, Feghali-Bostwick CA, Varga J. The early growth response gene Egr2 (Alias Krox20) is a novel transcriptional target of transforming growth factor-beta that is up-regulated in systemic sclerosis and mediates profibrotic responses. Am J Pathol. 2011;178(5):2077-2090.

186. Chen ZH, Kim HP, Sciurba FC, Lee SJ, Feghali-Bostwick C, Stolz DB, Dhir R, Landreneau RJ, Schuchert MJ, Yousem SA, Nakahira K, Pilewski JM, Lee JS, Zhang Y, Ryter SW, Choi AM. Egr-1 regulates autophagy in cigarette smoke-induced chronic obstructive pulmonary disease. PLoS One. 2008;3(10):e3316.

187. Wang C, Zhu G, He W, Yin H, Lin F, Gou X, Li X. BMSCs protect against renal ischemia-reperfusion injury by secreting exosomes loaded with miR-199a-5p that target BIP to

inhibit endoplasmic reticulum stress at the very early reperfusion stages. FASEB J. 2019;33(4):5440-5456.
188. Zhang X, Liu L, Dou C, Cheng P, Liu L, Liu H, Ren S, Wang C, Jia S, Chen L, Zhang H, Chen M. PPAR Gamma-Regulated MicroRNA 199a-5p Underlies Bone Marrow Adiposity in Aplastic Anemia. Mol Ther Nucleic Acids. 2019;17:678-687.
189. Delic D, Wiech F, Urquhart R, Gabrielyan O, Rieber K, Rolser M, Tsuprykov O, Hasan AA, Kramer BK, Baum P, Kohler A, Gantner F, Mark M, Hocher B, Klein T. Linagliptin and telmisartan induced effects on renal and urinary exosomal miRNA expression in rats with 5/6 nephrectomy. Sci Rep. 2020;10(1):3373.
190. Kim SK, Kim G, Choi BH, Ryu D, Ku SK, Kwak MK. Negative correlation of urinary miR-199a-3p level with ameliorating effects of sarpogrelate and cilostazol in hypertensive diabetic nephropathy. Biochemical pharmacology. 2021;184:114391.
191. Agarwal V, Bell GW, Nam J-W, Bartel DP. Predicting effective microRNA target sites in mammalian mRNAs. eLife. 2015;4:e05005.
192. Pakravan G, Foroughmand AM, Peymani M, Ghaedi K, Hashemi MS, Hajjari M, Nasr-Esfahani MH. Downregulation of miR-130a, antagonized doxorubicin-induced cardiotoxicity via increasing the PPARgamma expression in mESCs-derived cardiac cells. Cell Death Dis. 2018;9(7):758.
193. Sun L, Xu T, Chen Y, Qu W, Sun D, Song X, Yuan Q, Yao L. Pioglitazone attenuates kidney fibrosis via miR-21-5p modulation. Life sciences. 2019;232:116609.
194. Ruby M, Gifford CC, Pandey R, Raj VS, Sabbisetti VS, Ajay AK. Autophagy as a Therapeutic Target for Chronic Kidney Disease and the Roles of TGF-β1 in Autophagy and Kidney Fibrosis. Cells. 2023;12(3).
195. Kim SI, Na HJ, Ding Y, Wang Z, Lee SJ, Choi ME. Autophagy promotes intracellular degradation of type I collagen induced by transforming growth factor (TGF)-β1. J Biol Chem. 2012;287(15):11677-11688.
196. Ding Y, Kim S, Lee SY, Koo JK, Wang Z, Choi ME. Autophagy regulates TGF-beta expression and suppresses kidney fibrosis induced by unilateral ureteral obstruction. J Am Soc Nephrol. 2014;25(12):2835-2846.
197. Kim WY, Nam SA, Song HC, Ko JS, Park SH, Kim HL, Choi EJ, Kim YS, Kim J, Kim YK. The role of autophagy in unilateral ureteral obstruction rat model. Nephrology (Carlton). 2012;17(2):148-159.

198. Wang L, Yin Y, Hou G, Kang J, Wang Q. Peroxisome Proliferator-Activated Receptor (PPARgamma) Plays a Protective Role in Cigarette Smoking-Induced Inflammation via AMP-Activated Protein Kinase (AMPK) Signaling. Med Sci Monit. 2018;24:5168-5177.
199. Eardley KS, Kubal C, Zehnder D, Quinkler M, Lepenies J, Savage CO, Howie AJ, Kaur K, Cooper MS, Adu D, Cockwell P. The role of capillary density, macrophage infiltration and interstitial scarring in the pathogenesis of human chronic kidney disease. Kidney Int. 2008;74(4):495-504.
200. Ochieng J, Furtak V, Lukyanov P. Extracellular functions of galectin-3. Glycoconjugate journal. 2002;19(7-9):527-535.
201. Brooimans RA, Stegmann AP, van Dorp WT, van der Ark AA, van der Woude FJ, van Es LA, Daha MR. Interleukin 2 mediates stimulation of complement C3 biosynthesis in human proximal tubular epithelial cells. J Clin Invest. 1991;88(2):379-384.
202. Gao S, Cui Z, Zhao MH. The Complement C3a and C3a Receptor Pathway in Kidney Diseases. Frontiers in immunology. 2020;11:1875.
203. Ishibashi M, Egashira K, Hiasa K, Inoue S, Ni W, Zhao Q, Usui M, Kitamoto S, Ichiki T, Takeshita A. Antiinflammatory and antiarteriosclerotic effects of pioglitazone. Hypertension. 2002;40(5):687-693.
204. Zamanian MY, Taheri N, Opulencia MJC, Bokov DO, Abdullaev SY, Gholamrezapour M, Heidari M, Bazmandegan G. Neuroprotective and Anti-inflammatory Effects of Pioglitazone on Traumatic Brain Injury. Mediators of inflammation. 2022;2022:9860855.
205. Agarwal R. Anti-inflammatory effects of short-term pioglitazone therapy in men with advanced diabetic nephropathy. Am J Physiol Renal Physiol. 2006;290(3):F600-605.
206. Yuan Q, Tang B, Zhang C. Signaling pathways of chronic kidney diseases, implications for therapeutics. Signal Transduct Target Ther. 2022;7(1):182.
207. Sanz AB, Sanchez-Niño MD, Ramos AM, Ortiz A. Regulated cell death pathways in kidney disease. Nature Reviews Nephrology. 2023;19(5):281-299.
208. Reiss AB, Voloshyna I, De Leon J, Miyawaki N, Mattana J. Cholesterol Metabolism in CKD. Am J Kidney Dis. 2015;66(6):1071-1082.
209. Gholaminejad A, Abdul Tehrani H, Gholami Fesharaki M. Identification of candidate microRNA biomarkers in renal fibrosis: a meta-analysis of profiling studies. Biomarkers. 2018;23(8):713-724.
210. Gholaminejad A, Abdul Tehrani H, Gholami Fesharaki M. Identification of candidate microRNA biomarkers in diabetic nephropathy: a meta-analysis of profiling studies. J Nephrol. 2018;31(6):813-831.

211. Roointan A, Gholaminejad A, Shojaie B, Hudkins KL, Gheisari Y. Candidate MicroRNA Biomarkers in Lupus Nephritis: A Meta-analysis of Profiling Studies in Kidney, Blood and Urine Samples. Molecular Diagnosis & Therapy. 2022.
212. Li J, Ma L, Yu H, Yao Y, Xu Z, Lin W, Wang L, Wang X, Yang H. MicroRNAs as Potential Biomarkers for the Diagnosis of Chronic Kidney Disease: A Systematic Review and Meta-Analysis. Frontiers in Medicine. 2022;8.
213. Wang C, Hu J, Lu M, Gu H, Zhou X, Chen X, Zen K, Zhang C-Y, Zhang T, Ge J, Wang J, Zhang C. A panel of five serum miRNAs as a potential diagnostic tool for early-stage renal cell carcinoma. Scientific Reports. 2015;5(1):7610.
214. Bhaskaran V, Nowicki MO, Idriss M, Jimenez MA, Lugli G, Hayes JL, Mahmoud AB, Zane RE, Passaro C, Ligon KL, Haas-Kogan D, Bronisz A, Godlewski J, Lawler SE, Chiocca EA, Peruzzi P. The functional synergism of microRNA clustering provides therapeutically relevant epigenetic interference in glioblastoma. Nat Commun. 2019;10(1):442.

9. PUBLICATIONS

Publications related to the thesis:

1. **Garmaa G**, Manzéger A, Haghighi S, Kökény G. HK-2 cell response to TGF-β highly depends on cell culture medium formulations. Histochemistry and Cell Biology. 2024;161(1):69-79. Impact factor, journal quartile – 2.3, Q1.
2. Manzéger A, **Garmaa G**, Mózes MM, Hansmann G, Kökény G. Pioglitazone Protects Tubular Epithelial Cells during Kidney Fibrosis by Attenuating miRNA Dysregulation and Autophagy Dysfunction Induced by TGF-β. Int J Mol Sci. 2023;24(21). Impact factor, journal quartile – 5.6, D1.
3. **Garmaa G**, Bunduc S, Kói T, Hegyi P, Csupor D. Ganbat D, Dembrovszky F, Meznerics F.A, Nasirzadeh A, Barbagallo C, Kökény G. A Systematic Review and Meta-Analysis of microRNA Profiling Studies in Chronic Kidney Diseases. Non-Coding RNA 2024; 10 (3)30. Impact factor, journal quartile – 4.3, Q1.
4. **Garmaa G**, Rita N, Kökény G. Panel miRNAs are potential diagnostic markers for chronic kidney diseases: a systematic review and meta-analysis. (accepted in BMC Nephrology). Impact factor, journal quartile – 2.2, Q2.

Publications not related to the thesis:

1. Tóth-Mészáros A, **Garmaa G**, Hegyi P, Bánvölgyi A, Fenyves B, Fehérvári P, Harnos A, Gergő D, Nguyen Do To U, Csupor D. The effect of adaptogenic plants on stress: A systematic review and meta-analysis. Journal of Functional Foods 2023 Vol. 108 Pages 105695, DOI: https://doi.org/10.1016/j.jff.2023.105695. Impact factor, journal quartile – 5.6, Q1.
2. Horváth IL, Bunduc S, Fehérvári P, Váncsa S, Nagy R, **Garmaa G**, Kleiner D, Hegyi P, Erőss B, Csupor D. The combination of ulinastatin and somatostatin reduces complication rates in acute pancreatitis: a systematic review and meta-analysis of randomized controlled trials. Sci Rep. 2022 Oct 26;12(1):17979. doi: 10.1038/s41598-022-22341-7. PMID: 36289288; PMCID: PMC9606296. Impact factor, journal quartile – 4.6, D1.
3. Enkhmaa D, Ganmaa D, Tanz LJ, Rich-Edwards JW, Stuart JJ, Enkhtur S, **Gantsetseg G**, Batkhishig B, Fitzmaurice G, Bayalag M, Nasantogtokh E, Bairey Merz CN, Shufelt CL. Changes in Vascular Function from Preconception to Postpartum Among Mongolian Women. J Womens Health (Larchmt). 2022 Jul 28. doi: 10.1089/jwh.2021.0360. Epub ahead of print. PMID: 35904927.

4. Ganbat D, Jugder B-E, Ganbat L, Tomoeda M, Dungubat E, Miyegombo A, **Garmaa G**, Takahashi Y, Fukuzawa R, Mori I, Shiomi T, Nakata A, Tomita Y. Use of the Naphthoquinone YM155 (Sepantronium Bromide) in the Treatment of Cancer: A Systematic Review and Meta-Synthesis. Oncologie, 2022 Jun 07; 0 (0): Vol. 1-31.
5. Ganmaa D, Uyanga B, Zhou X, **Gantsetseg G**, Delgerekh B, Enkhmaa D, Khulan D, Ariunzaya S, Sumiya E, Bolortuya B, Yanjmaa J. Vitamin D Supplements for Prevention of Tuberculosis Infection and Disease. New England Journal of Medicine. 2020 Jul 23;383(4):359-68.
6. Ganmaa D, Enkhmaa D, Baatar T, Uyanga B, **Gantsetseg G**, Helde TT, McElrath TF, Cantonwine DE, Bradwin G, Falk RT, Hoover RN. Maternal Pregnancy Hormone Concentrations in Countries with Very Low and High Breast Cancer Risk. International Journal of Environmental Research and Public Health. 2020 Jan;17(3):823.
7. Bromage S, Enkhmaa D, Baatar T, **Garmaa G**, Bradwin G, Yondonsambuu B, Sengee T, Jamts E, Suldsuren N, McElrath TF, Cantonwine DE. Comparison of seasonal serum 25-hydroxyvitamin D concentrations among pregnant women in Mongolia and Boston. The Journal of steroid biochemistry and molecular biology. 2019 Oct 1;193:105427.
8. Ganmaa D, Khudyakov P, Buyanjargal U, Baigal D, Baatar M, Enkhamgalan N, Erdenebaatar S, Ochirbat B, Burneebaatar B, Purevdorj E, Purevsuren Y, **Gantsetseg G**, Erdenetuya G, Martineau, Adrian R. Risk factors for active tuberculosis in 938 QuantiFERON-positive schoolchildren in Mongolia: a community-based cross-sectional study. BMC infectious diseases. 2019 Dec;19(1):532.
9. Enkhmaa D, Tanz L, Ganmaa D, Enkhtur S, Oyun-Erdene B, Stuart J, Chen G, Carr A, Seely EW, Fitzmaurice G, Buyandelger Y, Sarantsetseg B, **Gantsetseg G**, Rich-Edwards, J. W.Randomized trial of three doses of vitamin D to reduce deficiency in pregnant Mongolian women. EBioMedicine. 2019 Jan 1;39:510-9.

10. ACKNOWLEDGEMENT

The experience I had at Semmelweis University has taught me valuable lessons that I will carry with me throughout my life. It wasn't just about completing my Ph.D. project but also about balancing my work and personal life, staying motivated, keeping an open mind, facing the realities of the scientific world, and remaining calm, strong, and kind in the face of adversity. This experience and my thesis would not have been possible without the generous professional and personal support of some incredible people around me. I feel honored to dedicate this part of my thesis to them.

I appreciate your invitation to study at Semmelweis for the first time, **Prof. László Rosivall**. Your kind words and encouragement during my stay were the building blocks I needed to grow and stay strong. I'm grateful for your support, which provided me with the necessary inspiration to keep going.

Thank you very much, **Prof. Gábor Kökény**. You are a skilled and professional professor, and I feel fortunate to have had the opportunity to work under your guidance. Initially, I was curious about microRNA regulation in kidney disease, and you welcomed my curiosity and provided valuable insights. Your encouragement and support have led me to explore this exciting scientific field further. Your dedication to science and time management principles taught me valuable career lessons.

Dear **Prof. Zoltán Benyó**, I wanted to express my gratitude for your generous support and understanding. You have been an exceptional leader and an inspiration for international PhD students like me. Your kind and compassionate attitude, coupled with your exceptional leadership abilities, have helped me grow both professionally and personally. I truly appreciate everything you have done for us.

Prof. Gábor Szénási, **Prof. András Balla,** and **Prof. Péter Légrády,** I am grateful for the time you spent reviewing my thesis. Your thoughtful comments and suggestions have been incredibly helpful in shaping my work. I truly appreciate your expertise and willingness to share it with me. Thank you to the **exam committee members**, **Prof. Péter Reismann, Dr. Tamás Kaucsár**, and **Prof. Balázs Sági**, who supported my PhD defense.

I appreciate your support, **Prof. Miklós Mózes**, and your cheerful and warm greeting every morning, which has been a source of inspiration. **Anna Manzéger**, I would like to express my gratitude for your invaluable technical support and training during my first years. Let's continue to listen to "The Hu" and share inspiration, even from afar. Hopefully, little **Lia** will join us. I wish all the best to her. I would also like to extend my appreciation to **Krisztina Fazekas** and **Rita Bencs**, for your valuable technical assistance and expertise, which was of immense help

throughout the journey. **Rita,** your kindness is truly exceptional. Thank you to all my current and former colleagues at the **Department of Theoretical and Translational Medicine**.

I am grateful for the financial support provided by the **Tempus Public Foundation** and the **SE250+ scholarship** for my PhD project training.

Dear **Tamás Kói, Stefania Bunduc**, **Péter Hegyi, Dezső Csupor, Rita Nagy, and colleagues at the TM centre**, I wanted to take a moment to express my sincere gratitude for your tremendous assistance and collaboration in our meta-analyses. The experience has been truly exhilarating, and I am thrilled to have had the opportunity to work with such talented and dedicated colleagues. Thank you again for your invaluable contributions to our project.

I want to express my gratitude to all my **friends** who have been with me through thick and thin, especially **Safaa, Kenan, Bálint, Sami, Mehdi, Zahra, Nino, Arezoo**, and **Zambaga**. I truly appreciate your support and warm hand during my journey. A special thank you to **Safaa** for being by my side, listening, and providing me with mental support during tough times.

I am immensely grateful to my mentors, who have played a vital role in shaping my life. I am incredibly fortunate to have such extraordinary mentors as **Dr. Ganmaa, Dr. Dariimaa, Dr. András, Dr. Munkhzol**, **Dr. Janet, Dr. Enkhmaa**, and **Dr. Khosbayar**, who have always supported and encouraged me. Thank you, my distant friends, **Naraa, Deegii, Javzaa, Uuganaa, Chinzo,** and **Odonoo**, and my friend in Hungary, **Soko**, neice **Baaska**, for supporting me mentally and spiritually.

I hold my dearest grandmother, **Purevsuren**, and my teacher, **Dr. Garid**, close to my heart. I miss them dearly every day, but I know they are in a better place and watching over us. I believe they would be proud of their daughter and the entire family. Furthermore, I extend my gratitude to my **great-grandfather**, who had a remarkable intelligence and spirit that inspired me. I promise always to remember his words and keep my word to him.

I want to take a moment to express my deepest gratitude towards my beloved family. My loving parents, **Garmaa** and **Erdenechimeg**, my wonderful sisters, **Jiimee, Duna**, and **Dodo**, and my brothers-in-law, **Batka and Batkhuu**, have been my constant source of support. To my little ones, **Babu, Anu, Agaraa,** and **Unkhruush,** thank you from the bottom of my heart for everything you have done for me. Your unconditional love and unwavering emotional and mental support have brought me to where I am today. I grew up learning to be the right person, always be honest, support those in need, and be persistent. All of these values were instilled in me thanks to my family's tireless commitment to my growth and well-being. Once again, I am genuinely grateful for all you have done for me.